Book of Abstracts

Faculty of Physics of the University of Vienna, Austria
September 15-19, 2013

Dear participant,

Welcome to the 34th International Symposium on Dynamical Properties of Solids – dyProSo XXXIV, at the Faculty of Physics, University of Vienna, which is organized by the Physics of Functional Materials Group.

dyProSo is a 4-day research meeting aiming to promote new ideas and concepts concerning excited states in condensed matter. The symposium is intended to stimulate discussions between young and experienced scientists working in this broad field, to foster scientific contacts and develop new ideas.

Advances in theory (ab-initio calculations, molecular dynamics and Monte Carlo simulations, new formulations and phenomenological models, etc.) and in experiment (optical spectroscopy, inelastic neutron and X-ray scattering, novel techniques, etc.) are presented.

The scientific programme of dyProSo XXXIV focuses on:

- Phonons, magnons and electromagnons
- Superconductors
- Carbon-based materials
- Multiferroics
- Relaxors
- Amorphous, liquid and soft matter
- Advances in experimental techniques and theory
- Materials at extreme pressure

There are 21 invited lectures, 25 contributed talks and 39 poster presentations. Following the tradition of DyProSo there are no parallel sessions.

I wish you a stimulating and exciting conference and a pleasant stay in Vienna.

On behalf oft he Local Organizing Committee of dyProSo XXXIV,

Wilfried Schranz (conference chairman)

Sponsors

University of Vienna

Springer Verlag

AVL, Graz, Austria

Austrian Airlines

Stadt Wien

International Advisory Board

A. Almeida (University of Porto, Portugal)
C. Ecolivet (CNRS/GMCM/UNIV Rennes, France)
J. Hlinka (Institute of Physics Prague, Czech Republic)
T. Janssen (University of Nijmegen, The Netherlands)
M. Kiskinova (ELETTRA Trieste, Italy)
J. Kulda (ILL Grenoble, France)
M.-H. Lemée-Cailleau (ILL Grenoble, France)
S. Lovesey (ISIS Oxford, United Kingdom)
B. Partoens (University of Antwerp, Belgium)
M. Pérez-Mato (University of Bilbao, Spain)
B. Roessli (PSI Villigen, Switzerland)
C. Thomsen (TU Berlin, Germany)

Programme Committee

W. Schranz (chairman, Austria)
C. Dellago (Austria)
J. Hlinka (Czech Republic)
J. Kreisel (Luxembourg)
G. Krexner (Austria)
H. Kuzmany (Austria)
R. Miletich (Austria)
O. Paris (Austria)
W. Petry (Germany)

Local Organizing Committee

Wilfried Schranz (chairman)
Martin Fally
Armin Fuith
Heinz Kabelka
Jürgen Klepp
Gerhard Krexner
Wolfgang Pichl^{+}
Marius Reinecker
Romano Rupp
Anna Marie Hermann (Secretary)

Table of contents

Programme

Sunday, September 15, 2013

18:00	Registration
19:00	Welcome reception

Monday, September 16, 2013

08:30 Registration

08:45 Opening

Multiferroics I	
09:00	**Nicola Spaldin** *Cosmic strings in multiferroics*
09:40	**Pierre Tolédano** *Magnetoelectric effects in antiferromagnets, weak ferromagnets and magnetic monopole-like systems*
10:20	**Annette Bussmann-Holder** *$EuTiO_3$: an almost multiferroic material with surprising novel strong spin-lattice coupling at elevated temperatures*

10.45 Coffee break

Phonons, magnons and electromagnons I	
11:15	**Standa Kamba** *Electromagnons: Electrically active spin excitations*
11:55	**Przemyslaw Piekarz** *Lattice dynamics in the rare-earth crystals and nanostructures*

12:20 Lunch

14:00	**Jirka Hlinka** *Unfolded phonon dispersion of antiferroelectric $PbZrO_3$*
14:25	**Istvan Kezsmarki** *Novel optical phenomena in multiferroics*
14:50	**Peter Babkevich** *$LiErF_4$: a model dipolar-coupled antiferromagnet*
15:15	**Alexandre Ivanov** *Phonon dispersion in symmetry related crystal structures: metallic phases in Sn*

15:40 Coffee break

Materials at extreme pressure	
16:10	**Sergio Speziale** *The elastic anisotropy of dense materials at extreme conditions: Experimental approaches and implications for deep Earth geophysics*
16:50	**Mael Guennou** *Combined instabilities of perovskites under pressure: $BiMnO_3$ and related Bi-based perovskites*
17:30	**J. Agostinho Moreira** *Unraveling the effect of high pressure in rare-earth manganites*
17:55	**Andreas Tröster** *High Pressure Landau Theory Applied to Strontium Titanate*

18:30 **Wine/Beer Poster session**

Tuesday, September 17, 2013

08:30 Registration

Amorphous, liquid and soft matter	
09:00	**Gerhard Gruebel** *Local Order in Liquids and Glasses*
09:40	**Leif Eric Hintzsche** *Defect states at c-Si/a- $Si_3N_xH_y$ interfaces*
10:05	**Bogdan Sepiol** *Atomic diffusion in network-forming glasses studied with X-ray photon correlation spectroscopy*
10:30	**Vasily Artemov** *Proton dynamics in liquid water and ice*

10:55 Coffee break

Relaxors	
11:25	**Francesco Cordero** *Polar and antiferrodistortive modes and their coupling in PZT by dielectric and anelastic measurements*

12:05 Lunch

14:00	**Marco Deluca** *Raman spectroscopy of lead-free relaxor ceramics*
14:40	**Rasa Pirc** *From lattice model to quantitative theory of relaxor ferroelectrics*
15:05	**Anna Böhmer** *Nematic susceptibility of hole- and electron-doped $BaFe_2As_2$ iron-based Superconductors*
15:30	**Jan Petzelt** *Broadband dielectric spectroscopy of $Ba(Zr,Ti)O_3$: dynamics of relaxors and diffuse ferroelectrics*

15:55 Coffee break

Carbon-based materials I	
16:25	**Brian LeRoy** *Imaging local electronic properties of graphene*
17:05	**Janina Maultzsch** *Resonance behavior of defect-induced Raman modes in carbon nanotubes*
17:45	**Miro Haluška** *Monitoring the fabrication process flow of SWCNT field effect transistors using Raman spectroscopy*

18:30 **Advisory Board Meeting**

Wednesday, September 18, 2013

08:30 Registration

Phonons, magnons and electromagnons II	
09:00	**Alois Loidl** *Electromagnons*
09:40	**Uladzislau Dziom** *Optical activity of electromagnon in multiferroic manganite*
10:05	**Laura Chaix** *THz Magnetoelectric Atomic Rotations in the Chiral Compound $Ba_3NbFe_3Si_2O_{14}$*

10:30 Coffee break

11:00	**Michael Leitner** *Temperature-dependent phonons in Fe: Implications on thermodynamics and diffusion*
11:25	**Björn Wehinger** *Lattice dynamics of silica polymorphs*
11:50	**Piotr Zielinski** *Dynamics of curved surfaces. True and leaky surface waves in cylindrical cavities*
12:15	**Cene Filipic** *Polarons in crystalline perfluorotetradecanoic acid monohydrate*

12:40 Lunch

Advances in experimental techniques and theory	
14:20	**Kai Rossnagel** *Shooting electronic structure movies with time-resolved photoemission*
15:00	**Michael A. Carpenter** *Elastic and anelastic relaxations associated with phase transitions in ferroic and multiferroic perovskites*
15:40	**Georg Kresse** *Methods beyond DFT: current status and future developments*

16:20 Coffee break

Carbon-based materials II	
16:50	**Ludger Wirtz** *Graphene and graphite intercalation compounds: dependence of the phonon dispersion on the environment*
17:30	**Jannik Meyer** *Exploring low-dimensional nano-carbon materials by high-resolution microscopy*

20:00 **Conference dinner**

Thursday, September 19, 2013

Superconductors	
09:00	**Philippe Bourges** *Novel magnetism in high-Tc copper oxides superconductors*
09:40	**Jitae Park** *Resonant magnetic excitations in iron-based superconductors*
10:20	**Christoph Meingast** *Thermodynamic study of the magneto-structural and superconducting transitions in Co-doped $BaFe_2As_2$*

10:45 Coffee break

11:15	**Jozef T. Devreese** *Mechanisms of superconductivity in strontium titanate and in a $LaAlO_3$-$SrTiO_3$ heterostructure*
11:40	**Vladimir Kozhevnikov** *Nonlocal effect and dimensions of Cooper pairs in Pippard superconductors*

12:05 **Refreshments**

Multiferroics II	
13:00	**Manfred Fiebig** *Extended magnetoelectric functionalities in improper ferroelectrics*
13:40	**Rui Vilarinho Silva** *Competing magnetic interactions and Spin-Phonon Coupling in Magnetoelectric Y-Substituted $GdMnO_3$*
14:05	**Markus Braden** *Neutron scattering studies on chiral multiferroics*
14:45	**Ekhard K. H. Salje** *Noise and Pattern Formation in Ferroic Materials*

15:30 **Closing**

Talks

Multiferroics I

Cosmic strings in multiferroics

Spaldin, Nicola (ETH Zurich, Zurich , CHE)

The first symmetry-lowering phase transition to occur after the Big Bang -- the so-called Grand Unification Transition -- is believed to have yielded cosmic strings, formed as topologically protected defects when symmetry-lowered regions of different phase intersected. It is extraordinarily difficult, however, to study cosmic string formation directly because of issues associated with replaying the Big Bang in the laboratory. Here I will show that the multiferroic hexagonal manganites -- with their coexisting magnetic, ferroelectric and structural phase transitions -- generate topologically protected defects at their domain intersections which are the crystallographic equivalent of cosmic strings.

The ferroic phase transitions are readily accessible in the laboratory, and the resulting domains straightforward to characterize, so the hexagonal manganites can be used to test the so-called "Kibble-Zurek" scaling laws proposed for defect-formation in the early universe. I will describe how electronic structure calculations and symmetry analysis allowed identification and quantification of the important features of the hexagonal manganites, and present experimental results of the first unambiguous demonstration of Kibble-Zurek scaling.

Magnetoelectric effects in antiferromagnets, weak ferromagnets and magnetic monopole-like systems

Tolédano, Pierre (Laboratory of Physics of Complex Systems, Picardie, FRA)

The intensive search for materials showing simultaneous magnetic and ferroelectric orders and the understanding of their properties have paved the way to the identification of new classes of magnetoelectric materials. We shall first describe theoretically the specific physical properties of the most celebrated multiferroic compounds in which the onset of the multiferroic phase across a second-order phase transition results from the coupling of two antiferromagnetic order-parameters. The “pseudo-proper” character of this coupling gives rise to a small induced “improper” electric polarization and critical anomalies typical of a “proper” ferroelectric transition. In the most widespread case of an incommensurate multiferroic phase the polarization results from non-linear magnetoelectric effects which forbid an electric-field induced magnetization. In some materials the continuous rotation of the phason mode allows a coupling between antiferromagnetic modes having the same symmetry. By contrast in commensurate multiferroic phases, direct and reversed linear magnetoelectric effect can be observed. The property of the multiferroic state to be antisymmetric with respect to time and space inversions has prompted a discussion of the relevance of the concept of the magnetic toroidal moment and its long-range order in antiferromagnets. In contrast with antiferromagnetic ordering which does not give rise to a macroscopic symmetry-breaking order-parameter, the toroidal moment is a macroscopic polar vector. Its existence allows predicting two distinguishable subclasses of magnetoelectric materials:

1) *Ferrotoroidic antiferromagnets* in which the toroidal moment constitutes the primary order-parameter with respect to the correlated antiferromagnetic order. In the absence of measurable physical quantity showing direct evidence of a toroidal moment, the primary ferrotoroidic mechanism should be reflected by the existence of magnetoelectric effects forbidden by the antiferromagnetic order, and denoting the predominant contribution of the toroidal moment to the internal magnetic field.
2) *Ferrotoroidic weak-ferromagnets* in which, for some definite symmetries of the multiferroic state, one can discriminate the toroidal moment and weak ferromagnetic contributions to the magnetoelectric effects. Another potential new class of magnetoelectric materials consists of spin-ice-like antiferromagnets, in which the elementary excitations have a magnetic charge behaving as a magnetic monopole. It has been suggested that for specific antiferromagnetic structures an electric dipole could be attached to each magnetic charge, opening the possibility of controlling the monopole-like charges by an electric field.

A theoretical analysis of the possible realization of such magnetoelectric systems will be discussed.

$EuTiO_3$: an almost multiferroic material with surprising novel strong spin-lattice coupling at elevated temperatures

Köhler, Jürgen (Max-Planck-Institute for Solid State Research, Stuttgart, GER); Guguchia, Zurab (Physik-Institut der Univ. Zürich, Zürich, CHE); Keller, Hugo (Physik-Institut der Univ. Zürich, Zürich, CHE); Bussmann-Holder, Annette (Max-Planck-Institute for Solid State Research, Stuttgart, GER)

$EuTiO_3$ (ETO) is antiferromagnetic at T_N=5.5K. In analogy to $SrTiO_3$ (STO) it exhibits a strong mode softening of a long wave length optic mode, reminiscent of ferroelectricity, however suppressed by quantum fluctuations. A strong spin lattice coupling is evident at low temperatures, since the dielectric constant exhibits an unusual drop at TN which can be erased by a magnetic field. The analogies between STO and ETO have recently been shown to be supplemented by the observation of an oxygen octahedral rotation at high temperatures (TS=282K) driven by the condensation of a zone boundary acoustic mode. It is shown that TS is strongly magnetic field dependent with a nonlinear enhancement of TS. This observation suggests that a very pronounced magneto-electric coupling is present at high temperatures which originates from correlated dynamic spin clusters as also evidenced by a finite muon spin rotation signal. Further, the phase diagram of mixed crystals of STO and ETO is presented where the high temperature as well as the low temperature transition temperatures are identified and shown to follow distinctly different composition dependencies.

Phonons, magnons and electromagnons I

Electromagnons: electrically active spin excitations

Kamba, Standa (Institute of Physics , Prague, CZE); Goian, V. (Institute of Physics , Prague, CZE); Kadlec, F. (Institute of Physics , Prague, CZE); Kadlec, C. (Institute of Physics , Prague, CZE); Vanek, P. (Institute of Physics , Prague, CZE); Kempa, M. (Institute of Physics , Prague, CZE); Gich, M. (Institut de Ciència de Materials de Barcelona , Bellaterra, ESP)

The fundamental differences between the static and dynamic magnetoelectric couplings will be explained. The microscopic origin of the static magneto-electric coupling, i.e. the change of magnetization with electric field or of electric polarization with magnetic field, is already well understood. Depending on the specific magnetic structure of the investigated materials, the exchange striction, inverse Dzyaloshinskii-Moriya interaction or the spin-dependent covalency between the metal d state and ligand p state may play the key role. In contrast, due to the dynamic magnetoelectric coupling, spin waves (magnons) can be excited by the electric component of the electromagnetic radiation; therefore, these excitations are called electromagnons (EMs). Unlike the antiferromagnetic or ferromagnetic resonances — i.e. magnons from the Brillouin zone (BZ) centre (**q**=0) excited by the magnetic component of the electromagnetic radiation —, the EMs are magnons with a general value of the wave vector q. In different magnetic structures, EMs can have wavevectors from the G point (**q**=0), from the BZ boundary (**q**=$\mathbf{Q}_{BZ}$), **q**=$\mathbf{q}_m$ or **q**=$\mathbf{Q}_{BZ}$ - 2$\mathbf{q}_m$ (here $\mathbf{q}_m$denotes the modulation wavevector of the magnetic structure). The reasons of EM activation in the THz permittivity spectra and their properties will be discussed for different compounds; among them, in the canonical spin-induced ferroelectric $TbMnO_3$ [1]. In this compound, the ferroelectricity is induced by a spin-orbit coupling (inverse Dzyaloshinskii-Moriya interaction), and two EMs are activated by the magnetostriction. An exotic example is $CaMn_7O_{12}$, whose polarization is the highest among all spin-induced ferroelectrics. In the multiferroic $CuFe_{1-x}Ga_xO_2$, an EM was observed only in the paraelectric phase with a collinear magnetic order, while it vanished from the THz spectra in the ferroelectric phase with an incommensurately modulated helimagnetic structure [2]. We will also show that the EMs are not limited to multiferroics — we have observed an EM in ε-Fe_2O_3, a pyroelectric ferrimagnet prepared in the form of nanograin ceramics. We have shown that by combining infrared, THz and inelastic neutron scattering experiments, the EM can be discerned from magnons or phonons; this was achieved for the first time without using a single crystal. In a broader perspective, the sensitivity of EMs not only to the static external magnetic field, but also to the external electric field opens a promising route for electrically controlled magnonics in the THz region.

[1] Takahashi Y. et al. Evidence for an electric-dipole active continuum band of spin excitations in multiferroic $TbMnO_3$, Phys. Rev. Lett. 2008, **101**, 187201
[2] Seki S. et al. Electromagnons in the spin collinear state of a triangular lattice antiferromagnet, Phys. Rev. Lett. 2010, **105**, 097207

Lattice dynamics in the rare-earth crystals and nanostructures

Piekarz, Przemyslaw (Institute of Nuclear Physics, Kraków, POL); Stankov, Svetoslav (Karlsruhe Institute of Technology, Karlsruhe, GER); Bauder, Olga (Karlsruhe Institute of Technology, Karlsruhe, GER); Lazewski, Jan (Institute of Nuclear Physics, Kraków, POL); Parlinski, Krzysztof (Institute of Nuclear Physics, Kraków, POL); Ruffer, Rudolf (European Synchrotron Radiation Facility, Grenoble, FRA)

The determination of the lattice dynamics of rare-earth metals has been the challenge for the experimental and theoretical methods [1]. This arises from the difficulties in accessing single crystals with high quality and from the tendency of most lanthanides to oxidize when exposed to air. In addition, the large absorption cross-section for thermal neutrons exhibited by some isotopes of rare-earths prohibits the application of the standard inelastic neutron scattering. The difficulties in theoretical studies of the rare-earth metals result from the localized character of 4f electrons, complex magnetic ordering, and strong spin-orbit coupling. Samarium is one of the most fascinating elements throughout the entire periodic table. At ambient conditions Sm crystalizes in a peculiar rhombohedral structure referred to as Sm-type. We have determined the phonon density of states (DOS) and the thermo-elastic properties of Sm [2] by in-situ low temperature nuclear resonant inelastic X-ray scattering (NRIXS) [3] on a (0001)Sm film and first principles calculations. The calculated phonon dispersion relations and phonon DOS for this structure has bee compared with the dhcp lattice, which is characteristic for the light lanthanides. Surprisingly, the dhcp unit cell, being by a factor of 2.2 smaller in height, exhibits more pronounced vibrational anisotropy in comparison to the Sm-type structure. The origin of this phenomenon is the different stacking layer sequence of atoms with local hexagonal and cubic symmetry in both unit cells. This modifies mainly the vibrational properties along the [0001] direction of the atoms at the hexagonal positions, whereas the atoms with cubic symmetry vibrate in a similar manner in both structures. Employing in-situ NRIXS, we have investigated the phonon DOS of ultrathin Eu films (2-24 monolayers) and compared the results with that of bulk Eu [1] and ab initio calculations. The experimental studies revealed a systematic shift of the phonon DOS to higher energies and significant suppression of the low-energy phonon modes as the film thickness is reduced. The observed phenomenon is attributed to the change in the crystal symmetry and the compression of the epitaxial Eu film induced by the lattice mismatch with the Nb(110) substrate.

S. Stankov acknowledges the financial support by the Initiative and Networking funds of the President of the Helmholtz Association and the Karlsruhe Institute of Technology (KIT) for the Helmholtz- University Young Investigators Group "Interplay between structure and dynamics in epitaxial rare- earth nanostructures" contract VH-NG-625. P. Piekarz J. Łażewski, and K. Parlinski acknowledge support by the Polish National Science Center (NCN) under Project No. 2011/01/M/ST3/00738.

[1] S. Stankov, P. Piekarz, A. M. Oleś, K. Parlinski, and R. Rüffer, Phys. Rev. B **78** , 18030 (2008).
[2] O. Bauder, P. Piekarz, A. Barla, I. Sergueev, R. Rüffer, J. Łażewski, T. Baumbach, K. Parlinski, and S. Stankov , to be published.
[3] S. Stankov, R. Rüffer, M. Sladecek, M. Rennhofer, B. Sepiol, G. Vogl, N. Spiridis, T. Slezak, and J. Korecki, Rev. Sci. Instrum. **79**, 045108 (2008).

Unfolded phonon dispersion of antiferroelectric $PbZrO_3$

Hlinka, Jiři (Institute of Physics, Czech Acad. Sci., Prague, CZE)

$PbZrO_3$ is an interesting model compound, either as an end-member of technologically relevant solid solutions with $PbTiO_3$ (piezoelectric PZT's) or as an example of an antiferroelectric material. The parent paraelectric phase is a simple cubic perovskite with a 5-atom unit cell (Pm3m, Z=1). Below the antiferroelectric phase transition (Tc ~ 500K), it turns into an orthorhombic Pnma (Z=8) structure. This phase transition can be understood as a result of the condensation of two order-parameters, for example one at the wave vector $\mathbf{k}_1$=(0.25,0.25,0), and the other at the wave vector $\mathbf{k}_2$=(0.5,0.5,0.5) [1]. Due to the multiplication of the unit cell, a large number of phonon modes becomes active in the infrared, Raman or hyper-Raman spectra below the phase transition. Interestingly, practically all these modes have been identified in our recent spectroscopic studies of $PbZrO_3$ single crystals [2,3]. Moreover, we shall show that one can frequently trace back the relation of these optically active modes to the phonon modes of the parent, high temperature cubic phase. This even allows us to reconstruct several low-frequency phonon dispersion branches within the reciprocal plane containing the $\mathbf{k}_1$ and $\mathbf{k}_2$ wave vectors, similarly as it was already done for the incommensurate and commensurate dielectric materials in the past [4].

[1] H. Fujishita and S. Hoshino, J. Phys. Soc. Jpn. **53**, 273 (1968).
[2] J. Hlinka, T. Ostapchuk, E. Buixaderas, J. Petzelt, J. Dec, J. Drahokoupil, M. Savinov and I. Gregora, in preparation.
[3] J. Hlinka, I. Gregora, T. Ostapchuk, E. Buixaderas, J. Petzelt, V. Laguta, and B. Hehlen, ongoing work.
[4] S. Kamba et al, J. Phys. Cond. Matt. **5**, 4401 (1993).

Novel optical phenomena in multiferroics

Kezsmarki, Istvan (Budapest University of Technology and Economics, Department of Physics, Budapest, HUN); Bordacs, Sandor (Budapest University of Technology and Economics, Department of Physics, Budapest, HUN); Szaller, David (Budapest University of Technology and Economics, Department of Physics, Budapest, HUN); Nagel, Urmas (National Institute of Chemical Physics and Biophysics, Tallinn, EST); Room, Toomas (National Institute of Chemical Physics and Biophysics, Tallinn, EST); Engelkamp, Hans (Radboud University Nijmegen High Field Magnet Laboratory, Nijmegen); Penc, Karlo (Institute for Solid State Physics and Optics, Wigner Research Centre for Physics, Budapest, HUN); Tokura, Yoshinori (RIKEN Center for Emergent Matter Science, Tokyo, JPN)

Simultaneous breaking of time-reversal and spatial inversion symmetries can lead to the emergence of new optical phenomena in multiferroics. As the most peculiar example, we have recently found that multiferroics can exhibit strong non-reciprocal directional dichroism, i.e. they absorb counter-propagating light beams with different strength [1,2]. Moreover, we have demonstrated that the absorbing and transparent directions of light propagation can be reversed by the application of either magnetic or electric fields. In the low-energy (THz, infrared) region of the electromagnetic spectrum directional dichroism is the consequence of the optical magnetoelectric effect, i.e. the coupled dynamics of the local magnetization and electric polarization. Collective spin modes in multiferroics, which are resonantly excited by both the electric and magnetic component of light, are the "elementary excitations" of such electromagnetic (or magnetoelectric) response. Here, we show that these electromagnetic resonances can efficiently generate directional optical anisotropy by studying several multiferroic compounds including $Ba_2CoGe_2O_7$ and $Ca_2CoSi_2O_7$. Our results imply that strong directional dichroism can be present in a large variety of multiferroic materials due to their coupled spin-polarization dynamics [3,4]. Besides its potential in photonics, detection of directional optical anisotropy also provides a tool to reveal the microscopic origins and key parameters of the magnetoelectric phenomena in multiferroics.

[1] I. Kezsmarki et al. *Enhanced Directional Dichroism of Terahertz Light in Resonance with Magnetic Excitations of the Multiferroic $Ba_2CoGe_2O_7$ Oxide Compound*, Phys. Rev. Lett. **106**, 057403 (2011).
[2] S. Bordacs et al. *Chirality of matter shows up via spin excitations*, Nat. Phys. **8**, 734 (2012).
[3] K. Penc et al. *Spin-Stretching Modes in Anisotropic Magnets: Spin-Wave Excitations in the Multiferroic $Ba_2CoGe_2O_7$*, Phys. Rev. Lett. **108**, 257203 (2012).
[4] D. Szaller et al. *Symmetry conditions for nonreciprocal light propagation in magnetic crystals*, Phys. Rev. B **87**, 014421 (2013).

$LiErF_4$: a model dipolar-coupled antiferromagnet

Babkevich, Peter (EPFL, Lausanne, CHE); Nikseresht, Neda (EPFL, Lausanne, CHE); Kovacevic, Ivan (EPFL, Lausanne, CHE); Ronnow, Henrik (EPFL, Lausanne, CHE)

The $LiErF_4$ is a unique model material representing a purely dipolar-coupled planar antiferromagnets. Dipolar interactions are a matter of long standing discussions due to their fundamental importance and generality to all magnetic systems ranging from bulk materials to nanomagnets. We have performed a comprehensive investigation of $LiErF_4$ including susceptibility, specific heat, elastic and inelastic neutron scattering and have obtained detailed information on the nature of the system including magnetic structure and the temperature-field phase diagram [1,2]. We have found that the thermal transition falls into the 2D XY/h $_4$ universality class [1], while the quantum phase transition is 3D. To date, very few experimental investigations have been reported on this compound. Exploiting large perfect crystals, negligible incoherent scattering, the large rare earth moment, and the existence of isotopes with and without the nuclear spins (therefore, demonstrating the effect of switching off the spin bath [3]), $LiErF_4$ represents an ideal model, where criticality and scaling relations can be explored in great detail.

[1] C. Kraemer et al, Science **336**, 1416 (2012)
[2] N. Nikseresht, PhD Thesis: http://infoscience.epfl.ch/record/178304
[3] H.M. Rønnow et al, Science **308**, 389 (2005)

Phonon dispersion in symmetry related crystal structures: metallic phases in Sn

Ivanov, Alexandre (Institut Max von Laue - Paul Langevin, Grenoble, FRA); Szakal, Alex (Wigner Research Centre for Physics, Budapest, HUN); Rumiantsev, Alexander (Russian Academy of Sciences, Moscow, RUS)

In the case of the phase transitions of the 1st order the relation between phonon spectra of the two phases may be not evident. A good starting point for such a comparison can be orientation relations between the crystal lattices of the two phases. Mathematically these orientation relations can be expressed through the existence of a common symmetry subgroup for symmetry groups describing structures of both phases. Using this approach we analyze the phonon dispersion in the two phases of metallic tin – the well known beta-Sn (called white tin) with a tetragonal space group and two atoms in the primitive cell and the other phase, called gamma-Sn, with a less common simple-hexagonal crystal structure with one atom in the primitive cell. The orientation relations between the two structures find their justification in the existing low-frequency vibration modes in the two structures. We complemented the existing experimental data with our more detailed measurements of the phonon dispersion in the two metallic phases of tin in order to compare the full sets and show the way in which different branches of the two phases should be compared. We notice that certain branches drastically change at the transition while the others remain practically unchanged in the whole Brillouin zone. A half of the 6 branches in the two-atomic white tin transforms to branches at the zone boundary in one-atomic gamma-tin with their correspondence described by the inelastic structure factors (or eigenvectors of phonon modes). A virtual transition from one structure to another is simulated with the help of a simple lattice dynamics model which takes into account the symmetry correspondence of the crystals structures of these phases of metallic Sn.

Materials at extreme pressure

The elastic anisotropy of dense materials at extreme conditions: Experimental approaches and implications for deep Earth geophysics

Speziale, Sergio (Deutsches GF, Potsdam, GER)

Determining the elastic properties of materials is fundamental both for their thermodynamic characterization and for the understanding of their mechanical behavior.The study of the elastic properties of condensed matter at extreme pressure and temperature conditions is a main focus of condensed matter physics, chemistry, and of geophysics. Several techniques can furnish partial information about average aggregate elastic moduli of solids and the compressibility of fluids at high pressure and temperature. However, the determination of the elastic anisotropy -the directional dependence of the elastic constants- at very high pressures is still a very challenging task. The measurement of the full elastic tensor of elastically anisotropic materials at simultaneous high pressures and temperatures is nowadays at the limit of our current capabilities and there are only very few techniques which are promising candidates to more routinely perform such measurements in the near future. In my talk I will introduce a selection of the main techniques to perform single-crystal elastic constants determinations at extreme pressures. Some of these techniques, such as Brillouin scattering and inelastic x-ray scattering, are based on inelastic scattering of electromagnetic radiation by acoustic phonons. I will highlight merits, limitations and perspectives of such methods with a special stress on the applications in mineral physics for the determination of reliable mineralogical models of the very deep interior of our planet consistent with the available global seismological and geochemical constraints.

Combined instabilities of perovskites under pressure: BiMnO3 and related Bi-based perovskites

Guennou, M (CRP Gabriel Lippmann, Luxembourg, LUX); Bouvier, P (Grenoble Institute of Technology, Grenoble, FRA); Toulemonde, P (Institut Néel, Grenoble, FRA); Kreisel, J (CRP Gabriel Lippmann, Luxembourg, LUX)

Over the past 10 years, many efforts have been devoted to the (re-)examination of structural distortions in perovskites under high-pressure and associated physical properties, in order to identify general trends and rules for their evolutions and interactions. Bismuth-based perovskites in particular show a remarkable variety of structures but have been less explored, partly because of their challenging synthesis.

In this work, the focus will be laid on recent results obtained on bismuth manganite $BiMnO_3$. This compound has a non-polar C2/c structure at ambient conditions and, from the point of view of structural distortions, combines strong octahedral tilts, Jahn-Teller distorted octahedra and a polar-active bismuth cation on the A-site with its characteristic s^2 lone pair electrons. Our investigations up to 60 GPa by XRD and Raman spectroscopy on both powder and single crystal $BiMnO_3$ samples have revealed a total of four phase transitions at 1, 7, 37 and 53GPa with a phase sequence $C2/c \rightarrow P2_1/c \rightarrow Pnma \rightarrow Cm \rightarrow$ (unknown). Particularly notable in this evolution are a strong reduction of the cooperative Jahn-Teller distortion in the *Pnma* phase, the emergence of an unexpected polar phase *Cm* at 37GPa, and an insulator-to-metal transition at 55 GPa.

These results will be put into perspective in the broader context of Bi-based perovskites under pressure. This includes in particular our own past investigations on the equally complex high-pressure behavior of $BiFeO_3$ in the same pressure range, characterized by unusual orthorhombic phases probably related to complex tilt systems. Based on these comparisons, tentative general trends will be summarized.

Unraveling the effect of high pressure in rare-earth manganites

Moreira Agostinho, J (IFIMUP, Porto, POR); Almeida, A (IFIMUP, Porto, POR)

Perovskite rare-earth manganites, $RMnO_3$, exhibit many fascinating phenomena, including orbital and charge ordering, half-metallic behaviour, a rich variety of magnetic orders, including modulated structures, and magnetoelectric coupling [1-4]. At ambient conditions, the rare-earth manganites, with R = La to Dy, exhibit an orthorhombically distorted perovskite structure, with Pnma symmetry, which can be derived from the ideal perovskite structure by tilt of the MnO_6 octahedra and by the cooperative Jahn-Teller distortion [4]. The balance of the competition between the antiferromagnetic and ferromagnetic exchange interactions, underlying the rich phase diagram of these compounds, has a well-established effect on the tilt angle of the octahedra.

In this contribution, we present a pressure-dependent study up to ~60 GPa of the lattice dynamics of $RMnO_3$, with R = Pr, Nd, Sm, Eu, Gd, Tb, and Dy, by Raman scattering, and of the structure of $RMnO_3$, with R = Pr, Sm, Eu, Gd, and Dy, by using synchrotron radiation diffraction. Experimental data yield a structural and insulator-to-metal phase transition at high pressure, for the studied compounds. It can be seen that the critical pressure increases as the ionic radius of the rare-earth ion decreases. Whenever the x-ray diffraction data exhibit enough quality, the symmetry of the high-pressure phase is presented.

The pressure dependence of the wave number of the Raman bands for different modes shows different slopes but no anomaly up to the critical pressure. Moreover, the slope of the linear portion of the wave number pressure dependence for the same mode has a different value for each compound, pointing out that the structural deformations induced by pressure are not accommodated in the same way for each one.

The analysis of the x-ray data enables us to determine the pressure dependence of the lattice parameters and volume. Within the orthorhombic phase, the compression is anisotropic, with the soft direction along the a-axis, and the hard direction along the b-axis. The compressibilities along the b and c-axis increase with decreasing ionic radius, while the compressibility along the a-axis decreases. The compressibility along the b-axis is slightly dependent on the rare-earth ion. Moreover, the pressure behavior of both axial and orthorhombic strain for the different compounds will be compared and their evolution discussed in order to evaluate the relative role of Jahn-Teller distortion and tilting of MnO_6 octhaedra. Their relative importance can also be inferred from the analysis of the wave number of the out-of-phase MnO_6 rotations and in-plane O2 symmetric stretching modes.

References:

[1] Fiebig M, J. Phys.D Appl. Phys, **38**, R123 (2005)
[2] Kimura T, Tokura Y, J. Phys.: Condens.Matter, **20**, 434204 (2008)
[3] Mochizuki M, Furukawa N, Phys. Rev. B, **80** 134416 (2009)
[4] Goto T, Kimura T, Lawes G, Ramirez AP, Tokura Y, Phys. Rev. Lett. **92**, 257201 (2004)

High Pressure Landau Theory Applied to Strontium Titanate

Tröster, Andreas (Vienna University of Technology, Vienna, AUT)

For decades, Landau theory has proven its value as one of the most useful and versatile approaches to gain an understanding of all kinds of phase transitions in condensed matter physics. In particular, its intimate linkage to group theory makes Landau theory an indispensable tool for analyzing and quantifying structural phase transitions in the solid state, in which strain frequently plays an important role as a primary or secondary order parameter.

While it is often possible to treat strain effects accompanying a thermally driven structural transition within a linearized elastic approximation, the large strain effects exhibited by high pressure phase transitions generally require a full nonlinear treatment of elastic energy. In this talk we explain how to set up a consistent calculation scheme for a Landau theory of high pressure phase transitions which systematically allows to take into account elastic nonlinearities and shows how to utilize available information on the pressure dependence of elastic constants taken form experiment or from DFT calculations.

Applied to the example of the high pressure cubic-tetragonal phase transition in $SrTiO_3$, a model perovskite which has played a central role in the development of the theory of structural phase transitions, our theory allows to obtain a quantitatively satisfying description of recent high precision experimental data and to make interesting predictions that still need to be tested by experiment.

Amorphous, liquid and soft matter

Local Order in Liquids and Glasses

Gruebel, Gerhard (DESY, Hamburg, GER)

The study of angular correlations in diffraction patterns was recently demonstrated to reveal bond orientational order of amorphous materials [1]. For electrons and visible light, related techniques were developed earlier [2]. By using coherent x-rays as probe, the intrinsic spatial and temporal averaging mechanism performed in conventional (incoherent) diffraction can be avoided. Instead, snapshots of the instantaneous positions of all particles in the beam are reflected in the coherent diffraction patterns, so called ”speckle patterns”. In order to uncover the hidden local symmetries in disordered matter such as liquids and glasses from the speckle patterns properly defined higher order correlation functions have to be devised and applied to the data. This method called X-ray Cross Correlation Analysis (XCCA) represents a promising tool to study disordered samples such as fast relaxing liquids at Free-Electron-Laser facilities in the hard X-ray regime. We will show applications of the XCCA technique to hard sphere liquids and glasses.

[1] P. Wochner, C. Gutt, T. Autenrieth, T. Demmer, V. Bugaev, A.D. Ortiz, A. Duri, F. Zontone, G. Grübel, and H. Dosch. Proc. Natl. Acad. Sci. **106**, 11511 (2009).
[2] N.A. Clark, B.J. Anderson, A.J. Hurd. Phys. Rev. Lett. **50**, 1459 (1983); J.M. Gibson, M.M.J. Treacy, T. Sun, and N.J. Zaluzec. Phys. Rev. Lett. **105**, 125504 (2010).

Defect states at c-Si/a-$Si_3N_xH_y$ interfaces

Hintzsche, Leif Eric (University of Vienna, Vienna, AUT); Jordan, Gerald (University of Vienna, Vienna, AUT); Marsman, Martijn (University of Vienna, Vienna, AUT); Lamers, Machteld (ECN Solar Energy, Petten, NLD); Weeber, Arthur (ECN Solar Energy, Petten, NLD); Kresse, Georg (University of Vienna, Vienna, AUT)

Amorphous silicon nitrides are deposited on crystalline silicon as antireflection and passivating coatings. Up to date detailed knowledge about the interfaces is largely lacking. We have investigated the electronic and structural properties of c-Si/a-$Si_3N_xH_y$ interfaces obtained by large scale ab initio molecular dynamics simulations. Over 500 independent samples have been generated for each considered stoichiometry to perform a reliable defect analysis. While the classes of dominant defect states coincided with previous bulk calculations, we found a considerably increased defect density at the interface. By applying an energy and spatially resolved defect analysis, we observed that most of the defect states originate from the first silicon nitride layer at the interface. Additionally, we examined passivation effects of hydrogen at the interface which play an important role to increase the efficiency of modern solar cells.

Atomic diffusion in network-forming glasses studied with X-ray photon correlation spectroscopy

Ross, Manuel (Dynamik Kondensierter Systeme, Wien, AUT); Leitner, Michael (Dynamik Kondensierter Systeme, Wien, AUT); Stana, Markus (Dynamik Kondensierter Systeme, Wien, AUT); Sepiol, Bogdan (Dynamik Kondensierter Systeme, Wien, AUT)

Condensed matter can be distinguished on the microscopic level into amorphous materials and crystals. For a crystal model system we applied a new method in our group which allows measuring dynamics on atomic length scales [1], in contrast to the typically used macroscopic methods like the tracer technique. By utilizing the most brilliant X-rays generated by high energy synchrotron sources and measuring in the diffuse regime of wide angle scattering, we extended X-ray photon correlation spectroscopy to the atomic range (aXPCS). Consecutively to this first successful application, we proved that our method performs in very good agreement with other measurement methods for different types of crystals [2].

Since the establishment of the random network theory of Zachariasen [3], research on glass has made large progress. The exact mechanisms of diffusion in glasses, however, are still far from being understood. Being able to observe atomic dynamics with aXPCS in crystal systems, the next step is to extend this method to the complex case of non-crystalline materials. One of physics' unsettled questions is the dynamic behavior of these amorphous materials.

In lead-silicate glasses, both components can act as network formers. We selected these systems as good candidates for studying diffusion in glasses with aXPCS. Our recent study in metallic glass [4] at temperatures around the glass transition showed highly non-equilibrium atomic mobility which was independently confirmed by another group [5, 6].

Another interesting class of materials are fast ionic conductors due to the increasing relevance of solid oxide fuel cell applications. As these materials are well known for their fast diffusive motion, they are also a promising candidate for pushing the limits of the accessible range for aXPCS. We investigated an alkali-borate ionic conducting glass, where the network structure decides the way ions diffuse and thus determines the conductivity of the material. Our analysis of two different compositions of lead-silica and of one composition of rubidium-borate glasses allows to draw conclusions on diffusion properties like the mean distance and a time scale of ionic motion and thereby to shed light on the processes which govern glassy dynamics. I will give an overview on our recent results obtained from measurements at the synchrotrons ESRF and PETRA III and discuss the consequences for our picture of the atomic dynamics in glasses.

As we have shown the feasibility of aXPCS only recently [1], there is a large field of systems to be explored with this new method. The talk of M. Stana within this conference will explain the principles of aXPCS and illustrate the experimental achievements in crystalline solids. This talk will show our approach to the diffusion mechanisms in network-forming glasses.

Our work was supported by the Austrian Science Fund (FWF): P22402.

[1] M. Leitner, B. Sepiol, L.-M. Stadler, B. Pfau, and G. Vogl, Nature Mat. **8**, 717 (2009).
[2] M. Stana, M. Leitner, M. Ross, and B. Sepiol, J. Phys.: Condens. Matter **25**, 065401 (2013).
[3] W. H. Zachariasen, J. Am. Chem. Soc. **54** (1932).
[4] M. Leitner, B. Sepiol, L.-M. Stadler, and B. Pfau, Phys. Rev. B **86**, 064202 (2012).
[5] B. Ruta et al., Phys. Rev. Lett. **109**, 165701 (2012).
[6] B. Ruta et al., J. Chem. Phys. **138**, 054508 (2013).

Proton dynamics in liquid water and ice

Artemov, Vasily (A.M. Prokhorov General Physics Institute RAS, Moscow, RUS); Pronin, Artem (Dresden High Magnetic Field Laboratory, Dresden, GER); Volkov, Alexander (A. M. Prokhorov General Physics Institute, Moscow, RUS)

In order to find the microscopic mechanism, responsible for the formation of the dielectric spectra of liquid water and ice and for the spectra transformation at 0 C, we analyze the experimental data on the permittivity and the dynamical conductivity (at frequencies 10^3-10^{11} Hz) in the framework of a recently developed model of proton transport in liquid water [1].

The model is in line with the modern concept that protons, H^+, and the hydroxyl ions, OH^-, are permanently generated and recombined in the volume of water and ice due to self-ionization of the H_2O molecules [2-4]. Since free protons are not observed, they are considered to localize after their birth (on femtosecond time scale) on the neighboring neutral H_2O molecules. The excess proton converts the H_2O molecule into a charged complex H_3O^+ with a positive charge q^+, and leaves a "proton hole", OH^-, with a negative "twin" charge q^-. Subsequently, the q^+ and q^- charges wander in a relay-race manner over the H_2Omolecules until they meet their partners to recombine.

We suggest that there are two possible recombination processes for the charges: the fast one (recombination with its own twin partner) and the slow one (recombination with a "foreign" partner). These processes reveal themselves as two well-separated absorption areas in the conductivity spectrum. Analogously to the materials with high ionic conductivity (the superionics), we describe the proton dynamics in terms of the Brownian diffusion of protons.

At the first stage, we find the model to fit comprehensively the experimental dielectric panorama of liquid water. The model reveals the giant concentrationof the H_3O^+ - OH^- ionic pairs, $N = 5\times10^{-26}$ m^{-3}, and a very short lifetime of an intact water molecule (0.1 to 1 ns, instead of commonly accepted 11 hours). The model shows, that the static permittivity is predominantly determined by *N*.

At the second stage, we find *N* and the diffusion length, ℓ, to be invariants at the water-ice phase transition, while the diffusion coefficient *D* of protons changes by 6.5 orders of magnitude. Such behavior of *N,* ℓ, and *D* perfectly describes the experimentally-observed transformation of the dielectric spectra at the phase transition at 0 C.

[1] A.A. Volkov, V.G. Artemov, A.V. Pronin, Proton Electrodynamics in Liquid Water, arXiv:1302.5048v1, 2013.
[2] H.J. Bakker, H.-K.Nienhuyst, Delocalization of Protons in Liquid Water, Science, Vol. 297, 587, (2002).
[3] A . Hassanali , M . K . Prakash , H . Eshet , M . Parrinello , On the Recombination of Hydronium and Hydroxide Ions in Water , PNAS , Vol . 108 , 20410 (2011).
[4] V.F. Petrenko, R.W. Whitworth. Physics of Ice, Oxford Univ. Press, 1999, p. 373.

Relaxors

Polar and antiferrodistortive modes and their coupling in PZT by dielectric and anelastic measurements

Cordero, Francesco (CNR-ISC, Istituto dei Sistemi Complessi, Roma, ITA); Craciun, F. (CNR-ISC, Istituto dei Sistemi Complessi, Roma, ITA); Trequattrini, F. (Università di Roma , Roma, ITA); Galassi, C. (CNR-ISTEC, Faenza, ITA)

In some multiferroic perovskites and related materials, the coupling of octahedral tilt modes with the polar and magnetic ones plays a role [1,2], and the mechanisms in pure ferroelectrics may also apply to other multiferroics.

Thanks to the combination of dielectric and anelastic spectroscopies, it has been possible to probe better than before the structural transitions involving the antiferrodistortive (AFD) tilt modes of the octahedra in PZT [3] and NBT-BT [4]. In PZT, close to the antiferroelectric phase, a new border T_{IT} is identified with te onset of disordered tilting, before the final long range ordered tilting of the *R3c* phase is established below T_T. Such a line merges with T_C, presumably giving rise to a combined ferroelectric-tilt transition. On the high-Ti side of our series of large grain ceramic samples, T_T does not cross the morphotropic phase boundary (MPB), but merges with it. On the other hand, in NBT-BT it had already been established that the instability to the ferroelectric state T_d coincides with the tilt transition between tetragonal $a^0a^0c^+$ and rhombohedral $a^-a^-a^-$ (in Glazer notation) over an extended range of Ba compositions.

Figure 1 Phase diagrams of PZT and NBT-BT where the combined polar-AFD transitions are vertically shaded. The tilt patterns are given in Glazer notation S/LRO = short/long range order.

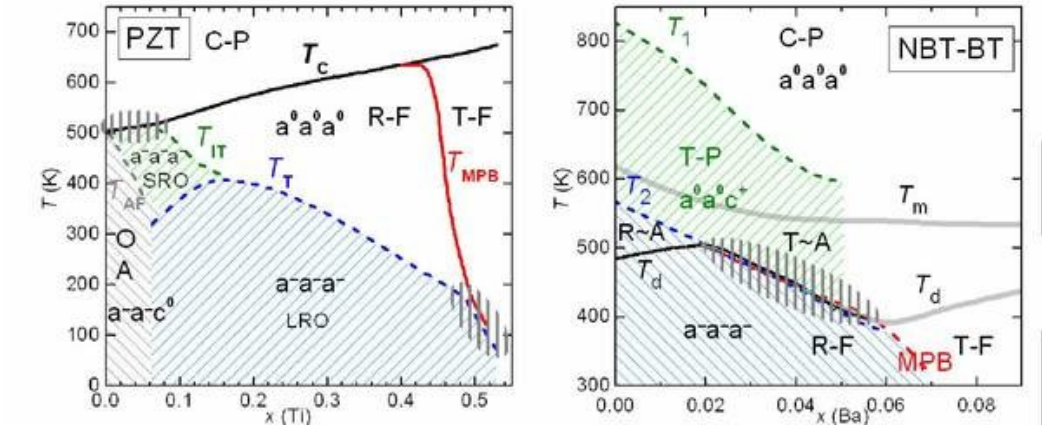

These lines of combined polar-tilt transitions are vertically hatched in Fig. 1, and it is suggested that they are a consequence of cooperative interaction between the polar and the AFD modes, as proposed for the trigger-type transitions in the multiferroic $BiFeO_3$ [2]. In PZT, the transition to the antiferroelectric orthorhombic phase involves both the antipolar and AFD modes, which, near the border with the FE phase, can condense at quite different temperatures.

[1] N. A. Benedek and C. J. Fennie, Phys. Rev. Lett. 106, 107204 (2011).
[2] I.A. Kornev and L. Bellaiche, Phys. Rev. B 79, 100105 (2009)].
[3] F. Cordero, F. Trequattrini, F. Craciun and C. Galassi, Phys. Rev. B 87, 094108 (2013).
[4] F. Cordero, F. Craciun, F. Trequattrini, E. Mercadelli and C. Galassi, Phys. Rev. B 81, 144124 (2010).

Raman spectroscopy of lead-free relaxor ceramics

Deluca, Marco (Materials Center Leoben Forschung GmbH, Leoben, AUT)

Relaxor ceramics are being nowadays increasingly studied for industrial applications involving the conversion of electrical into mechanical energy and vice-versa. Following the environmental regulations that impose finding a suitable lead-free alternative to replace the dominant lead-based electroceramics, bismuth- or barium-based relaxors are currently under consideration for actuator applications.

In this talk, the use of Raman spectroscopy for the characterization of this class of materials will be presented. Due to its sensitivity to the short-range structure, this technique is especially effective if used together with dielectric, piezoelectric measurements or X-ray diffraction, methods that generally give a macroscopic picture of the structure and properties of the material. Raman spectroscopy can be used to detect phases, coexistence of phases, and their transition in dependence of electric field, pressure and temperature. Several examples of the application of this technique to the study of relaxors will be given, including sodium bismuth titanate (BNT), the most promising lead-free ferroelectric, and A-site and B-site substituted barium titanate (BT)-based ceramics. The relationship between the structures revealed by Raman spectroscopy and the dielectric and electro-mechanical properties of these compositions will be also discussed.

The complementary role of Raman spectroscopy with other techniques will be highlighted, and also its capability to distinguish structural features that can be ascribed to differences in the production process of these materials.

From lattice model to quantitative theory of relaxor ferroelectrics

Pirc, Rasa (Jozef Stefan Institute, Ljubljana, SVN); Novak, N. (Jozef Stefan Institute, Ljubljana, SVN); Kutnjak, Z. (Jozef Stefan Institute, Ljubljana, SVN)

Relaxor ferroelectrics are random displacive systems such as substitutionally disordered perovskite oxides, in contrast to dipolar glasses which can be regarded as randomly diluted order-disorder type ionic solids. There are several common features in the two cases, for example, a broad temperature peak in the ac dielectric susceptibility, a splitting between the ac and the quasistatic field-cooled susceptibilites, and a broad distribution of relaxation times characterized by a Vogel-Fulcher type divergence of the longest relaxation time. A clear distinction between the above two categories can been made by comparing the characteristic temperature dependence of the NMR line shape and the associated EA order parameter. It is now widely recognized that the crucial degrees of freedom in relaxors are the so-called polar nanoregions (PNRs), which are formed at relatively high temperatures and are characterized by possessing reorientable dipole moments of variable lengths. In dipolar glasses, however, the dipoles have a fixed length and are thus analogous to magnetic spin glasses, however, with the addition of random electric fields.

It has been argued in the past that a key factor in the formation of PNRs are strong random electric fields acting on the lattice ions. Here we adopt this view in the framework of a high temperature Born-Meyer-type ionic lattice potential as a starting point towards a mesoscopic quantitative theory of relaxors. Next we show that the random fields can be exactly eliminated by a simple gauge transformation to a deformed lattice, where randomness now appears in the harmonic terms in the potential. By introducing a set of eigenvectors and eigenvalues of the harmonic potential, we initiate a coarse graining procedure leading to a set of collective modes, which are identified as PNRs. In a simplest approximation, these are described by pseudospins of variable lengths, which are restricted by a global spherical condition. In this representation, weak residual random fields acting on the PNRs may exist Thus we recover the spherical random bond-random field (SRBRF) model of relaxor ferroelectrics [1], which has been used in the past to predict a number of relaxor properties, such as the FC static susceptibility and the NMR line shape in various systems. More recently, the SRBRF model has been applied to the analysis of the heat capacity in PMN crystals and PLZT ceramics obtained by high resolution calorimetry [2].

[1] R. Pirc and R. Blinc, Phys. Rev. B **60**, 13470 (1999); R. Blinc, J. Dolinšek, A. Gregorovič, B. Zalar, C. Filipič, Z. Kutnjak, A. Levstik, and R.Pirc, Phys. Rev. Letters **83**, 424 (1999).
[2] N. Novak, R. Pirc, M. Wencka, and Z. Kutnjak, Phys. Rev. Letters **109**, 037601 (2012); N. Novak, R. Pirc, and Z. Kutnjak, Europhys. Lett. **102**, 17003 (2013).

Magnetoelectric relaxor 0.8PFN-0.2PMW

Levstik, Adrijan (Jozef Stefan Institute, Ljubljana, SVN); Filipič, Cene (Jozef Stefan Institute, Ljubljana, SVN)

Solid solution $0.8Pb(Fe_{1/2}Nb_{1/2})O_3$ - $0.2Pb(Mg_{1/2}W_{1/2})O_3$ (0.8PFN-0.2PMW) is a magnetoelectric relaxor which shows broad and frequency dependent maxima both in the electric as well as in the magnetic susceptibilities. The Vogel-Fulcher type dielectric relaxor freeze-out is accompanied by a significant magnetic anomaly demonstrating magnetoelectric coupling and thus magnetoelectric effect.

Strain induced ferroelectricity was observed directly at low temperatures in $KTaO_3$ thin films and the temperature-strain phase diagram was determined.

Replaced by

Nematic susceptibility of hole- and electron-doped $BaFe_2As_2$ iron-based Superconductors

Böhmer, Anna (Karlsruhe Institute of Technology, Eggenstein-Leopoldshafen , GER)

Superconductivity in the Fe-based superconductors occurs when a spin-density-wave (SDW) transition of the parent compound is suppressed by either physical pressure or through chemical doping. Associated with the SDW transition is a structural transition, which breaks the four-fold symmetry of the lattice. The structural transition is thought to be driven by electronic degrees of freedom (spin and/or orbital), fluctuations of which may drive the superconducting pairing. Here, we study these fluctuations by examining the 'nematic' susceptibility, i.e. the susceptibility associated with the spin/orbital ordering over a wide temperature and doping range. The nematic susceptibility of hole-doped $Ba_{1-x}K_xFe_2As_2$ and electron-doped

$Ba(Fe_{1-x}Co_x)_2As_2$ iron-based superconductors is obtained from measurements of the elastic shear modulus using a three-point bending setup in a capacitance dilatometer. We find that nematic fluctuations, although weakened by doping, extend over the whole superconducting dome in both systems, suggesting their close tie to superconductivity. Evidence for quantum critical behavior of the nematic susceptibility is, surprisingly, only found for $Ba(Fe_{1-x}Co_x)_2As_2$, the system with the lower maximal Tc value. The high resolution of our experiment allows us to study the change of this susceptibility upon entering the superconducting state in great detail.

Broadband dielectric spectroscopy of $Ba(Zr,Ti)O_3$: dynamics of relaxors and diffuse ferroelectrics

Petzelt, Jan (Institute of Physics ASCR, Praha 8, CZE); Nuzhnyy, Dmitry (Institute of Physics ASCR, Praha 8, CZE); Bovtun, Viktor (Institute of Physics ASCR, Praha 8, CZE); Savinov, Maxim (Institute of Physics ASCR, Praha 8, CZE); Canu, Giovanna (Institute for Energetics and Interphases, NRC, Genoa, ITA); Buscaglia, Vincenzo (Institute for Energetics and Interphases, NRC, Genoa, ITA)

$Ba(Zr_xTi_{1-x})O_3$ (BZT-x) solid solution is a very attractive and intensively studied system because it is lead free, isovalent, and passes from standard ferroelectric behaviour of neat $BaTiO_3$ (x=0) over diffuse ferroelectric behaviour ($0.15<X_3$ (BZO, x=1). Dielectric responses of ceramics with x=0, 0.2, 0.4, 0.6, 0.7, 0.8, 1 were investigated from Hz frequencies up to the infrared using several techniques in a broad temperature range (10 - 700 K). In neat BZO the dielectric response is fully determined by polar phonons, the lowest-frequency one being of the Last type, unlike in $BaTiO_3$, where it is of the Slater type. On the other hand, response in BTO in a broad range around the ferroelectric transition near ~400 K is dominated by an overdamped central mode (CM) in the THz range in addition to the soft phonon mode [1]. In all the studied BZT samples the lowest-frequency phonon mode in the 100 cm^{-1} range is almost not softening and the response below room temperature is dominated by two additional CM relaxations: The higher-frequency one in the 10^{10}-10^{11} Hz range, which is not very temperature dependent, and the lower-frequency one which is slowing down from the GHz range and below room temperature it is thermally activated and broadening. At low temperatures it merges into a near-constant loss background, which decreases with increasing x. In the case of diffuse transition in BZT-0.2, the CM softens only to the GHz range near the transition temperature and below it only the near-constant loss background dominates the response below ~1 GHz. The picture of polar nanoregions in BZT differs from that in heterovalent relaxors, because they are pinned to the nanoregions of the BTO clusters (frozen in our temperature range), where from first-principle theories it follows that the Ti^{4+} ions are off-centered as in the neat BTO whereas the Zr^{4+} ions remain centered as in the neat BZO. Therefore we assign the soft CM to the hopping of the off-centered Ti^{4+} ions. The origin of the higher-frequency CM might be connected with the polar nanoregion dynamics (e.g. fluctuations of their boundaries inside the BTO nanoclusters). Unlike BTO, the dynamic instability, which is responsible for the diffuse ferroelectric and relaxor behavior in BZT, is mainly due to the hopping dynamics of the off-centered Ti^{4+} ions rather than due to the soft phonons and therefore the diffuse transition in BZT is essentially of the order-disorder type.

[1] D. Nuzhnyy, J. Petzelt, M. Savinov, T. Ostapchuk, V. Bovtun, M. Kempa, J. Hlinka, V. Buscaglia, M. T. Buscaglia, P. Nanni, *Phys. Rev.* B**86**, 014106 (2012).

Carbon-based materials I

Imaging local electronic properties of graphene

LeRoy, Brian (University of Arizona, Tucson, USA)

Scanning probe microscopy is a powerful tool to probe low-dimensional systems. The local information provided by scanning probe microscopy is invaluable for studying effects such as interactions and scattering. Using this approach, we have probed the local electronic properties of graphene.

Monolayer graphene is a single atomic sheet of carbon atoms in a honeycomb lattice. The honeycomb lattice creates a unique linear dispersion relation and the charge carriers behave as massless fermions near the Dirac point. We have studied the effect of charged impurities and the underlying substrate on the local density of states. We find that long-range scattering from charged impurities locally shifts the charge neutrality point leading to electron and hole doped regions. By using boron nitride as a substrate, we observe an improvement in the electronic properties of the graphene as well as a moire pattern due to the misalignment of the graphene and boron nitride lattices. We find that the periodic potential due to the boron nitride substrate creates a set of 6 new superlattice Dirac points in graphene. The ultraflat and clean nature of graphene on boron nitride devices allows for the observation of scattering from buried step edges, which is used to map the dispersion relation. More complicated graphene heterostructures can be created by adding additional layers or other two-dimensional materials. Our latest results with trilayer graphene and rotated bilayers will also be discussed.

Resonance behavior of defect-induced Raman modes in carbon nanotubes

Maultzsch, Janina (Technische Universitaet Berlin, Berlin, GER)

In carbon nanotubes, the well-known defect induced Raman mode (D mode) and its second-order mode (2D mode) are due to a double-resonant Raman scattering process. Because of the double resonance, the frequencies of the D and 2D modes are expected to be dispersive with the excitation wavelength, as observed in graphene and graphite as well. Although such a dispersion is readily observed in carbon nanotube ensembles, so far the D and 2D-mode dispersion of a single, chiral-index identified nanotube has not been followed over a large excitation wavelength range.

Single-tube measurements were either performed on high-quality suspended nanotubes, or on tubes where any Raman signal was assigned a priori to exclusively nanotubes being resonantly excited.

Here we show by resonance Raman scattering on chiral-index enriched carbon nanotubes that the D and 2D-mode dispersion measured in nanotube ensembles is indeed dominated by the contribution of nanotubes in resonance [1]. We observe a diameter dependence of the D and 2D modes and, dependent on the diameter range, can attribute certain components of the D and 2D modes to metallic or semiconducting nanotubes. These results solve a longstanding question about the double-resonance Raman process in carbon nanotubes and furthermore help characterizing chemically functionalized nanotubes.

Furthermore, we will present results on tip-enhanced Raman scattering on semiconductor nanostructures, giving information about strain, composition and crystal structure on the nanometer scale [2].

[1] J. Laudenbach, F. Hennrich, H. Telg, M. Kappes, and J. Maultzsch, Phys. Rev. B **87**, 165423 (2013).

[2] E. Poliani, M.R. Wagner, J.S. Reparaz, M. Mandl, M. Strassburg, X. Kong, A. Trampert, C.M. Sotomayor Torres, A. Hoffmann, and J. Maultzsch, Nano Lett. accepted, doi: 10.1021/nl401277y (2013).

Monitoring the fabrication process flow of SWCNT field effect transistors using Raman spectroscopy

Haluška, Miro (MNS ETH Zurich, Zurich, CHE); Liu, Wei (MNS ETH Zurich, Zurich, CHE); Chikkadi, Kiran (MNS ETH Zurich, Zurich, CHE); Suess, Tobias (MNS ETH Zurich, Zurich, CHE); Muoth, Matthias (MNS ETH Zurich, Zurich, CHE); Hierold, Christofer (MNS ETH Zurich, Zurich, CHE)

Field effect transistors (FETs) utilizing individual single-walled carbon nanotubes (SWCNTs) as active channels may be used for different sensor applications, for example for low power consumable chemical sensors for NO2 detection [1, 2, 3]. For a successful and reliable implementation of SWCNTs in future devices, some bottlenecks still remain to be solved. One of them is the fact that the electrical characteristics of carbon nanotube FETs (CNFETs) exhibit uncontrollable variations that cannot be explained solely by the different properties of the incorporated SWCNTs. The individual fabrication steps can also affect the CNFET characteristics by altering the nanotube properties and/or interfaces between the nanotube, metal and substrate, respectively. In this work, we focus on the identification of fabrication steps affecting the properties of SWCNTs and CNFETs. Changes in the SWCNT properties and the final CNFET characteristics were monitored by Raman spectroscopy and electrical measurements, respectively.

SWCNTs for CNFETs were synthesized on Si/SiO_2 substrates from ferritin-based Fe catalyst nanoparticles [4] by LPCVD at 850°C in CH_4/H_2 [5]. As-grown SWCNTs were electrically contacted by using either standard photo or electron-beam lithography. Each CNFET consists of Cr/Au source and drain electrodes connected by a SWCNT and a back gate electrode formed by a highly p-doped Si substrate. The chip on which the CNFET devices have been fabricated was completely passivated by an Al_2O_3 film formed by atomic layer deposition immediately after metal contact deposition. Finally, windows were etched into the passivation film to expose the SWCNTs to the gas environment, while the metal-nanotube contact areas remained passivated [2].

The presence of carbonaceous impurity clusters was detected by Raman spectroscopy after lithographic processes had been applied. The Raman spectra of the clusters have two characteristic peaks with similar intensities and maxima around 1340 and 1600 cm^{-1} measured with a 532 nm excitation laser line. We attribute the origin of these carbonaceous clusters to photoresist residues remaining on the chip even after cleaning with N-methyl pyrrolidone (NMP) at 80°C [6]. The clusters were often attached to SWCNTs. These impurities can increase the metal-nanotube contact resistance, broadened the hysteresis, and induce nanotube doping in an uncontrolled manner.

Another process step which influences CNFET characteristics is the etching of the sensor windows into the Al_2O_3 passivation layer on top of the SWCNTs. Raman spectra of SWCNTs in the open sensor window show shifts of the G band when compared to those from the passivated section of a nanotube.

By monitoring the CNFET gas sensor fabrication flow, we have identified some problematic fabrication steps and suggested preventing the direct exposure of the nanotubes to the resist [7, 8]. The CNFETs fabricated in this way exhibit n-type transistor characteristics with an on-state resistance from 25 to 46 kOhm. This result is an important contribution towards the fabrication of CNFET devices with reproducible characteristics.

[1] J. Kong et al., Science **287** (2000) 622.
[2] M. Mattmann et al., Appl. Phys. Lett. **94** (2009) 183502.
[3] T. Helbling et al., Nanotechnology **20** (2009) 434010.

[4] K. Chikkadi et al., Microelectronic Eng. **88** (2011) 2478.
[5] L. Durrer et al., Nanotechnology **20** (2009) 355601.
[6] L. Durrer, PhD thesis, ETH No. 18947, “Controlled Single-Walled Carbon Nanotube growth for sensing applications” (2010).
[7] S.-W. Lee et al.: 36th Int. conference on Micro and Nano Engineering(MNE), Genoa, Italy, 2010.
[8] W. Liu et al., Int. Conference on Solid-State Sensors, Actuators and Microsystems, Barcelona, Spain, 2013.

Phonons, magnons and electromagnons II

Electromagnons

Loidl, Alois (Experimental Physics V, Augsburg, GER); Schmidt, M. (University of Augsburg, Augsburg, GER); Deisenhofer, J. (University of Augsburg, Augsburg, GER)

In today's electronics ferroelectrics and ferromagnets play a key role and are used in a wide range of applications. The quest for multiferroic materials, where these two phenomena are intimately coupled is of great fundamental and technological importance. A material that is ferroelectric and ferromagnetic at room temperature certainly is the holy grail of multiferroic research and promises various applications, involving, e.g., the switching of the magnetization by electric fields. During the last decade it became clear that there exist different routes to multiferroicity, including magnetic materials with charge-order driven or spin driven mechanisms.

Electromagnons are the generic excitations of multiferroics and can be characterized as spin waves carrying dipolar weight via a strong magnetoelectric coupling. Electromagnon excitations were theoretically predicted already 40 years ago [1] and only recently were experimentally observed in spin-driven multiferroic rare-earth manganites [2]. Electromagnons constitute a fundamental new class of excitations in ferroelectric magnets. In rare-earth perovskite manganites - via strong magnetic frustration - spiral spin order is established at low temperatures, which concomitantly induces improper ferroelectric order. In the ferroelectric and magnetic phase, electromagnon excitations gain optical weight via a strong coupling to low-lying phonon modes. Theoretical models to explain character and nature of electromagnons include purely electronic processes like spin currents [3], small lattice distortions via an inverse Dzyaloshinskii-Moriya interaction [4,5] or Heisenberg exchange coupling [6].

In this talk we will discuss the recent status of experiments and theoretical modeling of the dynamics of multiferroics. We report on recent experimental observations of electromagnon excitations in different classes of multiferroics using submillimeter-wave and THz spectroscopy, we study their coupling to phonon excitations and compare with existing theoretical models. Specific attention is paid to new observations in $Eu_{1-x}Ho_xMnO_3$ [7] were polarization switching has been observed as function of temperature, but also to new systems like the triangular magnet α-$CaCr_2O_4$ [8].

[1] V. G. Baryakhtar, I. E. Chupis, Soviet Physics-Solid State **11**, 2628, 1970
[2] A. Pimenov et al., Nature Phys. **2**,, 97, 2006
[3] H. Katsura et al., Phys. Rev. Lett. **98**,, 027203, 2007
[4] M. Mostovoy, Phys. Rev. Lett. **96**,, 067601, 2006
[5] I. A. Sergienko, E. Dagotto, Phys. Rev. B **73**,, 094434, 2006
[6] R. V. Aguilar et al., Phys. Rev. Lett. **102**,, 047203, 2009
[7] Zhenyu Chen et. al., 2013, unpublished
[8] M. Schmidt et al., 2013, unpublished

Optical activity of electromagnon in multiferroic manganite

Dziom, Uladzislau (TU Wien, Wien, AUT); Pimenov, Anna (TU Wien, Wien, AUT); Pimenov, Andrei (TU Wien, Wien, AUT); Shuvaev, Alexey (TU Wien, Wien, AUT)

Theoretical models, describing properties of rare-earth manganite multiferroics, predict a magnetoelectric coupling between certain components of electric and magnetic susceptibilities. In particular geometry the coupling should lead to rotation of the plane of polarization. We have experimentally observed this optical activity in multiferroic manganite $DyMnO_3$ in frequency range 90 – 800 GHz. Dysprosium manganite undergoes transition into ferroelectric state at T=19 K. Below this temperature linearly polarized radiation passing through the sample acquires a crossed component t_c, provided ferroelectric domains are predominantly oriented along one of the two possible directions. Orientation of the predominant static polarization P determines the sign of t_c, allowing to probe the state of the sample by measuring the amplitude of the optical activity.

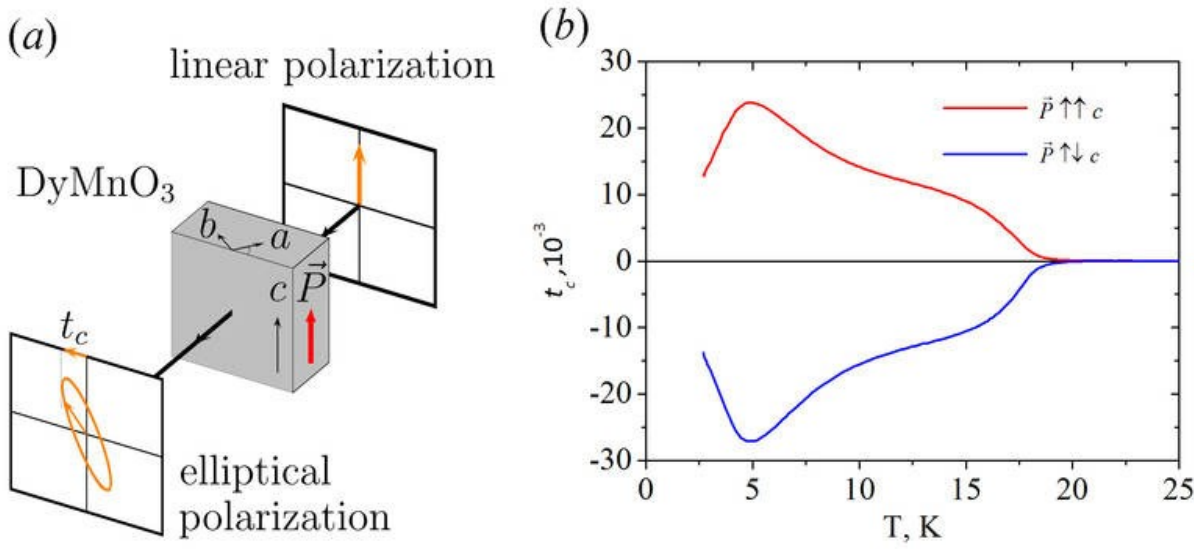

Fig. 1 (a) Mutual orientation of the sample and the incident terahertz wave, enabling the magnetoelectric coupling to cause a rotation of the polarization plane. (b) Temperature dependence of the signal in crossed polarizers at frequency 212 GHz.

THz Magnetoelectric Atomic Rotations in the Chiral Compound $Ba_3NbFe_3Si_2O_{14}$

Chaix, Laura (Institut Laue-Langevin, Grenoble Cedex 9, FRA); de Brion, Sophie (Institut Néel, CNRS and Université Joseph Fourier, Grenoble Cedex 9, FRA); Lévy-Bertrand, Florence (Institut Néel, Grenoble cedex 9, FRA); Simonet, Virginie (Institut Néel, CNRS and Université Joseph Fourier, Grenoble cedex 9, FRA); Ballou, Rafik (Institut Néel, CNRS and Université Joseph Fourier, Grenoble cedex 9, FRA); Canals, Benjamin (Institut Néel, CNRS and Université Joseph Fourier, Grenoble cedex 9, FRA); Lejay, Pascal (Institut Néel, CNRS and Université Joseph Fourier, Grenoble cedex 9, FRA); Brubach, Jean-Blaise (Synchrotron SOLEIL, Gif-sur-Yvette, FRA); Creff, Gaëlle (Synchrotron SOLEIL, Gif-sur-Yvette, FRA); Willaert, Fabrice (Synchrotron SOLEIL, Gif-sur-Yvette, FRA); Roy, Pascale (Synchrotron SOLEIL, Gif-sur-Yvette, FRA); Cano, Andres (ESRF, Grenoble , FRA)

Magneto-electric phenomena, involving cross coupling between electric and magnetic degrees of freedom, are attracting considerable attention [1]. Beyond static properties of improper multiferroism, dynamical magneto-electric effects have been identified in the form of electromagnons, i.e. magnons dressed with charges, hence excitable by an electric field [2]. Here we report experimental evidence of the dual phenomenon, that are atomic vibrations dressed with orbital currents, hence excitable by a magnetic field, which we recently found out in the chiral compound $Ba_3NbFe_3Si_2O_{14}$, by X-ray absorption THz spectroscopy [3]. $Ba_3NbFe_3Si_2O_{14}$ belongs to the family of non-centrosymmetric langasite materials. It crystallizes in the non-centrosymmetric trigonal space group P321, thus displaying a structural chirality. The only ions bearing a magnetic moment are Fe^{3+}, which are distributed over a triangular lattice of triangles in the (**a,b**) plane perpendicular to the ternary axis **c**. Below T_N=27 K, an antiferromagnetic order is stabilized with a propagation vector **k** =(0, 0, 1/7). The Fe^{3+} magnetic moments are arranged in the same triangular configuration on each triangle of an (**a,b**) plane. This ferro-chiral configuration is helically propagated along the perpendicular direction **c**. A fascinating discovery was that a single magnetic triangular chirality together with a single magnetic helical chirality is stabilized in an enantiopure single crystal [4]. Our recent investigations by X-ray absorption THz spectroscopy performed on the AILES beam line at the SOLEIL synchrotron facility evidenced three different excitations at 5 K: the first one, around 13 cm^{-1s} disappears at T_N and is assigned to a magnon. The other two, at 23 cm^{-1} and 29 cm^{-1}, persist up to four times T_N. The former is excited when the THz magnetic field is parallel to the (**a,b**) plane while the later is excited when the THz electric field is along the **c** axis. We argue that both excitations arise from a mode of atomic rotation whose magneto-electric activity unveils the occurrence of a static helical electric polarization.

[1] N. A. Spaldin and M. Fiebig, Science **309**, 391 (2005); S.-W. Cheong and M. Mostovoy, Nature Materials 6, 13 (2007)
[2] A. Pimenov, A. A. Mukhin, V. Y. Ivanov, et al., Nature Physics **2** (2006) 97 ; S. Petit, et al., Phys. Rev. Lett. **99**, 266604 (2007) ; S. Pailhès, *et al.*, Phys. Rev. B **79**, 134409 (2009).
[3] L. Chaix, S. de Brion, F. Lévy-Bertrand, V. Simonet et al., Phys. Rev. Lett. **110**, 157208 (2013)
[4] K. Marty, *et al.*, Phys. Rev. Lett., **101** (2008) 247201; K. Marty, *et al.*, Phys. Rev. B **81**, 054416.

Temperature-dependent phonons in Fe: Implications on thermodynamics and diffusion

Leitner, Michael (Technische Universität München, Garching b. München, GER); Neuhaus, Jürgen (Technische Universität München, Garching b. München, GER); Nicolaus, Karl (Technische Universität München, Garching b. München, GER); Petry, Winfried (Technische Universität München, Garching b. München, GER); Hennion, Bernard (Laboratoire Leon Brillouin, Gif-sur-Yvette CEDEX, FRA); Hiess, Arno (European Spallation Source AB, Lund, SWE)

Apart from its technological relevance, the system of pure iron is clearly also a worthwhile subject for fundamental research: At ambient pressure it crystallizes in the bcc δ structure, undergoing a transition to the fcc γ phase at decreased temperature. Very unusually, upon a further temperature lowering, it transforms martensitically back to a bcc (α-)phase, and finally develops a ferromagnetic ordering.

Here we report measurements of the phonon dispersions at various temperatures over all these phases by inelastic neutron scattering. Generally, the anharmonic effects lead to a softening of the phonons, which we describe by modelling the dispersions in terms of a Born-von Kármán model with temperature-dependent force constants (the so-called quasi-harmonic approximation).

From these parametrizations we can compute the vibrational contributions to the energy and entropy differences at the phase transitions. We find that while the latent heats arise mainly from the electronic contributions, the vibrational contributions to the entropy can not be neglected. Especially the γ ↔ δ-transition is driven mainly by the increased vibrational entropy of the open bcc high-temperature structure, in contrast to theoretical treatments that claim magnetic origins for the stability of the δ phase [1].

Additionally, we compute the temperature-dependent vacancy migration enthalpies, which are proportional to the ω-2-moment of the vibrational densities of states [2]. We find that their temperature variation can reproduce the behaviour of the self-diffusion coefficient around the ferromagnetic transition [3]. Further, we conclude that due to lattice softening, in general the parameters deduced from Arrhenius fits of diffusivities should be seen only as phenomenological quantities.

[1] H. Hasegawa and D. G. Pettifor, Phys. Rev. Lett. **50**, 130 (1983).
[2] H. R. Schober, W. Petry, and J. Trampenau, J. Phys.: Condens. Mat. **4**, 9321 (1992).
[3] M. Lübbehusen and H. Mehrer, Acta Metall. Mater. **38**, 283 (1990).

Lattice dynamics of silica polymorphs

Wehinger, Björn (European Synchrotron Radiation Facility, Grenoble, FRA)

The silica polymorphs alpha-quartz, coesite and alpha-cristobalite were investigated with particular interest on the first peak in the density of vibrational states. The combination of thermal diffuse scattering, inelastic x-ray scattering and ab initio lattice dynamics calculations was used for the study of the lattice dynamics at arbitrary momentum transfers. The recovery of the full lattice dynamics allowed for the localisation of the critical points responsible for Van Hove singularities and the attribution of their vibrational character and the topology in energy momentum space [1,2]. Quite remarkable we find that the critical points responsible for the first peak are located at the zone boundary in the case of all three silica polymorphs under investigation. The topology of the energy surface in the vicinity of the critical points is different, but despite this, the associated displacement patterns are very similar: The largest displacement is observed for oxygen. The vibration consists mainly of a tetrahedron tilt, accompanied by a small distortion. The observation has impact on the thermodynamics and atomic dynamics of glasses which are much more similar to those of crystals than previously thought [3].

[1] A. Bosak, M. Krisch, D. Chernyshov, B. Winkler, V. Milman, K. Refson, and C. Schulze-Briese. *New insights into the lattice dynamics of alpha-quartz*. Z. Kristallogr., **227**(2):8491, 2012

[2] B. Wehinger, A. Bosak, A. Chumakov, A. Mirone, A. Winkler, N. ubrovinskaia, V. Brazhkin, and T. Dyuzheva and M. Krisch. *Lattice dynamics of coesite*. J. Phys.: Condens. Matter **25**, 275401, 2013

[3] A. Chumakov, G. Monaco, A. Fontana, B. Bosak, R. Hermann, D. Bessas, B. Wehinger, A. Crichton, M. Krisch, R. Rüffer, G. Baldi, G. Carini Jr, G. D'Angelo, E. Gilioli, G. Tripodo, M. Zanatta, B. Winkler, V. Milmann, K. Refson, M. Dove, N. Dubrovinskia, L. Dubrovinsky, R. Kedig, and Y. Yue. *The role of disorder in the thermodynamics and atomic dynamics of glasses*. submitted.

Dynamics of curved surfaces. True and leaky surface waves in cylindrical cavities

Zielinski, Piotr (Institute of Physics, Cracow University of Technology and The H. Niewodniczanski Institute of Nuclear Physics PAN, Kraków, POL); Sobieszczyk, Pawel (The H. Niewodniczanski Institute of Nuclear Physics PAN, Kraków, POL)

The problem of wave propagation in cavities of different size scales is interesting in many applications starting from seismic phenomena [1] by the ultrasonic defectoscopy [2] and blood transport in arteries [3] to micro and nanopores useful in studies of molecular systems. Although the history of studies on the dynamics of cylindrical boreholes in elastic media is, for these reasons, rather long the results known till now concern mainly so called true surface waves, i.e. the excitations with infinite life times (if internal friction effects in the medium are neglected). It turns out, however, that apart from the above secular waves the cylindrical geometry gives rise to a number excitations that radiate their energy into the bulk in a fairly slow way. Such excitations are called surface leaky waves. A particularity of concave surfaces is that a part of the leaky waves are subsonic, i.e. they show real parts of frequencies below the band of bulk waves. The dynamics of the subsonic leaky waves and that of the typical supersonic leaky waves is somewhat different [4], the former being characterized by a strong reactive amplitude, whereas the latter show a maximum in the local density of states. A number of examples will be presented along with the effect of coating the surface with different layers in search for a rare phenomenon of true surface waves within bands of bulk waves [5].

[1] G. Stilke, Geophysical Prospecting, **7**, 273 (1959)
[2] N. Barshinger, J.L. Rose, I IEEE Trans. Ultrason. Ferroelectr. Freq. Control. **51**, 1547 (2004)
[3] K. Jagielska, D. Trzupek, M. Lepers, A. Pelc, and P. Zieliński, Phys. Rev. E**76**, 066304 (2007)
[4] P. Sobieszczyk and P. Zieliński, poster at this conference
[5] D. Trzupek, P. Zieliński, Phys. Rev. Lett., **103** (2009) 075504

Polarons in crystalline perfluorotetradecanoic acid monohydrate

Filipič, Cene (Jozef Stefan Institute, Ljubljana, SVN)

The ac electrical conductivity and dielectric constant of perfluorotetradecanoic acid monohydrate (PFTDA) were investigated in the frequency range from 1 Hz to 1 MHz and the temperature range from 5 K to 300 K. At temperatures below 300 K the ac conductivity and dielectric constant follow the universal dielectric response (UDR) typical of hopping or tunneling of localized charge carriers. The analysis of the temperature dependence of the UDR parameter s in terms of the theoretical model for small polarons revealed that below 300 K this mechanism governs the charge transport in PFTDA.

Shooting electronic structure movies with time-resolved photoemission

Rossnagel, Kai (University of Kiel, Kiel, GER)

The still recent development of ultrashort-pulsed photon sources operating in the extreme ultraviolet to X-ray regime, free-electron lasers (FELs) and high-harmonic-generation (HHG) sources, has opened broad avenues in the study of the dynamic properties of materials on the fundamental time scales of atomic and electronic processes. One popular possibility is to take stroboscopic diffraction patterns of molecules and crystals, thus capturing the motion of atoms in reciprocal space in real time. This is often referred to as molecular movie making. Yet equally fascinating is the idea to use the unique characteristics of FEL and HHG radiation to shoot electronic structure movies, i.e., to directly observe what the electrons are doing on the ultrafast time scale [1]. Here the method of choice is time- and angle-resolved pump-probe photoemission spectroscopy (trARPES): an intense optical laser pulse collectively excites the valence electrons in a material and the electron dynamics leading the system back to equilibrium is monitored at different time delays by measuring the kinetic energies and emission angles of photoelectrons created by an ultrashort extreme ultraviolet or X-ray probe pulse [2].

A productive test bed for the application of this novel technique can be found in correlated materials in which the interaction between electronic and lattice degrees of freedom leads to emergent behavior in the form of, e.g., superconductivity, metal-insulator transitions, lattice, charge, orbital, or spin order. The great allure of trARPES is that it combines spectral and momentum selectivity with femtosecond time resolution. It can therefore provide direct dynamical information on the electronic degrees of freedom that should, in principle, enable us to identify the dominant degrees of freedom in a correlated material via their characteristic response times and temporal signatures as well as to determine the strength and nature of the interactions between these degrees of freedom.

The goal of this talk is to show, by way of examples taken from the family of layered transition-metal dichalcogenides, that this hypothesis is indeed true. Specifically, we will show that different types of correlated insulators can be classified by trARPES in the time domain [3].

[1] K. Rossnagel, Synch. Rad. News **25:5**, 12 (2012).
[2] T. Rohwer *et al.*, Nature **471**, 490 (2011).
[3] S. Hellmann *et al.*, Nat. Commun. **3**, 1069 (2012).

Elastic and anelastic relaxations associated with phase transitions in ferroic and multiferroic perovskites

Carpenter, Michael (University of Cambridge, Cambridge, GBR)

Ferroelectric and (anti)ferromagnetic transitions are typically characterised by measurements of some effective order parameter (electric or magnetic dipole moment) and of the order parameter susceptibility (dielectric constant and magnetic susceptibility). The first represents the equilibrium state, as controlled by the first derivative of free energy with respect to the order parameter, and the second is determined by the second derivative. Their dependence on temperature and frequency, together with loss properties in dynamic measurements, combine to give detailed insights into the underlying nature and mechanisms of both phase transitions and relaxational phenomena.

The analogous properties in relation to ferroelastic aspects of ferroic and multiferroic materials are strain and elastic compliance, so that dynamic measurements of elastic and anelastic properties provide complementary information on the specific role of strain coupling and strain relaxation. An important difference, however, is that ferroelectric and (anti)ferromagnetic ordering processes are almost invariably coupled with strain so that it has a pervasive influence on most phase transitions whatever the primary driving mechanism might be. In this context, Resonant Ultrasound Spectroscopy, operating at frequencies of ~0.1-1 MHz, has provided a particularly sensitive means of investigating the strength and dynamics of strain/order parameter coupling, the susceptibility of the driving order parameter and the mobility of ferroelastic twin walls.

Some recent examples among perovskites include combined octahedral tilting and antiferromagnetic phase transitions in $KMnF_3$ [1], relaxor behaviour in $Pb(Mg_{1/3}Nb_{2/3})O_3$ [2] (PMN), relaxor/ferroelectric behaviour in $Pb(Zn_{1/3}Nb_{2/3})O_3$-$PbTiO_3$ [3] (PZN-PT) and $Pb(In_{1/2}Nb_{1/2})O_3$-$Pb(Mg_{1/3}Nb_{2/3})O_3$-$PbTiO_3$ [4] (PIN-PMN-PT), antiferromagnetic ordering in $Bi_{0.90}Nd_{0.1}FeO_3$ [5] (BNFO) and $Bi_{0.74}Ca_{0.36}FeO_{0.18}$ (BCFO), Jahn-Teller/charge order + antiferromagnetic ordering in $Pr_{0.48}Ca_{0.52}MnO_3$ [6] (PCMO), and high spin/low spin + octahedral tilting in $LaCoO_3$ [7] (LCO).

In general, improper ferroelastic ($KMnF_3$) and ferroelectric (PZN-PT, PIN-PMN-PT) transitions are accompanied by large softening of the elastic constants due to significant coupling of the order parameter with strain. Ahead of ferroelectric transitions there is generally also a substantial softening which is due to coupling of dynamical, local clustering which also gives rise to central peak effects in Raman and Brillouin spectra and which couples with acoustic modes. This is generally attributed to polar nano regions (PNR's) which can even be stable/static well into the stability field of the parent cubic phase of relaxor materials (PMN, PIN-PMN-PT, PZN-PT). In these, a likely aspect of the overall behaviour is the development of tweed microstructures. By way of sharp contrast, the coupling of magnetic ordering with strain can be weak, with a resulting and typical stiffening of the elastic constants in proportion to the square of the order parameter, rather than softening (BNFO, BCFO). In PCMO, antiferromagnetic ordering gives no detectable change in elastic properties but the effect of an applied magnetic field can be seen in the suppression of the structural phase transition associated with charge ordering. Patterns of acoustic loss are also comparably diverse. It is, in principle, possible to modify the RUS experimental set-up so as to be able to investigate the phenomological diversity of strain coupling effects under the influence of simultaneous changes in temperature, magnetic field and electric field.

[1] Carpenter et al. (2012) Phys. Rev. B **85**, 224430.
[2] Carpenter et al. (2012) J. Phys.: Cond. Matt. **24**, 045902.
[3] Farnsworth et al. (2011) Phys. Rev. B **84**, 174124.
[4] Nataf et al. (2013) J. Appl. Phys. **113**, 124102.
[5] Schiemer et al. (2012) J. Phys.: Cond. Matt. **24**, 125901.
[6] Carpenter et al. (2010) Phys. Rev. B **82**, 134123.
[7] Zhang et al. (2011) J. Phys.: Cond. Matt. **23**, 145401.

Methods beyond DFT: current status and future developments

Kresse, G (Universität Wien, Wien, AUT); Grüneis, A (Universität Wien, Wien, AUT); Booth, G (Universität Wien, Wien, AUT); Alavi, A (Universität Wien, Wien, AUT);

The properties of all materials arise largely from the quantum mechanics of their constituent electrons under the influence of the electric field of the nuclei. The solution of the underlying many-electron Schrödinger equation is a 'non-polynomial hard' problem, owing to the complex interplay of kinetic energy, electron–electron repulsion and the Pauli exclusion principle. The dominant computational method for describing such systems has been density functional theory, although the accuracy of this method is not well established for materials under i.e. extreme conditions.

Quantum-chemical methods—based on an explicit ansatz for the many-electron wavefunctions and, hence, potentially more accurate—have not been fully explored in the solid state owing to their computational complexity, which ranges from strongly exponential to high-order polynomial in system size. Here the application of an exact technique, full configuration interaction quantum Monte Carlo to a variety of real solids, is reported providing for the first time reference many-electron energies that are used to rigorously benchmark the standard hierarchy of quantum-chemical techniques, up to the 'gold standard' coupled-cluster ansatz, including single, double and perturbative triple particle–hole excitation operators [1].

We show the errors in cohesive energies predicted by this method to be small, indicating the potential of this computationally polynomial scaling technique to tackle current solid-state problems.Furthermore simpler methods that recover the important ingredients of the many electron solution, such as the random phase approximation to the correlation energy and various improvements to this method are discussed [2,3].

[1] George H. Booth, Andreas Grüneis, Georg Kresse, and Ali Alavi, *Towards an exact description of electronic wavefunctions in real solids*, Nature **493**, 365-370 (2013).
[2] J. Harl and G. Kresse, *Accurate bulk properties from approximate many-body techniques*, Phys. Rev. Lett. **103**, 056401-1 -- 4 (2009).
[3] L. Schimka, J. Harl, A. Stroppa, A. Gruneis, M. Marsman, F. Mittendorfer, and G. Kresse, *Accurate surface and adsorption energies from many-body perturbation theory*, Nature Materials **9**, 741-744 (2010).

Carbon-based materials II

Graphene and graphite intercalation compounds: dependence of the phonon dispersion on the environment

Wirtz, Ludger (University of Luxembourg, Luxembourg)

Since graphene is an atomically thin 2D material, its properties can be strongly influenced by the environment. In particular, the substrate on which it is deposited can modify the phonon and electronic dispersions. Obviously, the "mechanical" interaction via chemisorption or physisorption influences the out-of-plane phonon modes. We show that, in addition, dielectric screening by the substrate can influence the Kohn-Anomaly of the highest optical phonon branch around K via a reduction of the electron-phonon coupling. We give several examples where this influence can be seen in Raman spectra and HREELS: graphene on boron nitride [1], graphene@Ir(111) [2], the buffer layer of graphene@SiC [3].

Furthermore, we present a combined experimental/theoretical study of the Raman spectra of potassium graphite intercalation compounds. In higher stages, several layers of graphene are alternating with one intercalant layer.

The inner layers remain weakly charged and electronically decouple from the outer layers that are adjacent to the intercalant layer and consequently carry most of the charge donated by the K ions. The Raman spectra (splitting of the G-line and shift of the 2D line) can be understood through the combined effect of charge transfer and lattice expansion [4].

References:

[1] F. Forster, A. Molina-Sánchez, S. Engels, A. Epping, K. Watanabe, T. Taniguchi, L. Wirtz, C. Stampfer arXiv:1212.3993 [cond-mat.mes-hall].
[2] M. Endlich, A. Molina-Sánchez, L. Wirtz, J. Kröger, submitted (2013).
[3] F. Fromm. M.H. Oliveira Jr., A. Molina-Sánchez, M. Hundhausen, J.M.J. Lopes, H. Riechert, L. Wirtz, and T. Seyller, New J. Phys. **15**, 043031 (2013).
[4] J. Chacon-Torres, L. Wirtz, T. Pichler, submitted (2013).

Exploring low-dimensional nano-carbon materials by high-resolution microscopy

Meyer, Jannik (University of Vienna, Physics department, Boltzmanngasse 5, 1090 Vienna, Austria Jannik.Meyer@univie.ac.at)

The microscopic characterization of two-dimensional materials, and low-dimensional matter in general, poses unique challenges but also opens unique new avenues that are not available with 3-D bulk structures or on he surfaces of 3D crystals. I will discuss some of these aspects in connection with high-resolution electron microscopic studies as well as scanning probe investigations.

The study of nano-carbons and other low-atomic number materials remains a particular challenge for high resolution transmission electron microscopy (HRTEM) owing to their intrinsically low contrast and high susceptibility to radiation damage. However, the recent developments in aberration-corrected electron optics open a route to a atomically-resolved studies of these materials at reduced electron energies, below the knock-on threshold of carbon atoms in graphene. I will present insights to this class of materials from electron microscopic studies with single-light-atom precision. Static deformations, topological defects, various vacancy configurations, the two-dimensional equivalent of dislocations, grain boundaries and substitutional dopants can be analyzed and exact atomic configurations are obtained.

At the same time, the electron microscope can be used to structure and modify graphene with highest resolution and with a direct feedback. We analyzed the mechanisms behind beam-driven structural changes and demonstrate how a controlled modification, beyond the ejection of atoms, can be achieved. In addition, substitutional doping of graphene can be obtained not only via a modified synthesis but also by electron irradiation effects.

As a complementary tool of atomic-level analysis, scanning probe microscopy and in particular scanning tunneling microscopy (STM) has been extensively used for studying graphene and related materials. Very recently, free-standing membranes of graphene have been explored by STM. I will show initial results from a dual-probe STM setup where a free-standing graphene membrane is probed simultaneously from opposing sides. At the closest point, the two probes are separated only by the thickness of the graphene membrane. This allows us to probe the deformations induced by one STM probe on a free-standing membrane with an independent second probe.

References:

J. C. Meyer et al., Nano Letters **8**, 3582 (2008)

A. Chuvilin et al., New Journal of Physics **11**, 083019 (2009)

J. C. Meyer et al., Nature Materials **10**, 209 (2011)

J. Kotakoski et al., Phys. Rev. Lett. **106**, 105505 (2011)

J. Meyer et al., Phys. Rev. Lett. **108**, 196102 (2012)

F. Eder et al., Nano Letters **13**, 1934 (2013)

Superconductors

Novel magnetism in high-T_c copper oxides superconductors

Bourges, Philippe (LLB/Orphée-CEA/CNRS, Gif sur Yvette, FRA)

One of the leading issues in high-Tc superconductors is the origin of the pseudogap phase in underdoped cuprates: below a certain temperature T*, cuprates exhibit a non-metallic behaviour in the normal state. Many theories attribute the pseudogap origin to the proximity of a competing state with superconductivity, but there is a wide disagreement about the nature of this state. Using polarized elastic neutron diffraction on triple-axis spectrometers at LLB/Orphée Reactor (CEA-Saclay), we establish a novel magnetic order firstly in the $YBa_2Cu_3O_{6+x}$ (YBCO) system, only in the underdoped regime and matching the pseudogap regime [1]. We have now generalized the observation in 4 different cuprates families: the magnetic order constitutes a genuine new phase of matter rather than a mere crossover phenomenon.

The observed magnetic order can be described as a Q=0 anti-ferromagnetic (AFM) order with two opposite magnetic moments per unit cell. It breaks time-reversal symmetry but preserves the translational symmetry, and actually gives rise to magnetic scattering at the proper Bragg peaks for the orbital moment phase which was originally predicted in the circulating current theory of the pseudogap state [2]. Recent experiments in detwinned YBCO samples allow to precise more accurately the magnetic model.

Further, two excitations associated with the novel magnetic order are also observed in the monolayer system $HgBa_2CuO_{4+}$ [3]. Their intensities rise below the same temperature T* and their dispersions are weak corresponding to Ising-like excitations. These novel excitations actually mix with conventional antiferromagnetic resonant fluctuations, which points toward a unifying picture of magnetism in the cuprates that will probably require a multiband description.

*Collaborators: Lucile Mangin-Thro, Yvan Sidis (LLB-Orphée), Yuan Li (Peking University), Guichuan Yu, Mun Chan, Yangmou Li, Martin Greven (Minnesota University), Paul Steffens (ILL Grenoble). Email: mailto:philippe.bourges@cea.fr

References

[1] P. Bourges, and Y. Sidis, C. R. Physique, 12, 461, (2011); V. Balédent et al , Phys. Rev. B, **83**, 104504 (2011); Yuan Li et al, Phys. Rev. B, **84**, 224508(2011); S. De Almeida-Didry, et al, Phys. Rev. B, **86**, 020504 (2012).
[2] C.M. Varma, Phys. Rev. B, **73**, 155113, (2006).
[3] Yuan Li et al, Nature **468**, 283 (2010) ; Nature Phys. **8**, 404 (2012).v

Resonant magnetic excitations in iron-based superconductors

Park, Jitae (FRM-II, Technical University Munich, Garching, GER)

After five years of the first report on the superconductivity in iron-based materials, there is no room for any doubt that the Fe-based superconductors are a class of unconventional and high-T_c superconductivity. As other well-known unconventional superconductors such as cuprates and heavy fermions, the antiferromagnetic spin fluctuation is suggested as a source of electron pairing in the superconducting state. One of the most compelling experimental evidence for certain correlation between the magnetic fluctuations and superconductivity is the magnetic resonant mode in the spin excitation spectrum; a sharp enhancement of magnetic excitations at the antiferromagnetic wave vector and characteristic energy (below $2\Delta_{SC}$) below the superconducting transition temperature. Moreover, the magnetic resonant mode carries important information about the superconductivity, for instance, the superconducting order parameter symmetry, pairing strength, and the electronic properties of the system. In this talk, I will present the momentum, energy, and temperature dependent inelastic neutron scattering data acquired over last years on various type Fe-based superconductors and discuss about our present understanding of iron-based superconductors.

Thermodynamic study of the magneto-structural and superconducting transitions in Co-doped $BaFe_2As_2$

Meingast, Christoph (Karlsruhe Institute of Technology, 76344 Eggenstein-Leopoldshafen, GER)

Superconductivity in the Fe-based superconductors occurs when a spin-density-wave (SDW) transition of the parent compound is suppressed by either physical pressure or through chemical doping. It is therefore important to understand the nature of the SDW transition in detail. Here we present thermodynamic (heat capacity and thermal expansion) data of the electron doped Co-Ba122 system. We extract the electronic components of both the heat capacity and thermal expansion by subtracting appropriate phonon backgrounds. From these data we construct the entropy landscape (via the heat capacity) and its pressure derivative (via the thermal expansion) versus temperature and doping. We discuss how superconductivity emerges out of this entropy landscape. From the thermal expansion data we show that uniaxial pressure is proportional to doping and, thus, also an appropriate tuning parameter in this system. Further, we find that many of the features predicted to occur for a pressure-tuned quantum critical system, in which superconductivity is an emergent phase hiding the critical point, are observed in this system. The electronic/magnetic Grüneisen parameters associated with the spin-density wave and superconducting transitions further demonstrate an intimate connection between both ordering phenomena.

Mechanisms of superconductivity in strontium titanate and in a $LaAlO_3$-$SrTiO_3$ heterostructure

Devreese, Jozef T. (TQC, Universiteit Antwerpen, Antwerpen, BEL); Klimin, Serghei (TQC, Universiteit Antwerpen, Antwerpen, BEL); Tempere, Jacques (TQC, Universiteit Antwerpen, Antwerpen, BEL); van der Marel, Dirk (Université de Genève, Genève, CHE)

We study theoretically superconducting phase transitions in bulk strontium titanate and in a $LaAlO_3$-$SrTiO_3$ heterostructure using an approach based on a dielectric function formalism. The phonon-mediated electron-electron interaction is suggested to be the dominating mechanism governing the superconducting phase transition in the heterostructure. The density dependence of the critical temperature has been calculated accounting for a recent theoretical model [1] of the band structure of strontium titanate and for all phonon branches including both LO and acoustic phonons. For a $LaAlO_3$-$SrTiO_3$ heterostructure, renormalization of the optical-phonon spectra due to the interfaces is accounted for. Comparison with experimental data is discussed.

[1] D. van der Marel, J. L. M. van Mechelen, and I. I. Mazin, Phys. Rev. B **84**, 205111 (2011).

This work was supported by FWO-V projects G.0356.06, G.0370.09N, G.0180.09N, G.0365.08, the WOG WO.035.04N (Belgium).

Magnetic flux density and critical field in the intermediate state of type-I superconductors

Kozhevnikov, Vladimir (Tulsa Community College, Tulsa, USA); Wijngaarden, Rinke (VU University Amsterdam, Amsterdam, NLD); de Wit, Jesse (VU University Amsterdam, Amsterdam, NLD); Van Haesendonck, Chris (KU Leuven, Leuven, BEL)

One of the central problems of contemporary superconductivity is the magnetic structure of the vortex core and elicitation of the microscopic parameters from the parameters of the mixed state (MS) in type-II materials. A similar problem, i.e. the magnetic structure of normal (N) domains and elicitation of the microscopic parameters from parameters of the intermediate state (IS) in type-I materials, is one of the longest standing problems, which was put forward by Peierls, F. London and Landau in the 1930s. Due to close relationship between MS and IS, a solution of the problem for the latter should help to solve it for the former. We will report on our recent study of the IS in a pure-limit Pippard superconductor (indium film with mean free path of 11 μm) placed in a magnetic field with independently controlled in- and out-of-plane components. We relied on simultaneous magneto-optical imaging and electrical transport measurements. The least expected observation is that the magnetic flux density in N-domains can be as small as 40% of the thermodynamic critical field H_c. This fact contradicts and hence overthrows the long-standing paradigm of superconductivity (Gorter and Casimir, 1934) stating that the N-phase is unstable at a field less than H_c. We will present a new and for the first time comprehensive theoretical model of the IS which consistently describes this and all other properties of the IS. Moreover, our model, based on rigorous thermodynamics, allows for quantitative determination of the domain-wall parameter and the coherence length. We will also discuss the possible impact of our model on modeling of the magnetic structure of the vortex cores in type-II superconductors.

*Supported by NSF (DMR 0904157)

Multiferroics II

Extended magnetoelectric functionalities in improper ferroelectrics

Fiebig, Manfred (Department of Materials, ETH Zurich, Zurich, CHE)

With the rise of the magnetoelectric multiferroics as compounds uniting coupled magnetic and ferroelectric order in a single phase of a material, there is an increasing awareness of the manifold mechanisms that can promote ferroelectric order. It was stimulated by the realization that the most established form of ferroelectricity – driven by the displacement of ions away from their high-symmetry position and orbital hybridization with one of its neighbors – is generally not very favourable in compounds already displaying magnetic order. This leads to the search for alternative forms of ferroelectric order more compatible with magnetism.

Among these compounds those with so-called improper ferroelectricity are particularly interesting. In improper ferroelectrics it is not the long-range dipolar order which drives the phase transition with the emergence of the spontaneous polarization. Instead the ferroelectric order is the consequence of another type of phase transition, often of the distortive or magnetic type, which permits the simultaneous emergence of the polarization. Because of the induced nature of the ferroelectric state, it can possess properties that are not normally found in conventional, i.e. proper, ferroelectrics. For example the classical forward-growth-type needle-like ferroelectric domains may not be present if the improper spontaneous polarization is small so that a strain distribution may determine the ferroelectric domain structure.

In relation to the magnetoelectric multiferroics it was realized that these "non-ferroelectric" properties of improper ferroelectrics bear a potential for novel physical phenomena with an outreach into new device concepts. In my talk I will discuss the unusual properties of several improper ferroelectrics. The experiments I will discuss were performed by optical second harmonic generation, scanning probe microscopy, and transport experiments. In the talk I may in particular refer to: (i) Ferroelectric domain patterns controlled by magnetic order and magnetic fields in multiferroics with magnetically induced ferroelectricity. This is observed in compounds like $MnWO_4$, $TbMnO_3$, and $TbMn_2O_5$. (ii) Topologically protected domains and functional domain walls in the hexagonal RMnO system (R = Sc, Y, In, Dy – Lu). Ferroelectricity in these compounds is induced by a distortive mode in a topological phase transition. It leads to protected meeting points of the six domain states. On the one hand, this enforces unfavourable domain walls with a head-to-head meeting of the polarization at the walls which leads to a conductivity depending on the orientation of the domain walls. On the other hand, the domain patterns follow universal scaling laws of the type that are also used to describe the evolution of the early universe.

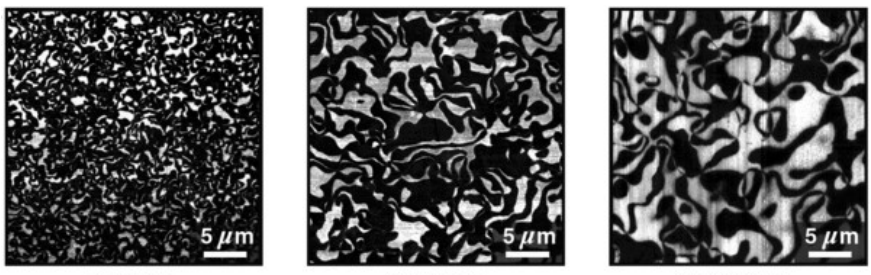

FIG.1.Improper ferroelectric domains on the z face of hexagonal $YMnO_3$ depending on the cooling rate through T_C. The density of the domain meeting points is related to universal scaling laws. See Phys. Rev. X **2**,041022 (2012).

Competing magnetic interactions and Spin-Phonon Coupling in Magnetoelectric Y-substituted $GdMnO_3$

Vilarinho Silva, Rui (IFIMUP and IN-Institute of Nanoscience and Nanotechnology, Porto, POR); Almeida, A. (IFIMUP and IN-Institute of Nanoscience and Nanotechnology, Porto, POR); Tavares, P. (Centro de Química, Vila Real, POR); Brochado Oliveira, J. (IFIMUP and IN-Institute of Nanoscience and Nanotechnology, Porto, POR); Sá, M. A. (IFIMUP and IN-Institute of Nanoscience and Nanotechnology, Porto, POR); Silva, J. M. M. (IFIMUP and IN-Institute of Nanoscience and Nanotechnology, Porto, POR); Agostinho Moreira, J. (IFIMUP and IN-Institute of Nanoscience and Nanotechnology, Porto, POR)

Magnetoelectrics are very interesting materials, as they exhibit magnetic and polar orders coupled together, opening new insights into fundamental knowledge and tailoring new multifunctional devices. Among the magnetoelectrics, some orthorhombic rare-earth manganites, with distorted perovskite structures, and general formula $RMnO_3$, with R = Eu to Dy, are the most studied [1]. In these compounds, ferroelectricity has been understood on the grounds of the inverse Dzyaloshinskii-Moriya model, where the modulated spin ordering induces lattice deformations, yielding electric polarization. The mechanisms driving the ferroelectricity in magnetic phases undoubtedly involve the interplay between spins and lattice instabilities, and thus, spin-phonon coupling. However, the existence of spin-phonon coupling is a necessary, but not sufficient condition for the existence of magnetoelectric effect, as a large number of transition metal oxides exhibit such coupling and no traces of magnetoelectricity was found.

In order to unravel the role of the spin-phonon coupling in the emergence of magnetoelectric effect, a systematic and detailed study of the lattice dynamics of several magnetoelectric materials is needed. In this scope, the aforementioned rare-earth manganites are interesting compounds, because they can be chemically modified in order to tune their physical properties, namely magnetoelectricity, through controlled lattice deformation. In these compounds, a complex interplay between spin-phonon coupling and magnetoelectricity is expected. The controlled isovalent substitution of the rare-earth ion in manganites by smaller ions, like Y^{3+}, Lu^{3+}, and Ho^{3+}, can distort the crystal lattice and the balance between competitive ferromagnetic and antiferromagnetic exchange interactions. Among the doped systems, the most studied are $Eu_{1-x}Y_xMnO_3$ and $Eu_{1-x}Lu_xMnO_3$, which exhibit a rather complex phase diagrams depending on the x-value. Another interesting system is $Gd_{1-x}Y_xMnO_3$, which has not been deeply studied.

In this work we present a detailed study of the structural, magnetic and lattice dynamic properties of Y-substituted $GdMnO_3$ ceramics ($Gd_{1-x}Y_xMnO_3$, with $0 \leq x \leq 0.4$). A thorough analysis towards the correlation between both structural and Raman modes parameters has been undertaken. Our results provide evidence for two main structural distortions of MnO_6 octahedra, arising from a cooperative Jahn-Teller and rotational distortions in these compounds. The temperature dependence of the B_{1g} symmetric stretching mode of the MnO_6 units has revealed either a positive or negative shift regarding the pure anharmonic temperature dependence of the phonon frequency, which strongly depends on the Y-concentration. This frequency renormalization is explained in terms of a competition between ferro and antiferromagnetic interactions. The relation between spin-spin correlation function, calculated from the magnetic specific heat data and the anomalous Raman mode frequency behavior is evidenced enabling the determination of the spin-phonon coupling parameter.

[1] Goto, T., Kimura, T., Lawes, G., Ramirez, a. P., & Tokura, Y., Physical Review Letters, **92**, 257201 (2004).

Neutron scattering studies on chiral multiferroics

Braden, Markus (Universität zu Köln, Köln, GER)

Neutron scattering with spherical polarization analysis is the ideal tool to analyze chiral magnetism. In multiferroics one may follow chiral components as function of temperature and electric field and thereby directly study the multiferroic hysteresis curves of chirality versus electric field [1]. In $MnWO_4$ the electric-field induced switching of chiral magnetism has been studied with a stroboscopic technique revealing remarkably slow dynamics of multiferroic domains. The time constants of the chiral switching in $MnWO_4$ are of the order of milliseconds but are strongly sample dependent. C ombining unpolarized and polarized neutron scattering studies, the frequencies and polarization patterns of magnetic excitations are determined. Evidence for an electromagnon, a hybridized phonon-magnon excitation, is obtained in $TbMnO_3$ [2] and for $MnWO_4$ and will be discussed in comparison to recent infrared reflectivity measurements. Phason-type magnetic excitations in $TbMnO_3$ are chiral for a propagation vector close to the magnetic zone centers and can be controlled by an external electric field. However, the chiral component is rapidly lost in the Brillouin zone and modes with opposed chirality are observed. $TbMnO_3$ also exhibits diffuse chiral scattering around the ferroelectric transition which can be poled by an electric field. Slightly above the ferroelectric transition in $TbMnO_3$ we find quasielastic chiral ordering without long-range order.

[1] T. Finger et al., Phys. Rev. B **81**, 054430 (2010)
[2] D. Senff et al., Phys. Rev. Lett. **98**, 137206 (2007) in collaboration with: M. Baum, S. Holbein, J. Stein, D. Senff, Th. Finger, A.C. Komarek, N. Aliouane, D. Argyriou, P. Steffens, A. Hiess, K. Schmalzl, L.P. Regnault, P. Link, K. Hradil, Y. Sidis, P. Becker- Bohatý, L. Bohatý,J. Leist, and G. Eckold

Noise and Pattern Formation in Ferroic Materials

Salje, E. K.H. (Cambridge University, Cambridge, U.K.)

Ferroic phase transitions often generate functional solids such as ferroelectrics, ferromagnets, or ferroelastics. The transition can generate micro structures whereby twinning in ferroelastics dominates also ferroelectric materials because the coupling between the ferroelectric polarization is usually very strong. The twin density can be high with distances between twin boundaries below 100nm. Twin boundaries sometimes contain functionalities which do not exist in the bulk. A typical example is ferrielectricity in twin boundaries of $CaTiO_3$ while the bulk has no polar properties. Such twin boundaries are subject to the new venture of 'Domain Boundary Engineering' where domain boundaries (and not the bulk) are the active elements of a device.

The key issue is how to form patterns which optimize the functionalities of the twin boundaries and what the dynamical behaviour of such patterns are. A first step is to optimize the boundary density which can lead to stripe domains and very mobile domain walls or totally jammed junction patterns when twin boundaries cross each other. Junctions are crossing points and determine whether the dynamic response is smooth (i.e. momentum driven) or jerky progression by avalanches). Defects and holes in porous materials eliminate the smooth movements and allow us to investigate the avalanche statistics of the evolving domain patters. The avalanche 'jerks' are then the noise in the response of such domain boundary devices and will determine the applicability of the device.

Experimental and simulation results will be presented. They show power law statistics with energy exponents near the mean field limit (1.3 - 1.8). The role of boundary conditions will be discussed.

Posters

P 1 Broad band dielectric investigation of TSCC single crystals

Mackeviciute, Ruta (Vilnius University, Vilnius, LTU); Ivanov, Maksim (Vilnius University, Vilnius, LTU); Banys, Juras (Vilnius University, Vilnius, LTU); Scott, James (Cambridge University, Cambridge, GBR)

The connection between ferroelectricity and organic molecules started in 1920 with the discovery of the first ferroelectric crystal, Rochelle salt, containing organic tartrate ions [1]. Organic ferroelectrics, such as tris-sarcosine calcium chloride (TSCC) [2] or diammonium hypodiphosphate (ADhP) [3] crystals, could be important not only for fundamental approach but also for versatile technical applications. TSCC crystal is well known organic ferroelectric which is studied more than 30 years but still is not investigated in a wide frequency range.

Dielectric measurements were performed in 110 K— 300 K temperature and 188 Hz – 46 GHz frequency range. Phase transition takes place at T_c = 129,3 K temperature and the maximum of the real part of dielectric permittivity is equal to 75. The temperature dependence of the real and imaginary parts of the dielectric permittivity could be divided into four temperature ranges: far above or below the Curie temperature ($T>>T_C$ and $T<<T_C$>) dispersion of dielectric permittivity is not observed. In the paraelectric phase close to T_C> we observe dispersion only in a high frequency range, i.e. in the gigahertz range. However, immediately below phase transition temperature we clearly observe dielectric dispersion in a wider frequency range (from 1.2 kHz to 46 GHz). Since this occurs in only the ferroelectric phase, it probably arises from domain wall dynamics.

[1] J. Valasek, Phys. Rev, 1921 Vol: 17, 475-481
[2] S. P. P. Jones, D. M. Evans, M. A. Carpenter, S. A. T. Redfern, J. F. Scott, U. Straube, V. H. Schmidt, Phys. Rev. B, 2011; **83**; 094102,
[3] P. Szklarz, M. Chanski, K. Slepokura, T. Lis, Chem. Mater, 2011; **23**; 1082-1084

P 2 Electromagnon in the hexagonal rare earth manganite $ErMnO_3$

Chaix, Laura (Institut Laue-Langevin, Grenoble , FRA); de Brion, Sophie (Institut Néel, CNRS and Université Joseph Fourier, Grenoble Cedex 9, FRA); Simonet, Virginie (Institut Néel, CNRS and Université Joseph Fourier, Grenoble Cedex 9, FRA); Lejay, Pascal (Institut Néel, CNRS and Université Joseph Fourier, Grenoble Cedex 9, FRA); Petit, Sylvain (CEA, Laboratoire Léon Brillouin, Gif-sur-Yvette, FRA); Cano, Andres (ESRF, Grenoble , FRA); Ressouche, Eric (CEA Grenoble, Grenoble , FRA); Regnault, Louis-Pierre (CEA Grenoble, Grenoble , FRA); Ollivier, Jacques (Institut Laue-Langevin, Grenoble , FRA); Ballou, Rafik (Institut Néel, CNRS and Université Joseph Fourier, Grenoble Cedex 9, FRA); Brubach, Jean-Blaise (Synchrotron SOLEIL, Gif-sur-Yvette, FRA); Willaert, Fabrice (Synchrotron SOLEIL, Gif-sur-Yvette, FRA); Roy, Pascale (Synchrotron SOLEIL, Gif-sur-Yvette, FRA)

The dynamical magneto-electric effect has been investigated so far in the form of electric-charge dressing of magnons called electromagnons, as observed recently in some multiferroics [1,2,3].

The low energy dynamical properties of the multiferroic hexagonal perovskite $ErMnO_3$ have been studied using FIR and THz spectroscopies and inelastic neutron scattering, with and without polarization analysis. These complementary spectroscopic tools have allowed us to ascribe the various observed excitations either to magnons induced by the Mn magnetic ordering, to crystal field transitions of the rare earth ions or to phonons. The $ErMnO_3$ compound is ferroelectric below T_C = 833K. A main antiferromagnetic order for the Mn^{3+} ions takes place below $T_N \approx$ 80K [4]. A complex phase diagram (magnetic field / temperature) is induced at low temperature with several transitions and spin reorientations due to the Mn-Er coupling. The dynamical spectra were obtained by measuring the THz transmission at the AILES beamline of the Synchrotron SOLEIL within a cryogenic environment. The wide-range energy [10cm^{-1} to 200cm^{-1}] combined with the natural polarization (98%) of the THz radiation allowed us measuring magnetic and structural excitations with different selection rules implying all possible geometries for the THz electric and magnetic field as regards to the crystal axis: **h//c e //b , h // b e//c** and **h** and **e** in the (**a,b**) plane .

Two intense absorption signals were detected at 6K for **h//c e // b** and **h // b e//c** around 18.5 cm^{-1} and 45 cm^{-1} respectively. Both absorptions disappear above T_N. For **h** and **e** in the (**a,b**) plane , no particular absorption was detected in this energy range. From comparison with inelastic neutron scattering and spin wave calculations, we assign the first signal to a standard magnon (**M**) whereas the signal at 45 cm^{-1} is attributed to an electromagnon (**EM**) [5].

[1] A. Pimenov, A. A. Mukhin, V. Y. Ivanov, et al., Nature Physics **2** (2006) 97.
[2] D. Senff, P. Link, K. Hradil, A. Hiess, L.P. Regnault, et al., Phys. Rev. Lett. **98**, 137206 (2007).
[3] S. Petit, F. Moussa, M. Hennion, et al., Phys. Rev. Lett. **99**, 266604 (2007) ; S. Pailhès, X. Fabrèges, L. P. Regnault, L. Pinsard-Godart, I. Mirebeau, F. Moussa, M. Hennion, and S. Petit, Phys. Rev. B **79**, 134409 (2009).
[4] M. Fiebig, C. Degenhardt, and R. V. Pisarev, Phys. Rev. Lett. **88**, 027203 (2001).
[5] L. Chaix *et al.*, in preparation.

P 3 Lattice Dynamics of Alkali Halides in the Anharmonic Regime

Kempa, Martin (Institute of Physics, ASCR Prague, Praha, CZE); Hlinka, Jirka (Institute of Physics, ASCR Prague, Praha, CZE); Marton, Pavel (Institute of Physics, ASCR Prague, Praha, CZE); Ondrejkovic, Petr (Institute of Physics, ASCR Prague, Praha, CZE)

Simple alkali halides, such as NaI or KBr, have been model examples of ionic crystals for decades, being studied both experimentally and theoretically. Recently, renewed interest in dynamics of alkali halides appeared, including incorporation of three-body interactions into the polarizable shell model [1], or a report on intrinsic localized mode in the phonon gap of NaI:Tl [2] at high temperatures.

Here we present our inelastic neutron scattering data on KBr and NaI, mainly the position and size of the energy gap in the phonon density of states in a wide range of temperatures from 10 to 700 K. The results reveal a pronounced temperature effect which effectively leads to closure of the phonon gap at temperatures in the range of 700–800 K. The results are discussed in the context of studies of possible intrinsic localized modes in the phonon gap of alkali halides. We have also attempted to induce the anharmonic lattice modes at low temperatures by UV excitation of the impurity electronic states of Tl+ substitution centers.

[1] U.C. Srivastava, R.S. Pandey, K.S. Upadayaya, Int. J. Phys. Sci. **5**, 972 (2010).
[2] M.E. Manley, A.J. Sievers, J.W. Lynn, S.A. Kiselev, N.I. Agladze, Y. Chen, A. Llobet, A. Alatas, Phys. Rev. B **79**, 134304 (2009).

P 4 Soft Mode in cubic $PbTiO_3$ observed by Hyper-Raman Scattering

Gregora, Ivan (Institute of Physics ASCR, Praha 8, CZE); Hlinka, Jirka (Institute of Physics ASCR, Praha 8, CZE); Hehlen, Bernard (LCVN, UMR CNRS 5587, Université Montpellier II, Montpellier, FRA); Kania, Antoni (University of Silesia, Katowice, POL)

The simple O_h^1(Z=1) perovskite structure of paraelectric $PbTiO_3$ has four zone centre optic modes, three F_{1u} polar modes and one F_{2u} non-polar vibration, all being triply degenerate. The lowest frequency F_{1u} is known to play the role of the soft mode. Hyper-Raman scattering (HRS) was used to get information on this mode from 1 K above the phase transition T_c up to ~ 930 K.

The results clearly show a single, well defined soft mode that obeys the Cochran law

$$\omega_0^2 = A\cdot(T - T_{SM}),$$

with $T_{SM} = T_C - 55$ K. The spectral response can be well modelled by a single damped harmonic oscillator: its eigenfrequency ω_0 softens down to ~17 cm^{-1} at T_C while the damping parameter (Γ) shows a very small variation with temperature. The crossover between the underdamped and overdamped regimes takes place at T_c+50 K.

It is realized that this mode is fully responsible for the Curie-Weiss behaviour of the dielectric permittivity of $PbTiO_3$ above T_c. The hyper-Raman results thus conclusively show that $PbTiO_3$ constitutes a clean example of a soft mode-driven ferroelectric system.

P 5 Strong effects of cation vacancies on the electronic and dynamical properties of FeO

Wdowik, Urszula D. (Institute of Technology, Pedagogical University, Cracow, POL); Piekarz, Przemyslaw (Institute of Nuclear Physics, Polish Academy of Sciences, Cracow, POL); Parlinski, Krzysztof (Institute of Nuclear Physics, Polish Academy of Sciences, Cracow, POL); Oles, Andrzej M. (Institute of Physics, Jagellonian University, Cracow, POL); Korecki, Józef (Institute of Catalysis and Surface Chemistry, Polish Academy of Sciences, Cracow, POL)

Electronic structure and vibrational dynamics of FeO crystal containing cation vacancies are theoretically studied within density functional theory incorporating strong local Coulomb interactions at Fe atoms.

Our investigations show a strong effect of Fe vacancies on the structural, electronic, and vibrational properties of wustite [1]. They also uncover qualitative difference between stoichiometric and defected FeO containing either 3% or 6% of cation vacancies. The insulating gap of iron oxide is reduced by about 50% due to unoccupied electronic bands introduced by trivalent Fe ions stabilized by cation vacancies. Significant changes in the electronic structure along with atomic displacements induced by cation vacancies affect strongly phonon dispersions via modified force constants, including those at atoms beyond nearest neighbors of defects. It is shown for the first time that theoretical phonon dispersions and their densities of states reproduce the results of inelastic neutron and nuclear resonant inelastic x-ray scattering experiments [2,3] only when Fe vacancies and Coulomb interaction are both included explicitly in *ab initio* simulations.

[1] U. D. Wdowik, P. Piekarz, K. Parlinski, A. M. Oleś, and J. Korecki, Phys. Rev. B **87**, 121106(R) (2013).
[2] G. Kugel, C. Carabatos, B. Hennion, B. Prevot, A. Revcolevschi, and D. Tocchetti, Phys. Rev. B **16**, 378 (1977).
[3] V. V. Struzhkin, H. K. Mao, J. Hu, M. Schwoerer-Bohning, J. Shu, R.J. Hemley, W. Sturhahn, M. Y. Hu, E. E. Alp, P. Eng, and G. Shen, Phys. Rev. Lett. **87**, 255501 (2001).

P 6 Surface wave propagation in systems showing true surface waves and surface resonances

Sobieszczyk, Pawel (Instytut Fizyki Jadrowej, Kraków, POL); Zielinski, Piotr (Instytut Fizyki Jadrowej, Kraków, POL)

A model consisting of a string embedded in an elastic medium and terminated by a harmonic oscillator is studied in the frequency and time domains to elucidate the physical effects of supersonic and subsonic leaky waves as well as that of true surface waves. A supersonic leaky wave manifests itself by a resonant maximum of the local density of states within the band of bulk waves and by an anomalous dispersion of the real part of the frequency dependent response function. The time domain impulse response then contains mainly resonant contribution from the poles of the response function in analogy to ordinary resonances. True surface waves show generally analogous behaviour. Here, however, the phenomenon is governed by dissipation mechanisms different from the radiation into the bulk. An important difference is that the impulse response contains equilibrated contributions due to the poles and due to the stop frequency gap in the case of true surface waves. The main manifestation of a subsonic leaky wave, i.e. a surface resonance with the frequency situated in the stop gap, is a sharp peak of the real part of the frequency-dependent response function just at the bottom of the bulk waves band. This is in certain analogy with a large reactive power in electric circuits. A strong destructive interference of the resonant part of the impulse response with the part due to the gap makes the time domain response fast attenuated. Similar but more rich phenomena occur at curved surfaces, e.g. on inner side of cylindrical cavity in an elastic medium. Local densities of states and the analogues of the reactive power will be shown in cases of practical interest in macroscopic and mesoscopic physics

P 7 Nematic susceptibility of hole- and electron-doped $BaFe_2As_2$ iron-based Superconductors

Böhmer, Anna (Karlsruhe Institute of Technology, Eggenstein-Leopoldshafen , GER)

Superconductivity in the Fe-based superconductors occurs when a spin-density-wave (SDW) transition of the parent compound is suppressed by either physical pressure or through chemical doping. Associated with the SDW transition is a structural transition, which breaks the four-fold symmetry of the lattice. The structural transition is thought to be driven by electronic degrees of freedom (spin and/or orbital), fluctuations of which may drive the superconducting pairing. Here, we study these fluctuations by examining the 'nematic' susceptibility, i.e. the susceptibility associated with the spin/orbital ordering over a wide temperature and doping range. The nematic susceptibility of hole-doped $Ba_{1-x}K_xFe_2As_2$ and electron-doped $Ba(Fe_{1-x}Co_x)_2As_2$ iron-based superconductors is obtained from measurements of the elastic shear modulus using a three-point bending setup in a capacitance dilatometer. We find that nematic fluctuations, although weakened by doping, extend over the whole superconducting dome in both systems, suggesting their close tie to superconductivity. Evidence for quantum critical behavior of the nematic susceptibility is, surprisingly, only found for $Ba(Fe_{1-x}Co_x)_2As_2$, the system with the lower maximal Tc value. The high resolution of our experiment allows us to study the change of this susceptibility upon entering the superconducting state in great detail.

P 8 Nonlocal effect and dimensions of Cooper pairs in Pippard superconductors

Kozhevnikov, Vladimir (Tulsa Community College, Tulsa, USA); Suter, Andreas (Paul Scherrer Institute, Villigen PSI, CHE); Fritzsche, Helmut (Chalk River Laboratories, Chalk River, Ontario, CAN); Gladilin, Vladimir (Universiteit Antwerpen, Antwerpen, BEL); Volodin, Alexander (KULeuven, Leuven, BEL); Prokscha, Thomas (Paul Scherrer Institute, Villigen PSI, CHE); Morenzoni, Elvezio (Paul Scherrer Institute, Villigen PSI, CHE); Temst, Kristiaan (KULeuven, Leuven, BEL); Van Bael, Margriet (KULeuven, Leuven, BEL); Van Haesendonck, Chris (KULeuven, Leuven, BEL); Indekeu, Joseph (KULeuven, Leuven, BEL)

A core concept of superconductivity is the formation of Cooper pairs. Beside the electric charge and the magnetic moment, the pairs are characterized by the size ξ_0 (Pippard coherence length) and the effective mass m*cp = 2Zm (m is mass of electron and Z is the renormalization factor). One more key microscopic parameter is the London penetration depth $\lambda_L(T)$ associated with the number density of the pairs. Knowledge of these parameters is a matter of fundamental importance. To ensure consistency ξ_0, Z and λ_L have to be measured simultaneously. Measurements of $\lambda_L(T)$ have being conducted over more than seven decades and provided crucially important information on the nature of superconductivity. However reliable absolute values of $\lambda_L(T)$ are just starting to emerge. A way to measure Z was discovered in the 1960s; currently Z is tabulated for many classical superconductors. Contrary, there was only one attempt to directly determine ξ_0; it was even stated that ξ_0 cannot be measured. The only known way for a direct determination of ξ_0 goes through the measurement of a nonlocal electrodynamic effect, a subtle phenomenon manifesting itself in a non-exponential decay of the magnetic field inside the superconductor. We will report on our recent direct and simultaneous determination of all three key microscopic parameters in two Pippard superconductors (In and Sn). This was achieved through high-resolution measurement of the nonlocal effect combining low-energy muon spin rotation spectroscopy and polarized neutron reflectometry. We will also discuss the application of the developed methodology to unconventional superconductors.

*Supported by NSF.

P 9 Spectroscopic characterization of charge-order fluctuations in organic superconductors

Masino, Matteo (Dipartimento di Chimica - Parma University, PARMA, ITA); Girlando, Alberto (Dipartimento di Chimica - Parma University, Parma, ITA); Dressel, Martin (Physikalisches Institut, Universitat Stuttgart, Stuttgart, GER); Drichko, Natalia (Dep. of Physics and Astronomy - Johns Hopkins University, Baltimore (MD), USA)

Organic superconductors, like other new classes of superconductors, are characterized by important electronic correlations. In the phase diagram of BEDT-TTF 1/4-filled organic conductors, a charge order (CO) metal to insulator phase transition is close to the superconducting ground state, with CO fluctuations in proximity of the instabilities. Fluctuations of charge-order can lead to attractive interactions and therefore have been invoked as mediators in the pairing mechanism.

Here we present the vibrational spectra of a wide range of BEDT-TTF organic conductors, ranging from metals to CO insulators and superconductors, in order to follow the charge value per lattice site for different types of ground states.

Infrared and Raman spectra show dramatic changes by varying temperature in band intensity, position and linewidth for the modes which are strongly coupled to the electronic system. The observed spectral features, which originates from CO and fluctuations of CO, can then be analyzed on the basis of an extension of the stochastic Kubo model to account for two-state exchange modulation in infrared and Raman spectroscopy. The analysis provides a full characterization of the charge distribution in the different ground states of the phase diagram, and identifies the fluctuating regime by monitoring the fluctuations rate, i.e. the velocity of charge "jump" from one molecule to the other.

P 10 Electrostatic barriers in 4H SiC with edge defects

Jochym, Pawel (Institute of Nuclear Physics, Cracow, POL); Piekarz, Przemyslaw (Institute of Nuclear Physics, Cracow, POL); Lazewski, Jan (Institute of Nuclear Physics, Cracow, POL); Sternik, Malgorzata (Institute of Nuclear Physics, Cracow, POL); Parlinski, Krzysztof (Institute of Nuclear Physics, Cracow, POL)

SiC is a promising material with many potential and current applications from high-performance semiconductor devices to the construction of thermo-nuclear fusion reactors. Unfortunately, it is notoriously difficult to grow a single, large monocrystal without substantial defects. The dislocations in the material have large influence on electronic properties of the material - particularly they lower the break-down voltage - which is one of the most important properties of the material when used as a substrate for electronic devices.

This paper presents the results of DFT calculations for the 4H SiC with Z-axis oriented edge dislocations and reports on methods used to calculate these barriers. The obtained data shows substantial lowering of electrostatic barriers along Z-axis where the dislocations are present. The results indicate the emergence of meandering tunnel-like structures where the barriers are lower and the transport of charges may be easier. These results show the possibility of computational investigation of this type of structures, offering guidance and help to experimental research in tackling the problem of imperfections occurring in the SiC and their influence on properties of the crystal.

P 11 Optimized Fourier Monte Carlo Simulation of Solid and Hexatic Membranes

Tröster, Andreas (Vienna University of Technology, Vienna, AUT)

The elastic behavior of the flat phase of solid membranes has recently been reinvestigated extensively as a result of the current enormous interest in graphene. As the effective Hamiltonian approach first worked out by Nelson and Peliti reveals, the resulting type of problem is that of a critical system with effective long-ranged interactions, which is notoriously difficult to tackle both theoretically as well as in simulation. We present an exciting refinement of our recently developed Fourier Monte Carlo algorithm, which promises to provide a new tailor-made approach to tackle critical behavior of general lattice systems with long-range interactions. On tuning the Monte Carlo acceptance rates separately for each wavevector, we are able to drastically reduce critical slowing down and thus observe critical behavior with excellent statistical accuracy. The power of our approach is illustrated by simulations results of the flat phase of solid and hexatic membranes, for which we calculate the out-of-plane correlation function $\langle |f(q)| \rangle^2 = G(q)$ and the related mean squared displacement $\langle (\Delta f)^2 \rangle$. For the solid case, a finite size scaling analysis for $\langle (\Delta f)^2 \rangle$ gives a numerical estimate for the critical exponent η which is markedly smaller than that derived from other recent simulations. Moreover, we find no signs of "intrinsic ripples". On the contrary, we argue that the observations of such ripples in earlier simulations are due to artifacts connected to the critical slowing down and the resulting lack of convergence of these simulations.

For the hexatic case, our simulations yield evidence for a logarithmic singularity $\eta = 0_{log}$.

P 12 Simulation of thermal rectification in a carbon nanotube via molecular dynamics

Foulaadvand, Ebrahim (IPM, Tehran, IRN)

We have investigated the thermal rectification phenomenon in a single-wall mass graded carbon nanotube by molecular dynamics simulation. Second generation Brenner potential has been used to model the inter atomic carbon interaction. Fixed boundary condition has been taken into account. We compare our findings to a previous study by Alaghemandi et al which has been done with a different potential and boundary condition. The dependence of the rectification factor R on temperature, nanotube diameter and length as well as mass gradient are obtained. It is shown that by increasing the temperature, the rectification decreases whereas by increasing the other parameters namely the mass gradient, diameter and the tube length it increases.

P 13 Dielectric properties of graphite filled epoxy resin composites

Kranauskaite, Ieva (Vilnius University, Vilnius, LTU); Macutkevic, Jan (Vilnius University, Vilnius, LTU); Banys, Juras (Vilnius University, Vilnius, LTU); Celzard, Alain (IJL-UMR CNRS and LERMAB-ENSTIB, Epinal, FRA); Bellucci, Stefano (INFN-Laboratori Nazionali di Frascati, Frascati, ITA)

Polymer composites with various carbon inclusions, like single- or multi- walled carbon nanotubes, carbon black, graphite or graphene are interesting for fundamental research and very attractive for various applications due to possibility to manipulate composite properties at nanoscale. The value of dielectric permittivity and electrical conductivity of these composites could be very high close to percolation threshold. However, despite of lot of publications is a lack of deep understanding relation between carbon filler microscopic properties and composite dielectric properties [1].

In this contribution were investigated epoxy resin composites filled with various size graphite flake inclusions, namely natural graphite (diameter of the graphite flakes are d = 500 – 750 μm), coarse graphite (d = 150 – 800 μm), medium graphite (d = 44 – 75 μm), fine graphite (d = 15 – 44 μm) and exfoliated graphite . The concentration of graphite inclusions was from 0.25 to 2.0 wt. %. Dielectric investigations were performed in frequency range from 20 Hz to 1 MHz, while the temperature interval was from 100 K to 450 K, by measuring loss tangent and capacity with LCR meter (HP – 4284A). The dielectric properties of all investigated composites, except composites with exfoliated graphite, are very similar to the dielectric properties of pure resin. At temperatures close to room temperature the dielectric dispersion in these composites is mainly caused by alfa relaxation in pure epoxy resin. At higher temperatures, similarly to pure epoxy resin electrical conductivity appears. The concentration dependence of conductivity activation energy and freezing temperature will be discussed in this presentation.

This research is funded by the European Social Fund under the Global Grant measure.

E-mail : ieva.kranauskaite@ff.stud.vu.lt

[1] W. Bauhofer, J. Z. Kovacs, *Composite Science and Technology* **69**, 1486 (2009).

P 14 Non dispersive Raman bands in the D-band region for double-walled carbon nanotubes with ultrasmall diameter

Kuzmany, Hans (Universität Wien, Wien, AUT); Chernov, A. I. (Universität Wien, Wien, AUT); Shi, L. (Universität Wien, Wien, AUT); Pichler, T. (Universität Wien, Wien, AUT); Kramberger, C. (Universität Wien, Wien, AUT); Kürti, J. (Eötvös University, Budapest, HUN); Gyimesi, B. (Eötvös University, Budapest, HUN)

Non-dispersive bands have been observed in the Raman spectrum of ferrocene grown double-walled carbon nanotubes (DWCNTs) for HiPco starting material. The new bands are in the frequency region of the D band and located at 1246, 1273, and 1360 cm^{-1}. They appear with highest intensity for transformation temperatures of 800° C and are resonance enhanced for excitation with red lasers. The outgoing resonance peaks at 633 nm which coincides with the resonance of a radial breathing mode of the inner tubes at 470 cm^{-1}, corresponding either to a (6,0) or to a (4.3) tube. Since non-dispersive D bands are very unusual in carbon nanotubes, the results are discussed within two contexts. In the first model the Raman line is ascribed to a double resonance Raman process activated by the periodic perturbation which is created by the outer tubes on the lattice of the inner tubes. Such interaction has been reported for bilayer graphene to result in a non-dispersive D band. Relevant phonon frequencies and optical transitions were evaluated on the level of DFT with chiral unit cells for the tubes. Results correlate well with the observed modes and with the observed resonances. Alternatively the bands may originate from a highly stabilized polyconjugated hydrocarbon which is grown during the transformation process to DWCNTs. In this case stability up to 800 °C is necessary for the encapsulated compounds.

P 15 Critical relaxation dynamic in $DyMnO_3$ multiferroic manganite

Schiebl, Markus (Technische Universität Wien, Wien, AUT); Shuvaev, Alexey (Technische Universität Wien, Wien, AUT); Pimenov, Anna (Technische Univerität Wien, Wien, AUT); Pimenov, Andrei (Technische Universität Wien, Wien, AUT)

We present the results of detailed dielectric investigations of the relaxation dynamic of $DyMnO_3$ multiferroic manganite. By applying the temperature and magnetic field-dependent dielectric spectroscopy in the frequency range between 10^{-1}-10^6 Hz we observe several simultaneously occurring relaxation processes. These relaxations are directly connected to the paraelectric-ferroelectric phase transition and to the polarization flop of the ferroelectric spin-cycloidal plane. Critical behavior near the phase transitions have been studied in detail. In agreement with previous results, the high frequency mode is associated with multiferroic relaxation dynamics of the domain walls.

P 16 Ferroelectricity and magnetism in (Sm, Fe)-doped $PbTiO_3$ perovskite ceramics

Craciun, Floriana (CNR Istituto dei Sistemi Complessi, Area della Ricerca Roma-Tor Vergata, Rome, ITA); Dimitriu, Elena (REGO Com, SRL, Bucharest, ROU); Grigoras, Marian (National Institute of Research and Development for Technical Physics, Iasi, ROU); Lupu, Nicoleta (National Institute of Research and Development for Technical Physics, Iasi, ROU); Cernea, Marin (National Institute of Materials Physics, Bucharest, ROU)

Many single-phase multiferroics are based on ferroelectric perovskite oxides substituted on the B.site with magnetic ions while keeping the A site occupied by a cation with a stereochemically active ns^2 lone pair, like Pb or Bi. An alternative way is to let B cation ferroelectric and substitute on the A site with magnetic rare earth (R) ions with a partially filled f shell. However this gives compounds with very low temperatures for magnetic ordering. In this study we follow yet a different path, by adding also a transition element with large ionic radius, like Fe^{2+} (r = 0.92 Å) besides an R (Sm^{3+}) ion, on the A site of $PbTiO_3$ (PT) while keeping B cation ferroelectric. Since the 3d orbitals of transition elements are less localized than 4f orbitals of R ions, the superexchange interaction through O 2p orbitals will be stronger. $(Pb_{0.845}Sm_{0.08}Fe_{0.035})(Ti_{0.98}Mn_{0.02})O_3$ceramic samples have been prepared by solid state reaction. The XRD analysis confirmed the obtaining of a pure crystalline phase of tetragonal P4mm symmetry with c/a about 1.05, as compared with 1.066 of pure PT. Temperature dependence of dielectric permittivity shows a strong anomaly at 662 K at the paraelectric-ferroelectric transition, about 100 K lower than in pure PT. The phase transition becomes of second order and polarization $P(T) \sim (T-T_c)^n$ with n ~ ¼ as near a tricritical point. A broad anomaly of dielectric permittivity is found below 140 K where magnetization also increases, due to the magnetoelectric coupling between ferroelectric and magnetic states. A good spontaneous ferroelectric polarization (14 μ C/cm^2) and moderate ferromagnetism (remanent magnetization M_r ~ 2.3 emu/g) have been found at T = 80 K. Slim magnetic hysteresis loops are measured even at room temperature (M_r ~ 0.1 emu/g). The dielectric constant is 190, tan δ ~ 0.005 and the piezoelectric g_{33} constant is 25 mV x m/N.

P 17 Magnetoelastic coupling and domain reconstruction in $La_{0.7}Sr_{0.3}MnO_3$ thin films epitaxially grown on $SrTiO_3$

Mota, D. A. (IFIMUP and IN-Institute of Nanoscience and Nanotechnology, Porto, POR); Romaguera Barcelay, Y. (IFIMUP and IN-Institute of Nanoscience and Nanotechnology, Porto); Almeida, A. (IFIMUP and IN-Institute of Nanoscience and Nanotechnology, Porto, POR); Sá, P. (Centro de Física. Universidade do Minho, Braga, POR); Almeida, B. G. (Centro de Física. Universidade do Minho, Braga, POR); Figueiras, F. (Department of Physics & CICECO, Aveiro, POR); Agostinho Moreira, J. (IFIMUP and IN-Institute of Nanoscience and Nanotechnology, Porto, POR)

Spintronics studies the properties of the electron spin, with a view to improve the efficiency of electronic devices and to enrich them with new functionalities. Such a broad definition implies that the range of subjects that fall under the umbrella of spintronics is inevitably very wide [1]. Several magnetic and semiconductors materials have been used for spintronics device applications and a large variety of spintronics effects have been studied. Nevertheless, only a few years ago, the incorporation of single-phase magnetoelectric multiferroic materials in spintronics devices has been undertaken [2].

The manganites are a unique class of materials with an extremely strong coupling between three fundamental degrees of freedom: electronic, spin and lattice order [3]. Of particular interest is $La_{0.7}Sr_{0.3}MnO_3$ (LSMO), showing both a Curie temperature of 360 K and an almost full spin polarization [4].

LSMO thin films grown coherently on cubic perovskite substrates are usually subjected to not only a biaxial strain due to lattice mismatch but also a further type of distortion, namely, angular distortion (or elastic shear). This angular distortion will also induce strain in the films and relax with increasing film thickness. $SrTiO_3$ (STO) substrates may induce a biaxial strain on the growing film due to the tetragonal distortion occurring below the antiferrodistortive phase transition (T_{STO}) at 105 K.

Epitaxial LSMO thin films, with different thickness ranging from 20 nm up to 330 nm, were deposited on (100)-oriented STO substrates by pulsed laser deposition, and their structure and morphology characterized at room temperature. High resolution X-rays diffraction (HR-XRD), atomic force microscopy and scanning electron microscopy were used to analyse film orientation and texture. The topography is uniform and the grain-size takes values between 30 to 50 nm, defining sharp squared cristallites. The HR-XRD study showed that as the LSMO films thickness increases, they start to relax the strained state and recover the bulk Curie temperature value by a non-homogeneous process. Magnetic properties of the as-processed thin films were characterized with a SQUID magnetometer in the vicinity of the antiferrodistortive STO phase transition (T_{STO}). The results reveal both an abnormal behaviour in the temperature dependent magnetization M(T) below T_{STO}, and an anomaly in the magnetoresistance and electrical resistivity close to the same temperature. Up to a critical thickness, of 155 nm, an in-excess magnetization is evidenced, whose temperature dependence evolves linearly with the square of the STO order parameter. The driving force is associated with a static magnetoelastic coupling between both TiO_6 and MnO 6 octahedra. Contrarily, above to the critical thickness an in-defect magnetization is observed also evolving linearly with the square of the STO order parameter, but with an inverted slope.

This unexpected reversed behaviour can be understood within the emergence in the upper layer of the film, observed by high resolution transmission electron microscopy, of randomly oriented magnetic domain reconstruction, which is needed to relax elastic energy stored in the film. The

relative magnitude and sign of the abnormal magnetization observed below T_{STO} is apparently dependent on those two competing, mutually interacting mechanisms.

[1] Sinova, J. & Zutic, I. (2012). *New moves of the spintronics tango*. Nature Materials. **11**:368-371.
[2] Bibes, M. & Barthelemy, A. (2007). *Oxide Spintronics*. IEEE Transactions on Electron Devices. **54**(5):1003-1023.
[3] Vlasko-Vlasov, V.K. et al. (2000). *Direct Magneto-Optical Observation of a Structural Phase Transition in Thin Films of Manganites*. Physical Review Letters. **84**:2239-2242.
[4] Perna, P. *et al.* (2011). *Tailoring magnetic anisotropy in epitaxial half metallic $La_{0.7}Sr_{0.3}MnO_3$ thin films*. Journal of Applied Physics. **110**(1):013919.

P 18 Resonant Magnetic X-ray Scattering Study of $DyMn_2O_5$

Johnstone, Graeme (Technische Universität Wien, Wien, AUT)

A series of resonant magnetic x-ray scattering experiments have been performed on the magnetoelectric multiferroic $DyMn_2O_5$, with measurements in both the hard and soft x-ray regimes. Using resonant magnetic x-ray scattering, the magnetic structure of $DyMn_2O_5$ has been determined in the ferroelectric phase. The ferroelectric phase of $DyMn_2O_5$ was previously shown to have the largest polarization of all of the members of the RMn_2O_5 (where *R* is a rare earth, Y or Bi ion) series of manganites. The magnetic structure observed is similar in character to that discovered in other members of the series, but differs in the direction of the ordered moments. In $DyMn_2O_5$ the Dy and Mn moments are approximately aligned with the *b*-axis, whereas in the other members of the series, the magnetic rare earth and Mn moments are approximately aligned with the *a*-axis.

P 19 The lattice dynamics and structural phase transitions in $Ca_3Mn_2O_7$ bulk ceramics and thin films

Goian, Veronica (Institute of Physics, Czech Academy of Science, Prague, CZE); Kamba, Stanislav (Institute of Physics, Czech Academy of Science, Prague, CZE); Adamo, Carolina (Department of Materials Science and Engineering, Cornell University, Ithaca, New York, USA); Vanek, Premysl (Institute of Physics, Czech Academy of Science, Prague, CZE); Drahokoupil, Jan (Institute of Physics, Czech Academy of Science, Prague, CZE); Seiner, Hanus (Institute of Thermomechanics, AS CR, Prague, CZE); Palatinus, Lukas (Institute of Physics, Czech Academy of Science, Prague, CZE); Klementova, Mariana (Institute of Physics, Czech Academy of Science, Prague, CZE); Svatuska, Michal (Institute of Physics, Czech Academy of Science, Prague, CZE); Benedek, Nicole (Materials Science and Engineering Program, The University of Texas at Austin, Austin, USA); Schlom, Darrell (Department of Materials Science and Engineering, Cornell University, Ithaca, New York, USA)

Based on *ab initio* calculations, a new type of ferroelectric phase transition was recently proposed in $Ca_3Mn_2O_7$, which crystallizes in Ruddlesden-Popper structure.[1] The ferroelectricity in such system should be induced by freezing of two nonpolar phonons from Brillouin zone boundary. If the modes of X^+_2 and X^-_3 symmetries will freeze simultaneously, I4/mmm phase will transform directly to $A2_1am$ orthorhombic structure and the phase transition is called the hybrid improper ferroelectric phase transition. If the modes will freeze gradually, paraelectric I4/mmm phase should transform to intermediate Cmcm (X^-_3 mode freezes first) or Cmca phase (X^+_2 mode freezes first) and after freezing of the second parameters, the ferroelectric $A2_1am$ orthorhombic structure will finally appear. The same calculations have shown that in biaxially strained $Ca_3Mn_2O_7$ films, the switching of polarization by electric field should cause 180° flip of magnetic moments by reversing the octahedral tilt.[1]

The aim of this contribution is to determine whether $Ca_3Mn_2O_7$ undergoes one hybrid or two successive phase transitions. We have combined X-ray and electron diffraction with measurements of heat capacity, resonant ultrasound and infrared (IR) spectroscopy. We investigated both bulk ceramics and strained $Ca_3Mn_2O_7$ thin films deposited using reactive molecular beam epitaxy on (110)$LuAlO_3$ and (110)$YAlO_3$ substrates (compressive strain up to 1.5 %).

Our room temperature electron and X-ray diffraction studies confirm $A2_1am$ crystal structure, which could be ferroelectric, but rather high conductivity of the ceramics did not allow us to perform measurements of ferroelectric hysteresis loops or temperature dependence of radio-frequency permittivity. X-ray diffraction reveal abrupt change near 670 K, thermal expansion coefficient exhibits the structural phase transition at 690 K. IR spectra of ceramics and thin films support improper-ferroelectric character of the phase transition near the same temperature. However, resonant ultrasound spectra and XRD of ceramics revealed two phase transitions; first one near 650 K and second one near 770 K. Although the theoretically predicted hybrid ferroelectric phase transition was not confirmed, the free energy landscape in slightly strained thin films should allow the electric field switching of magnetization.

[1] N. Benedek N. and C.J. Fennie, Hybrid improper ferroelectricity: A mechanism for controllable polarization-magnetization coupling, Phys. Rev. Lett., 2011, **106**, 107204

P 20 The sequence of phase transitions in $Ca_3Mn_2O_7$: a molecular dynamics study

Etxebarria, Inigo (University of the Basque Country, Bilbao, ESP); Madariaga, Julene (University of the Basque Country, Bilbao, ESP); G. Cubero, Iván (University of the Basque Country, Bilbao, ESP); Petralanda, U. (Euskal Herriko Unibertsitatea, Bilbao, ESP); Madariaga, Gotzon (University of the Basque Country, Bilbao, ESP)

$Ca_3Mn_2O_7$ belongs to the Ruddlesden-Popper series with a succession of two $CaMnO_3$ perovskite blocks stacked along the [001] direction and separated by CaO layers. It is ferroelectric and weakly ferromagnetic in the low temperature monoclinic phase (s. g. 36, $CmC2_1$) and tetragonal at high temperatures (s. g. 139, I4/mmm). The monoclinic phase includes three main distortions with respect to the tetragonal parent phase, two rotational (X_2^+, X_3^-) and a polar one (Γ_5^-) coupled by a trilinear coupling (~ γ $X_2^+X_3^-\Gamma_5^-$) [1]. This kind of coupling has been identified in several ferroelectrics and it is considered a promising mechanism to realize a strong coupling between ferroelectricity and ferromagnetism [2]. According to TEM experiments [3] and *ab initio* calculations [1] the sequence of phase transitions is I4/mmm (139) → Cmcm (63) → $Cmc2_1$ (36). It corresponds to the freezing of the X_3^- distortion first, and at lower temperatures the X_2^+distortion becomes non-zero.

In this work, the experimental low temperature phase has been expressed in terms of symmetry-adapted modes with the aid of AMPLIMODES (www.cryst.ehu.es) [4], and only the amplitudes and polarization vectors of the three main symmetry-adapted modes ($X_2^+X_3^-$ and Γ_5^-) have been used to fit the parameters of a minimal force model: a rigid-ion scheme with only Coulomb charges and Buckingham repulsive terms. Calculations of the energy maps in the space spanned by the X_2^+, X_3^- and Γ_5^- distortions are consistent with Ref. 2 showing that the trilinear term plays a crucial role in stabilizing the monoclinic ground state of the simulated crystal. Further, molecular dynamics simulations do not seem to agree with previous works; according to our results the sequence of phase transitions should be I4/mmm (139) → Cmca (64) → $Cmc2_1$ (36). This sequence implies the freezing of the X_2^+ mode at higher temperatures than the X_3^-. The possible reasons of the discrepancy between our results and experiments are also discussed.

[1] N. A. Benedek and C. J. Fennie. Phys Rev. Lett. **106**, 107204 (2011).
[2] P. Ghosez and J. M. Triscone, Nat. Mater. **10**, 269 (2011).
[3] L. Bendersky, M. Greenblatt and R. Chen, J. Solid State Chem. **174**, 418 (2003).
[4] D. Orobengoa, C. Capillas, M. I. Aroyo, and J. M. Perez-Mato, J. Appl. Cryst. **42**, 820 (2009)

P 21 Ultrasonic relaxation near phase transitions in crystals of $Sn_2P_2S_6$ family

Samulionis, Vytautas (Physics Faculty of Vilnius University, Vilnius, LTU); Banys, Juras (Physics Faculty of Vilnius University, Vilnius, LTU); Vysochanskii, Yulian (Uzhgorod University, Uzhgorod, UKR)

The crystals of $Sn_2P_2S_6$ (SPS) family are very interesting because of the large piezoelectric sensitivity, photoconductivity and ferroelectric properties what allows them to use as multifunctional materials in solid state electronics. The substitution sulphur or tin by other chemical elements in this material leads to appearance of tricritical points, incommensurate phase and the Lifshitz point providing unique possibility to investigate the dynamic critical behaviour. In this way ultrasonic studies which can characterize all kind of phase transitions are useful. The ferroelectric phase transition in SPS occurs at 337 K. At S to Se substitution phase transition temperature decreases and the incommensurate phase appears when content of selenium > 0.4. At tin by lead substitution the chemical bonds ionicity in solid solutions $(Pb_ySn_{1-y})_2P_2S_6$ increases and temperature of the ferroelectric transition rapidly decreases down – from 337 K at y = 0 till 0 K near y = 0.6, and the phase diagram becomes complicated. After substitution of two ions Sn by CuIn, AgIn and CuCr the large family of two dimension layered crystals was obtained. In these layered crystals copper electronic distribution perpendicular to the layer can be modeled by two vertically disposed Cu positions: one in centre and the other slightly shifted from octahedral centre. The incomplete occupancy of these sites induces a static or dynamic kind of disorder and it is the reason of phase transitions. $CuCrP_2S_6$ crystal is antiferroelectric below 155 K and antiferromagnetic below Neel temperature of 32 K. Here we present ultrasonic investigations of these crystals of SPS family. Ultrasonic measurements were carried out by pulse echo method in the frequency range 10-30 MHz. The temperature dependencies of longitudinal ultrasonic attenuation and velocity revealed the critical anomalies near phase transitions in these crystals and solid solutions with different content of selenium and lead. It was shown that the critical ultrasonic velocity anomalies were quite sharp and large, especially for longitudinal waves propagating along polar axis. But along this axis there is large domain scattering of ultrasonic wave and velocity dispersion related to domains, because these crystals are uniaxial ferroelectrics. Therefore directions perpendicular to polar axis b or c were chosen for precise ultrasonic velocity and attenuation measurements. The change of ultrasonic velocity at phase transition was found to be of order 20-30 %. Such large velocity changes results in large ultrasonic attenuation near the phase transitions. The critical attenuation anomaly appeared in the narrow temperature region close to the phase transition. The ultrasonic attenuation and velocity data in ferroelectric phase had been described by Landau theory including sixth order terms in free energy expansion. The order parameter relaxation time, calculated from ultrasonic data, was different depending on composition and structure of SPS crystals. Near phase transitions the variety of ultrasonic phenomena such as acoustoelectric interaction, acoustoelectric voltage, dynamic ultrasonic attenuation oscillations and photostimulated shift of phase transition down to lower temperatures were observed and investigated in these SPS family crystals.

P 22 Dielectric and impedance spectroscopy of relaxor $0.94(Na_{0.5}Bi_{0.5}TiO_3)$-$0.06BaTiO_3$ ceramics

Ivanov, Maksim (Vilnius University, Vilnius, LTU); Bucinskas, Kestutis (Vilnius University, Vilnius, LTU); Banys, Juras (Vilnius University, Vilnius, LTU); Kazakevicius, Edvardas (Vilnius University, Vilnius, LTU); Sapper, Eva (Technische Universität Darmstadt, Darmstadt, GER); Rödel, Jürgen (Technische Universität Darmstadt , Darmstadt, GER)

Ever since the discovery of piezoelectric effect, piezoelectric materials have been rapidly developed and widely used. The most widely used piezoelectric materials are relaxor $Pb(Zr,Ti)O_3$ (PZT)-based ceramics because of their superior piezoelectric properties. However due to legislative enforcements, representatively the European RoHS/WEEE regulations [1], lead-free piezoelectric materials have been extensively studied last decade. Among the studied materials, relaxor $(1-x)(Na_{0.5}Bi_{0.5}TiO_3)$-$xBaTiO_3$ ceramic family has been of particular interest because of the similar piezoelectric properties to PZT ceramics [2].

In the present work the dielectric and impedance properties of clean and 1mol% Fe doped $0.94(Na_{0.5}Bi_{0.5}TiO_3)$-$0.06BaTiO_3$ ceramics in 20Hz-1GHz frequency range and 300-1000K temperature range are investigated. The measurements of dielectric permittivity were performed during cooling cycle with 1K/min temperature variation rate. Complex resistivity was calculated using dielectric permittivity data.

Dielectric anomaly and two conductivity processes were distinguished with Arrhenius behavior of σ_{DC}. Possible cause of conductivity processes is discussed.

References

[1] Official Journal of the European Union **46** (L37) pp. 19-23 (2003).
[2] Thomas R. Shrout, Shujun J. Zhang, J. Electroceram. **19**, pp. 111-124 (2007).

P 23 Dielectric investigations of $Bi_3Gd_1Ti_3O_{12}$ ceramics

Palaimiene, Edita (Vilnius University, Vilnius, LTU); Banys, Juras (Vilnius University, Vilnius, LTU); Khomchenko, Vladimir (University of Coimbra, Coimbra, POR)

The Aurivillius phases are a class of layered bismuth oxide materials, which have attracted considerable interest due to the observation of fatigue-free behavior in thin-film nonvolatile memory applications [1].Their structure can be described as a bidimensionnal one consisting of $(Bi_2O_2)^{2+}$ layers divided by a stacking of perovskite units of composition $(A_{n-1}B_nO_{3n+1})^{2-}$ along the *c*-axis, whose bismuth titanate compounds allow the preparation of a great number of ferroelectrics materials having a high Curie temperature, a good stability of piezoelectric properties and a good resistivity vs. temperature [2]. Here we present the dielectric studies of $Bi_{4-x}Gd_xTi_3O_{12}$ – family ceramics.

Dielectric permittivity measurements of $Bi_3Gd_1Ti_3O_{12}$ ceramic was performed in the frequency range from 1 kHz to 1 MHz and in the temperature range 30 K to 1050 K. Obtained results can be divided into two parts: the low temperature part, where the glass like dispersion occurs at very low temperatures, and the high temperature part, where, especially at low frequencies, the conductivity processes dominate in the dielectric spectra (Fig.1).

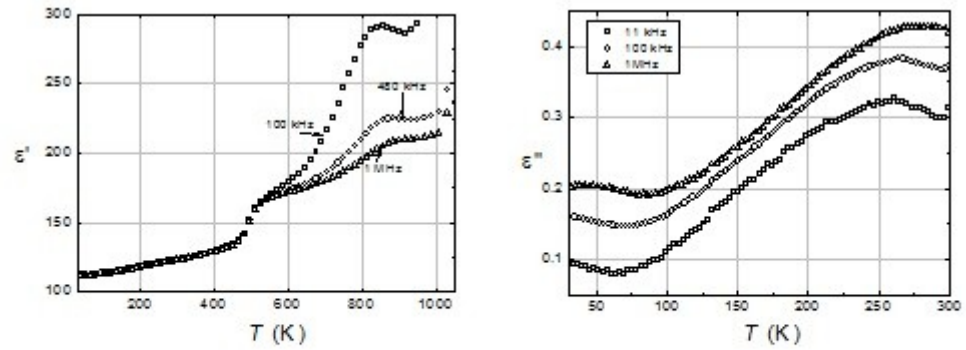

Fig. 1. Temperature dependence of the real and imaginary parts of the dielectric permittivity at different frequencies.

[1] V.A. Khomchenko et al., Effect of Gd substitution on ferroelectric and magnetic properties of $Bi_4Ti_3O_{12}$, Materials Letters **64** (2010) 1066–1068

[2] E.C. Subbarao, A family of ferroelectric bismuth compounds, J. Phys. Chem. Solids **23** (1962) 665–676

P 24 Origin of polar nano regions (PNR) in relaxor ferroelectrics: nonlinearity, discrete breather formation, and charge transfer

Bussmann-Holder, Annette (Max-Planck-Institute for Solid State Research, Stuttgart, GER)

A central issue in the physics of relaxor ferroelectrics is the origin of the formation of polar nano regions (PNR) below some characteristic temperature scale. While it is often attributed to chemical disorder, random bond – random field appearance, local symmetry lowering, it is shown here that the huge intrinsic nonlinearity of ferroelectrics gives rise to spatially limited excitations of discrete breather (DB) type, which interact strongly and self-consistently with the remaining lattice. This scenario corresponds to a two-component approach to relaxor physics with distinctive signatures in the dielectric spectra and strong charge transfer effects. The theoretical results are compared to broadband dielectric spectroscopy, which provides clear evidence for the two-component scenario and the emergence of DB like dynamics with decreasing temperature.

P 25 Cavitation in water at negative pressures

Menzl, Georg (Computergestützte Physik, AUT); Geiger, Philipp (Universität Wien, Wien, AUT); Dellago, Christoph (Universität Wien, Wien, AUT)

Water can be prepared at negative pressures in a metastable state due to the free energy penalty imposed by the cost of the interface associated with bubble nucleation. Remarkably, due to its strong surface tension, strongly negative pressures in excess of -150 MPa have been reached experimentally before the liquid broke under the mechanical tension and cavitation occurred, which has implications for many biological processes like water transport in trees. Recent interest in the topic is magnified by the discrepancy between the theoretical prediction for the cavitation pressure and the values obtained via different experimental methods [1].

While the cavitation rates at a given pressure and temperature can readily be obtained from experiment [2], the microscopic mechanism of cavitation in water and as such the underlying reason for the large deviation from theory remains unclear. Furthermore, while experimental work has to deduce the free energetics of the system from cavitation rates, the size of the critical cluster and the height of the nucleation barrier are directly accessible in simulation.

We develop a local order parameter to measure the formation of bubbles which corresponds to the change in system volume due to the presence of the bubble when compared to the metastable liquid. This definition of the order parameter coincides with the Gibbs dividing surface between the metastable bulk liquid and the bubble, yielding a thermodynamically consistent bubble volume. Using this order parameter we compute free energy barriers and the size of critical bubbles for cavitation events at various negative pressures. We subsequently analyze structural properties of the critical bubbles to obtain a microscopic picture of the transition.

In order to facilitate direct comparison between our results and experiments we compute cavitation rates at conditions where the free energy landscape of the system is comparable to experiments.

[1] F. Caupin, E. Herbert, Comptes Rendus Physique, **7**, 1000 (2006)
[2] M. El Mekki Azouzi, C. Ramboz, J.F. Lenain, F. Caupin, Nature Physics **9**, 38 (2013)

P 26 Composites of inorganic nanoparticles and polyurea elastomers - a multiscale problem

Reinecker, Marius (University of Vienna, Vienna, AUT); Fuith, Armin (University of Vienna, Vienna, AUT); Soprunyuk, Viktor (University of Vienna, Vienna, AUT); Fally, Martin (University of Vienna, Vienna, AUT); Sánchez-Ferrer, Antoni (ETH Zurich, Zurich, CHE); Mezzenga, Raffaele (ETH Zurich, Zurich, CHE); Mrzel, Ales (J. Stefan Institute, Ljubljana, SVN); Schranz, Wilfried (University of Vienna, Vienna, AUT)

Polyurea elastomers synthesized by sol/gel chemistry [1] are quite new materials with high potential for applications. They exhibit a phase separated nanostructure [1] with rigid urea domains (hard domains) embedded in a matrix of flexible polymer chains (soft domains). Pure polyurea elastomers undergo two glass transitions [2] at T_{g1}=-65°C and T_{g2}=T_{g1}+25°C attributed to cooperative motions of molecular segments in the soft domains (T g1) and to regions of restricted mobility near the hard nanodomains (T_{g2})

We performed dynamic mechanical analysis (DMA) measurements on three different polyurea elastomers JD-4000 (M_n=4024 g/mol, d=7.3 nm), JD-2000 (M_n=1991 g/mol, d=6.4 nm) and JD-400 (M_n=428 g/mol, d=4.4 nm). It turns out that the properties of the two glass transitions can be tuned by changing the distance d between the hard domains. For the smallest distance d=4.4 nm the second glass transition at T_{g2} even vanishes. According to the so called EHM model [3] the second glass transition can only occur, if the regions of restricted mobility near the hard nanodomains overlap, i.e. when the distance between the nanodomains goes beyond a critical limit of about 5-10 nm. In this picture for the JD-400 sample the regions of restricted mobility would be too small to exhibit their own glass transition. This is in quite good agreement with the assumption of so called cooperatively rearranging regions (CRRs), which are increasing up to several nm when the glass transition is approached. The properties of polymers can also be significantly changed by incorporating nanoparticles, due to their high surface/volume ratio. Here we use nanocomposites of new polyurea elastomers filled with 0.1, 0.5 and 1 wt-% MoS_2 which opens a unique possibility to study the multiscale behavior of these materials.

Acknowledgements: The present work was performed in the frame of the COST Action MP0902 (COINAPO – Composites of Inorganic Nanotubes and Polymers). Financial support by the Austrian Science Fund (FWF) P23982-N20 is gratefully acknowledged.

[1] A. Sánchez-Ferrer, D. Rogez and P. Martinoty, Macromol. Chem. Phys. **211**,1712 (2010).
[2] A. Fuith, M. Reinecker, A. Sánchez-Ferrer, R. Mezzenga, A. Mrzel, M. Knite, I. Aulika, M. Dunce and W. Schranz, Sensors & Transducers **12**, 71 (2011).
[3] A. Eisenberg, B. Hird and R. B. Moore, Macromolecules **23**, 4098 (1990).

P 27 Dynamic phases of colloidal monolayers sliding on commensurate substrates

Hasnain, Jaffar (University of Vienna, Vienna, AUT); Jungblut, Swetlana (University of Vienna, Vienna, AUT); Dellago, Christoph (University of Vienna, Vienna, AUT)

We report on numerical simulations of a monolayer of charge-stabilized colloids driven over a substrate potential by an external DC force. Using overdamped Langevin dynamics we studied the locked-to-sliding transition for various interparticle interaction strengths as a function of the driving force. A detailed analysis of the dynamical trajectories shows that the sliding dynamics is characterized by varying degrees of correlation leading to strongly collective effects. For weak interactions, the diffusion of individual defects is responsible for the motion of the monolayer. As the interaction strength is increased, there is a continuous transition towards distinct density compression and decompression zones are responsible for the motion of the monolayer. For very strong interactions, a type of stick-slip mechanism emerges, in which the sliding of the monolayer is mediated by the propagation of collective distortion waves. Our predictions can be tested experimentally with 2D arrangements of colloidal particles exposed to periodic light fields.

P 28 Atomic dynamics of the Zr-Be metallic glass probed by inelastic x-ray scattering

Syrykh, Gennady (NRC "Kurchatov Institute", Moscow, RUS); Veligzhanin, Alexey (NRC "Kurchatov Institute", Moscow, RUS)

We report on the preliminary results of the collective dynamic investigation in Zr-Be metallic glass by an inelastic X-ray scattering (IXS). In our previous experiment [1] the dynamical structure factors S(Q,E) of Zr-Be metallic glasses have been measured by inelastic neutron scattering (INS) at IN4 spectrometer (ILL) in the range of momentum transfers,

Q = 14 – 70 nm^{-1}. The acoustic- like and optic- like dispersion relations were observed. The lack of any kinematic restrictions for IXS would permit us to access the desired region of the first pseudo-Brillouin zone (< 14nm^{-1}). The experiment was performed at ID 28 spectrometer (ESRF) at an incident photon energy of 17794 eV, using the silicon (999) setup, providing an overall energy resolution of 3 meV (FWHM). Spectra for 3 angular settings of the spectrometer arm, consisting of 9 independent analyzers, were recorded, spanning a momentum transfer region from 4 to 27 nm^{-1}. The instrumental response function was recorded by measuring the scattering from a cooled (10K) disordered sample (Plexiglas). It turned out that an elastic contribution obtained by such method, do not correspond well to the ZrBe spectra for some analyzers. In many cases the resolution functions exceed the Be-Zr spectra at low energy region (up to 10 meV) and at high energy region (beyond 35 meV). Reliable informationwas obtainedwith only threeanalyzersthat allowus to extractthe peak positionandwidth ofthe acoustic-like mode.The presence of intensity above 30 meV indicates that optic-like mode may be registered. The difficulty of the search for optic mode lies in the fact that we are looking for a weak signal on a high wing of the Lorentzian resolution function. Therefore the high-frequency tail of the instrumental response function must be measured very accurately in order to yield reliable information on the elastic contribution. The IXS results were compared with those obtained by INS. The work was supported by RFBR (project 12-02-00860-a)

The authors are very grateful to Michael Krisch and Alexei Bosak for their help with the experiment, and a useful discussion of the results.

[1] G.F. Syrykh et al.: Condens. Matter **20**, 104241 (2008).

E-mail for corresponding author: sgf@isssph.kiae.ru

P 29 Defect states in amorphous silicon nitrides: a-$Si_3N_xH_y$

Fang, Changming (University of Vienna, Vienna, AUT); Watts, Thomas (University of Vienna, Vienna, AUT); Jordan, Gerald (University of Vienna, Vienna, AUT); Marsman, Martijn (University of Vienna, Vienna, AUT); Lamers, Machteld (ECN Solar Energy, Petten, NLD); Weeber, Arthur (ECN Solar Energy, Petten, NLD); Kresse, Georg (University of Vienna, Vienna, AUT); Hintzsche, Leif Eric (University of Vienna, Vienna, AUT)

Amorphous silicon nitrides are commonly deposited as passivation layers on Si based solar cells with their stoichiometries depending mainly on the applied deposition process. By using ab initio molecular dynamics simulations, we investigated important structural and electronic properties, such as atomic coordination and electronic defect states, for different silicon nitride stoichiometries. We found two dominant defect classes in silicon nitrides: (a) under-coordinated Si atoms and (b) states localized on Si-Si bonds. Furthermore, we observed that in sub-stoichiometric silicon nitrides, percolation networks with longer Si chains lead to a considerable number of delocalized defect states in the band gap. While hydrogen can passivate under-coordinated Si atoms, electronic defects related to the latter class are hardly changed. These findings suggest that the dominant defect class also changes depending on the stoichiometry and the concentration of hydrogen.

P 30 Dielectric investigation on PVDF embedded with ferrite nanoparticles

Svirskas, Sarunas (Vilnius University, Vilnius, LTU); Seputis, Mantas (Vilnius University, Vilnius, LTU); Banys, Juras (Vilnius University, Vilnius, LTU); Martins, Pedro (Centro/Departamento de Física, Universidade do Minho, Braga, POR); Lanceros-Mendez, Senentxu (Centro/Departamento de Física, Universidade do Minho, Braga, POR)

Polyvinylidene fluoride is well known for its high piezoelectric response compared to other polymers. PVDF has several phases of which polar β phase is of huge interest for various applications [1]. Several comprehensive studies of PVDF composites with various ferroelectric materials such as barium titanate or PZT [2,3] were performed in order to further increase the electromechanical properties of PVDF. Moreover, inclusions of ferrites in the PVDF might give rise to a multiferroic state [4]. Coupled ferroelectric and ferromagnetic phenomena would be attractive for multifunctional devices.

In this work we present dielectric spectroscopy results for PVDF with inclusions of $CoFe_2O_4$ (0.01, 1 ,10 wt. %), $NiZnFe_2O_4$ (10 wt. %) and $NiFe_2O_4$ (10 wt. %). Dielectric properties were measured in 20 Hz – 1 GHz frequency range and 100 K - 380K temperature range. A comparison of the dielectric properties of these composites will be made. Also, the impact of different concentration and different inclusions to activation energy of dipoles will be discussed.

References

[1] V. Sencadas et al. J. MACROMOL. SCIE. B-Pysics Vol. 48 (3) pp. 514-525 (2009)
[2] B. Hilczer et. al. J. Non-Cryst. Solids Vol.305(1-3), pp. 167-173 (2002).
[3] S. F. Mendes, C. M. Costa, C. Caparros, V. Sencadas, S. Lanceros-Mendez, J. Mat. Sci. Vol. 47(3), pp. 1378-1388 (2012);
[4] P. Martins, C. M. Costa, G. Botelho, S. Lanceros-Mendez, J. M. Barandiaran, J. Gutierrez, Mat. Chem. and Phys., Vol. 131(3), pp. 698-705 (2012).

P 31 Low-frequency elastic properties of water confined in nanoporous materials

Soprunyuk, Viktor (University of Vienna, Vienna, AUT); Reinecker, Marius (University of Vienna, Vienna, AUT); Schranz, Wilfried (University of Vienna, Vienna, AUT)

The behaviour of water in nanopores at low temperatures is a field of current interest. In this work we investigated the phase transitions of water (freezing/melting transition and glass transition) by investigation and comparing low frequency elastic properties of the water confined in nanoporous materials with different sizes of pores. We used two types of porous samples: vycor glass (producer: Corning Inc., New York, USA) with pore size of 7 nm and gelsil glasses (producer: 4F International Co., Gainsville, FL, USA) with pore sizes of 2.6 nm and 5 nm.

The low-frequency elastic measurements were performed by the parallel plate method using a dynamical mechanical analyser - DMA 7 and a Diamond DMA (producer: Perkin Elmer Inc., USA). The measurements have been performed at cooling and heating runs with a rate of temperature 1 - 1.5 K/min. The temperature investigation region was 100 K – 275 K and the frequency range in our experiments was 0.1 – 100 Hz.

The bulk water in the pores 2.6 nm, 5 nm and 7 nm undergoes first order phase transitions at lowered temperatures (15 – 40 K) then the freezing/melting phase transitions of ambient water. The heating curves show clear hysteresis of this phase transition.

Concerning the glass transition, the obtained results show clear shifting of glass transitions to lower temperatures with decreasing pores sizes. The average activation energy calculated from the results equal ~ 46.14 +/- 0.38 kJ/mol (or 0.478 +/- 0.004 eV) in good agreement with the literature data [1].

Acknowledgements : The present work was supported by the Austrian Science Fund (FWF) P23982-N20.

[1] P.Pissis, J.Laudat, D.Daoukaki, A.Kyritsis. J. of Non-Crystaline Silods **171**, 201-207 (1994).

P 32 Nucleation and growth of cluster crystals

Leitold, Christian (Computergestützte Physik, AUT); Lechner, Wolfgang (Institute of Quantum Optics and Quantum Information, Innsbruck, AUT); Mladek, Bianca (Max F. Perutz Laboratories, Wien, AUT); Dellago, Christoph (University of Vienna, Wien, AUT)

We study the formation of cluster phases in the GEM-n system for n=4[1]. The interaction between two particles separated by a distance *r* is given by

$$u(r) = \varepsilon \exp(-r_4/\sigma_4),$$

where ε andσ determine the energy and length scale, respectively. Due to the finite value of this pair potential for zero separation between two particles, the system can form a cluster crystal. In such a crystal, at high enough densities a number of particles can sit on top of each other at one single lattice site. In addition, hopping events can occur where a single particle jumps from its cluster to an adjacent one at another lattice site. The GEM-n potential can be seen as the effective interaction of certain amphiphilic dendrimers, which are also able to form cluster crystals[2]. In our work, we investigate which microscopic mechanisms lead to the formation of such a GEM-4 cluster crystal from a supercooled liquid in the low-temperature region of the phase diagram. To achieve this goal, we apply umbrella sampling with replica exchange to calculate the free energy as a function of a number of order parameters of the system. We study both planar and spherical interfaces. We also investigate the properties of the critical nuclei of the liquid-to-fcc2 transition. Furthermore, the application of transition interface sampling, again with replica exchange[3], helps us in finding the important transition pathways taking the system from the supercooled liquid to the different cluster crystal states.

[1] Kai Zhang, P. Charbonneau and B. M. Mladek, PRL **105**, 245701 (2010)
[2] D. A. Lenz, B. M. Mladek, C. N. Likos, G. Kahl, and R. Blaak, JPCB **115** (22), 7218 (2011)
[3] P. G. Bolhuis, JCP **129**, 114108 (2008)

P 33 Investigating phase transitions of copper sulfide using a neural network potential

Singraber, Andreas (Universität Wien, Wien, AUT); Behler, Jörg (Ruhr-Universität Bochum, Bochum, GER); Dellago, Christoph (Universität Wien, Wien, AUT)

The choice of an appropriate potential for a given system is a crucial part of any molecular dynamics (MD) simulation and determines if critical parts of the true dynamics are correctly reproduced or missed. While the combination of ab initio methods and MD provides high accuracy its application is restricted to small system sizes due to computional cost. Empirical potentials available for many systems are much faster but their fixed functional form inevitably introduces inaccuracies. The recently developed neural network (NN) potential method [1] combines several positive aspects of both worlds.

In this poster we present a neural network potential for copper sulfide (Cu_2S) and show its application in a study of the superionic properties of high chalcocite. At ambient conditions the copper atoms fill fixed intersticial positions within the sulfur hexagonal sublattice of low chalcocite. Upon heating the system above 376 K the copper atoms gain high mobility while the sulfur atom positions are only slightly changed leaving their rigid crystalline structure intact. This phase transition has recently been observed in experiments using transmission electron microscopy in copper sulfide nanorods [2]. We show that our NN potential is capable of correctly reproducing an ab initio potential energy surface, which allows us to investigate the phase transition on the atomistic level with great accuracy and computational efficiency. By use of this novel potential we observed for the first time the phase transition in a simulation which is not accessible with ab initio methods due to system size and trajectory length. In addition we were able to determine diffusion constants and structural properties in good agreement with experimental data.

[1] J. Behler and M. Parrinello, Phys. Rev. Lett. **98**, 146401 (2007)
[2] H. Zheng et al., Science **333**, 206 (2011)

P 34 Techniques of estimation of electrostatic barriers in 3D

Jochym, Pawel (Institute of Nuclear Physics, Cracow, POL)

We present a 3D image analysis - based method for calculating the electrostatic barriers in the crystal. The method is based on modified basin filling algorithm with bisection search for the value of the barrier.

The method is presented using 4H SiC as an example.

P 35 Multimode finite space model for open-ended coaxial line dielectric spectroscopy

Jablonskas, Dziugas (Vilnius University, Vilnius, LTU); Lapinskas, Saulius (Vilnius University, Vilnius, LTU); Rudys, Saulius (Vilnius University, Vilnius, LTU); Ivanov, Maksim (Vilnius University, Vilnius, LTU); Banys, Juras (Vilnius University, Vilnius, LTU)

Open-ended coaxial line (OCL) methods are often used in broadband dielectric spectroscopy (DS) in frequencies of 10 MHz and higher [1]. Also, such methods are preferred in many cases, because a lot of broadband circuit analyzers contain coaxial ports, thus a complex high frequency adapters are not required, since the line type is the same. Another good thing about OCL in DS is that frequency dependence of reflectance of OCL has no resonant behavior, thus dielectric permittivity equations give unambiguous solutions. OCL method in DS can be applied assuming that OCL is immersed in free space containing sample material [2]. All these benefits verify OCL as attractive method for DS.

However, the main disadvantage of OCL method is complex mathematical model. Also, not in every real life situation free space assumption is valid, because most of the times a size of sample is no larger than 10 mm. Thus, a model with respect to finite sample size is required. Finite space model can be assumed as transmission line rather than antenna as in free space model. Electrodynamical problems of transmission lines are easier to solve, than antenna system ones. Also, the model of discrete elements is not an option, since it gives large errors in higher frequencies and it is crucial, that solution finding would not be time consuming, as it is typical flaw of digital models.

Taking into account the mentioned requirements an analytical multimode finite space model of OCL was created. The system on which the model is based, consists of coaxial line probe inside a cylindrical waveguide filled with sample material, which can be liquid matter, soft matter, powder matter, etc. The model and experimental procedure will be presented.

References

[1] F. Kremer, A. Schönhals, “Broadband Dielectric Spectroscopy”, Springer, 2003.
[2] E. C. Brudette, F. L. Cain, J. Seals *“In Vivo* Probe Measurement Technique for Determining Dielectric Properties at VHF Through Microwave Frequencies”, IEEE Trans. Microwave Theory and Tech., vol. 28, p. 414-426, 1980.

P 36 Non-destructive Measurement of Dielectric Permittivity and Magnetic Permeability of Disc Shaped Materials in Microwave Frequency Range

Rudys, Saulius (Vilnius university, Vilnius, LTU)

The aim of this work is to measure dielectric permittivity and magnetic permeability of disk-shaped magneto dielectric samples in radio frequency range using non destructive measurement methods.

Conventional magnetic permeability measurement methods like shortened coaxial cavity method [1] and partially filled coaxial line method [2] both requires using disc samples with drilled hole. First method works only up to 1GHz frequency range. As for second method, it is complicated to place sample into the line and resolve magnetic permeability when dielectric permittivity is much higher than magnetic permeability

Methods of microstrip and modified open ended coaxial line were chosen in order to measure μ and ε in desired range of values. Numerical methods were used for calculation of these properties because of parasitic capacitance and inductance on connection ports in microstrip line case and there were no full wave model in modified open ended coaxial line case. $Ba_{0.15}Sr_{0.85}Fe_{12}O_{19}$ ceramics was used to check our measurement methods. To verify dielectric permittivity measurement results obtained using microstrip technique, method of capacitor on shortened coaxial end was used

References

[1] 16454A Magnetic Material Test Fixture: http://www.home.agilent.com/en/pd-1000000509%3Aepsg%3Apro-pn-16454A/magnetic-material-test-fixture?&cc=LT&lc=eng .

[2] S-parameter method, reflection and transmission mode, coaxial tube and waveguide type dielectric constant, dielectric loss tangent, permeability, measurement system No. DPS08 , http://www.keycom.co.jp/eproducts/dps/dps8/page.html

P 37 Studies of atomic scale diffusion by x-ray photon correlation spectroscopy

Stana, Markus (Dynamik Kondensierter Systeme, Wien, AUT); Leitner, Michael (Technische Universität München, Forschungs-Neutronenquelle Heinz Maier-Leibnitz (FRM II), Garching, GER); Ross, Manuel (Universität Wien, Department of Physics, Dynamics of Condensed Systems, Wien, AUT); Sepiol, Bogdan (Universität Wien, Department of Physics, Dynamics of Condensed Systems, Wien, AUT)

Quasielastic Neutron Scattering (QNS) has proven successful in investigating diffusive dynamics at the atomic level in solid state physics. “Due to the limited resolution, however, there are lower limits for the diffusion coefficient, $D > 10^{-7}$ cm^2 s^{-1}, and for the jump rates, $T^{-1} > 10^8$ s^{-1}, respectively” [1]. There have been, of course, numerous improvements over the last decade, but QNS is in general still limited to measurements in the vicinity of the melting transition. Furthermore, because of the specific scattering cross section of neutrons, it favours selected atoms like hydrogen or lithium. The driving force of our studies in the last years was to develop a method which can study atomic motion at the fundamental level in a spectrum of solids as broad as possible. A secondary objective was to find a method with a better resolution in order to enlarge the accessible range of temperatures towards lower jump rates. This allows investigating new physics in the low temperature regime and does not imply a limitation to solids which are only stable at extremely high temperatures.

The new technique of X-ray photon correlation spectroscopy, which was developed to work on the atomic scale by our group, operates in the time regime rather than in the energy regime. Atomic scale X-ray photon correlation spectroscopy (aXPCS) is therefore not subject to the limitations mentioned above. Its resolution towards faster dynamics is only limited by the intensity of the X-ray beam and the readout time of the detector, two fields which are rapidly progressing and towards slower dynamics it is limited by the stability or rather the time of the experiment. Furthermore, there is practically no restriction to certain elements for this technique (with the limitation to elements equal to or heavier than sodium but the progress in this field is also startling fast). It should also be mentioned that aXPCS measures chemical fluctuations rather than self diffusion. With this technique it is therefore possible to investigate atomic scale diffusion in the temperature range of intermetallic phases or to study dynamics of glasses well below glass transition temperatures. The first successful aXPCS experiment was carried out only few years ago by our group [2]. This talk will give an introduction to this new technique as well as an overview of what we have been able to experimentally achieve since then, like measuring jump frequencies in the order of $T^{-1} \sim 10^{-3}$ s^{-1} in solid solutions [3] or studying diffusion mechanisms in metallic glasses [4]. Application of the aXPCS technique for dynamics in network-forming glasses will be presented in the talk by B. Sepiol during this conference.

This work was supported by the Austrian Science Fund (FWF): P22402.

[1] R. Hempelmann *Quasielastic Neutron Scattering and Solid State Diffusion,* Oxford: Clarendon (2000).
[2] M. Leitner, B. Sepiol, L.-M. Stadler, B. Pfau and G. Vogl Nature Mat. **8**, 717 (2009).
[3] M. Stana, M. Leitner, M. Ross and B. Sepiol J. Phys.: Condens. Matter **25** (2013) 065401.
[4] M. Leitner, B. Sepiol, L.-M. Stadler and B. Pfau, Phys. Rev. B **86**, 064202 (2012).

P 38 Application of holographic nanoparticle-polymer composites in neutron-optics

Klepp, J (Universität Wien, Wien, AUT); Fally, M (Universität Wien, Wien, AUT); Tomita, Y (University of Electro-Communications, Tokyo, JPN); Pruner, Ch (Universität Salzburg, Salzburg, AUT)

All neutron-optical phenomena are governed by the neutron-optical potential or, equivalently, the neutron refractive-index. Thus, an important task in the design of neutron-optical elements is structuring the neutron refractive-index of materials in an efficient way. For this purpose we use materials that are sensitive to light combined with holographic techniques to produce holographic diffraction gratings for neutron-optics. Recent experiments with holographic gratings have demonstrated that two- and three-port beam-splitters as well as free-standing film mirrors for cold and very-cold neutrons are feasible by exploiting the Pendellösung interference effect known in dynamical diffraction theory [1,2,3,4,5,6]. Holographic gratings containing superparamagnetic nanoparticles to produce business card-size neutron polarizers working in comparably low external magnetic induction are being developed [6,7]. From these advancements, novel neutron-scattering instrumentation and techniques are expected.

[1] M. Fally, J. Klepp, Y. Tomita, T. Nakamura, C. Pruner, M.A. Ellabban, R.A. Rupp, M. Bichler, I. Drevensek-Olenik, J. Kohlbrecher, H. Eckerlebe, H. Lemmel, and H. Rauch, Phys. Rev. Lett. **105**, 123904 (2010).
[2] J. Klepp, C. Pruner, M.A. Ellabban, Y. Tomita, H. Lemmel, H. Rauch, M. Fally, Nucl. Instrum. Methods Phys. Res., Sect A **634**, S59 (2011)
[3] J. Klepp, C. Pruner, Y. Tomita, C. Plonka-Spehr, P.Geltenbort, S. Ivanov, G. Manzin, K.H. Andersen, J. Kohlbrecher, M.A. Ellabban, and M. Fally, Phys. Rev. A **84**, 013621 (2011)
[4] J. Klepp, Y. Tomita, C. Pruner, J. Kohlbrecher, and M. Fally, Appl. Phys. Lett. **101**, 154104 (2012).
[5] J. Klepp, C. Pruner, Y. Tomita, K. Mitsube, P. Geltenbort, and M. Fally, Appl. Phys. Lett. **100**, 214104 (2012).
[6] J. Klepp, C. Pruner, Y. Tomita, P. Geltenbort, I. Drevensek-Olenik, S. Gyergyek, J. Kohlbrecher, M. Fally, Materials **5**, 2788 (2012).
[7] J. Klepp, I. Drevensek-Olenik, S. Gyergyek, C. Pruner, R.A. Rupp, and M. Fally, J. Phys.: Conf. Ser. **340**, 012031 (2012)

P 39 Ferroic Species Revisited

Janovec, Václav (Institute of Physics, Academy of Sciences, Prague, CZE)

The profound role of symmetry in structural phase transitions were recognized by Lev D. Landau who found that (i) different phases of a crystal are credibly specified by their symmetries expressed by corresponding groups, (ii) if at a phase transition symmetry decreases, i.e. if the symmetry group F of one (*ordered*) phase is a proper subgroup of symmetry group G of the other (*disordered*) phase,

$$G > F, \qquad (*)$$

then there exists a a quantity, called the *order parameter*, which describes quantitatively the difference between both phases. The physical nature of the order parameter allows to classify transitions into ferroelectric, ferromagnetic and others.

Subsequently, Keitsiro Aizu formulated crystallographical equivalence between group-subgroup relations (*). This enabled him to define classes of symmetrically equivalent reductions (*) which he called ***ferroic species***. Ferroic species play for structural phase transitions similar role as crystallographical point groups have for homogeneous crystals. Aizu listed 212 species for non-magnetic phase transitions and recently Litvin found all 1601 magnetic species.

It has appeared that the relation (*) determines many basic features of corresponding phase transitions and domain structures, e.g, spontaneous properties (which enable detailed classification of phase transitions and ordered phases), basic properties of domain structures (number of domain states, distinction of domains, orientation of compatible domain walls, symmetries and tensor properties of domain walls), etc. These results have general validity for all transitions belonging to each species.

We shall recapitulate the main of these advances and give references where the corresponding explicit results for all species can be found.

P 40 $LiYbF_4$: a model dipolar-coupled antiferromagnet

Kovacevic, Ivan (EPFL, Lausanne, CHE)

Rare-earth compounds continue to attract much interest owing to their unusual magnetic properties. Our recent investigations of $LiErF_4$ have revealed that while the thermal transitions appears to fall into the 2D XY/h4 universality class, the quantum phase transition is 3D [1]. We are now examining $LiYbF_4$ which is predicted to display similar properties. We are interested in trying to understand the low temperature quantum mechanical interactions. Particularly if there is evidence of dimensional reduction, as found in $LiErF_4$.

References:

[1] C. Kraemer et al, Science **336**, 1416 (2012)

Authors Index

List of participants

Almeida Abílio,
Universidade do Porto
Rua do Campo Alegre, 687, 4169-007 Porto
Portugal
amalmeid@fc.up.pt

Artemov Vasily
A.M. Prokhorov General Physics Institute RAS
Vavilov str. 38, Moscow
Russian Federation
vartemov@bk.ru

Babkevich Peter,
EPFL LQM, 1015 Lausanne
Switzerland
peter.babkevich@epfl.ch

Böhmer Anna,
Karlsruhe Institute of Technology
Hermann-von-Helmholtz-Platz 1, 76344 Eggenstein-Leopoldshafen
Germany
anna.boehmer@kit.edu

Bourges Philippe,
LLB/Orphée-CEA/CNRS
Laboratoire Léon Brillouin, 91191 Gif sur Yvette
France
philippe.bourges@cea.fr

Braden Markus
Universität zu Köln
Zülpicher Str. 7750937 Köln
Germany
braden@ph2.uni-koeln.de

Bussmann-Holder Annette,
Max-Planck-Institute FKF
D-70569 Stuttgart
Germany
a.bussmann-holder@fkf.mpg.de

Carpenter Michael,
University of Cambridge
Dept. of Earth Sciences, CB2 3EQ Cambridge
United Kingdom
mc43@esc.cam.ac.uk

Chaix Laura
Institut Laue-Langevin
6 Rue Jules Horowitz
Grenoble Cedex 9
France
chaixl@ill.fr

Cordero Francesco,
CNR-ISC Istituto dei Sistemi Complessi
Area della Ricerca di Roma - Tor Vergata,
I-00133 Roma
Italy
francesco.cordero@isc.cnr.it

Craciun Floriana,
CNR Istituto dei Sistemi Complessi, Area della Ricerca Roma-Tor Vergata
Via del Fosso del Cavaliere, 100, I-00133 Rome
Italy
floriana.craciun@isc.cnr.it

Dellago Christoph,
Computergestützte Physik
Universität Wien, 1090 Wien
Austria
christoph.dellago@univie.ac.at

Deluca Marco,
Materials Center Leoben Forschung GmbH
Roseggerstrasse 12, 8700 Leoben
Austria
marco.deluca@mcl.at

Devreese Jozef,
Universiteit Antwerpen
Campus Drie Eiken -gebouw N, BE-2610 Antwerpen-Wilrijk
Belgium
jozef.devreese@ua.ac.be

Dziom Uladzislau,
TU Wien
Wiedner Hauptstraße 8-10, 1040 Wien
Austria
dziom@ifp.tuwien.ac.at

Etxebarria Inigo,
University of the Basque Country
Fisika Aplikatua II Saila, 48080 Bilbao
Spain
inigo.etxebarria@ehu.es

Fally Martin,
Physik Funktioneller Materialien
Universität Wien, 1090 Wien
Austria
martin.fally@univie.ac.at

Fiebig Manfred,
ETH Zurich
Department of Materials, 8093 Zurich
Switzerland
manfred.fiebig@mat.ethz.ch

Filipič Cene
Jozef Stefan Institute
Jamova 39, Ljubljana
Slovenia
cene.filipic@ijs.si

Foulaadvand Ebrahim,
Department of Nanosciences
IPM, Farmaniyeh str., Tehran,
Iran
foolad@iasbs.ac.ir

Fuith Armin,
Physik Funktioneller Materialien
Universität Wien, 1090 Wien
Austria
armin.fuith@univie.ac.at

Goian Veronica,
Institute of Physics, Czech Academy of Science
Na Slovance 2, 18221 Prague
Czech Rep
goian@fzu.cz

Gregora Ivan,
Institute of Physics ASCR Prague
Na Slovance 2, 18221 Praha 8
Czech Rep
gregora@fzu.cz

Gruebel Gerhard,
DESY
Notke Strasse 85, 22607 Hamburg
Germany
gerhard.gruebel@desy.de

Guennou Mael,
CRP Gabriel Lippmann
41, rue du Brill, L-4422 Belvaux
Luxemburg
guennou@lippmann.lu

Haluška Miro
Micro and Nanosystems
ETH Zürich, CH-8092 Zürich
Switzerland
haluska@micro.mavt.ethz.ch

Hasnain Jaffar,
Computergestützte Physik
Universität Wien,
Austria
jaffar.hasnain@univie.ac.at

Hintzsche Leif Eric,
Computergestützte Materialphysik
Universität Wien, 1090 Wien
Austria
leif.eric.hintzsche@univie.ac.at

Hlinka Jiri,
Institute of Physics, Czech Acad. Sci.
Na Slovance 2, 181 21 Prague
Czech Rep
hlinka@fzu.cz

Ivanov Alexandre,
Institut Max von Laue - Paul Langevin
6, rue Jules Horowitz, 38042 Grenoble
France
aivanov@ill.fr

Ivanov Maksim,
Vilnius university
Sauletekio 9/3 817 k., 10222 Vilnius
Lithuania
maksim.ivanov@ff.vu.lt

Janovec Václav
Institute of Physics, Czech Acad. Sci.
Na Slovance 2, 181 21 Prague
Czech Republic
janovec@fzu.cz

Jochym Pawel,
Institute of Nuclear Physics
ul. Radzikowskiego 15, 31-342 Cracow
Poland
pawel.jochym@ifj.edu.pl

Johnstone Graeme,
Technische Universität Wien
Wiedner Hauptstrasse 8-10, 1040 Wien
Austria
graeme.johnstone@ifp.tuwien.ac.at

Kabelka Heinz,
Physik Funktioneller Materialien
Universität Wien, 1090 Wien
Austria
heinz.kabelka@univie.ac.at

Kamba Stanislav,
Institute of Physics, Academy of Sciences of the Czech Republic
Na Slovance 2, 18221 Prague 8
Czech Rep
kamba@fzu.cz

Kempa Martin,
Institute of Physics, ASCR Prague
Na Slovance 2, 18221 Praha
Czech Rep
kempa@fzu.cz

Kezsmarki Istvan,
Budapest University of Technology and Economics, Department of Physics
Budafoki ut 8., 1111 Budapest
Hungary
kezsmark@dept.phy.bme.hu

Klepp Jürgen,
Physik Funktioneller Materialien
Universität Wien,
Austria
juergen.klepp@univie.ac.at

Kozhevnikov Vladimir
Tulsa Community College
Tulsa 909 S. Boston Ave
U.S.A.
vladimir@itf.fys.kuleuven.be

Kovacevic Ivan,
EPFL SB ICMP LQM, 1015 Lausanne
Switzerland
ivan.kovacevic@epfl.ch

Kranauskaite Ieva,
Vilnius University
Sauletekio av. 9, III b., LT-10222 Vilnius
Lithuania
ieva.kranauskaite@ff.stud.vu.lt

Kresse Georg,
Computational Materials Physics
Universität Wien, 1090 Wien
Austria
georg.kresse@univie.ac.at

Krexner Gerhard,
Physik Funktioneller Materialien
Universität Wien, 1090 Wien
Austria
gerhard.krexner@univie.ac.at

Kuzmany Hans,
Universität Wien
Universität Wien, 1090 Wien
Austria
hans.kuzmany@univie.ac.at

Lang Wolfgang,
Elektronische Materialeigenschaften
Universität Wien, 1090 Wien
Austria
wolfgang.lang@univie.ac.at

Leitner Michael,
Technische Universität München
Forschungs-Neutronenquelle Heinz Maier-Leibnitz, 85747 Garching b. München
Germany
michael.leitner@frm2.tum.de

Leitold Christian,
Computergestützte Physik
Universität Wien,
Austria
christian.leitold@univie.ac.at

LeRoy Brian,
University of Arizona
1118 E. 4th St., 85721 Tucson
Ud States of Am
leroy@physics.arizona.edu

Levstik Adrijan
Jozef Stefan Institute
Jamova 39, Ljubljana
Slovenia
adrijan.levstik@ijs.si

Loidl Alois,
University of Augsburg
Center for Electronic Correlations and Magnetism, 86135 Augsburg
Germany
alois.loidl@physik.uni-augsburg.de

Mackeviciute Ruta,
Vilnius University
Sauletekio al. 9, IIIb, 817, LT-10222 Vilnius
Lithuania
ruta.mackeviciute@ff.vu.lt

Maultzsch Janina,
Technische Universität Berlin
Hardenbergstr. 36, 10623 Berlin
Germany
janina.maultzsch@physik.tu-berlin.de

Meingast Christoph,
Karlsruhe Institute of Technology
Hermann-von-Helmholtz-Platz 1, 76344
76344 Eggenstein-Leopoldshafen
Germany
christoph.meingast@kit.edu

Menzl Georg,
Computergestützte Physik
Universität Wien,
Austria
georg.menzl@univie.ac.at

Meyer Jannik C.,
Physik Nanostrukturierter Materialien
Universität Wien, 1090 Wien
Austria
jannik.meyer@univie.ac.at

Michel Karl-H.,
University of Antwerp
CMTPhysics Groenenborgerlaan 171, B-2020 Antwerp
Belgium
ktdm@skynet.be

Miletich-Pawliczek Ronald
Universität Wien
Institut für Mineralogie und Kristallographie
A-1090 Wien, Althanstrasse 14 (UZAII)
Austria
ronald.miletich-pawliczek@univie.ac.at

Moreira Joaquim,
Universidade do Porto
Departamento de Física e Astronomia, 4169-007 Porto
Portugal
jamoreir@fc.up.pt

Mota D. A.,
IFIMUP and IN-Institute of Nanoscience and Nanotechnology
Departamento de Física e Astronomia, 4169-007 Porto
Portugal
dmota86r@gmail.com

Palaimiene Edita,
Vilnius University
3 Universiteto St, LT-01513 Vilnius
Lithuania
edita.masiukaite@ff.stud.vu.lt

Park Jitae,
FRM-II, Technical University Munich
Lichtenbergstr. 1, 85748 Garching
Germany
jitae.park@frm2.tum.de

Petry Winfried,
Forschungs-Neutronenquelle Heinz Maier-Leibnitz (FRM II) - TUM
Forschungs-Neutronenquelle Heinz Maier-Leibnitz, 85748 Garching
Germany
winfried.petry@frm2.tum.de

Petzelt Jan,
Institute of Physics ASCR
Na Slovance 2, 182 21 Praha 8
Czech Rep
petzelt@fzu.cz

Piekarz Przemyslaw,
Institute of Nuclear Physics
ul. Radzikowskiego 152, 31-342 Kraków
Poland
piekarz@wolf.ifj.edu.pl

Pimenov Anna,
Vienna University of Technology
Wiedner Hauptstraße 8-10 1040 Wien, 1040 Vienna
Austria
anna.pimenov@ifp.tuwien.ac.at

Pirc Rasa,
Jozef Stefan Institute
Jamova 39, 1000 Ljubljana
Slovenia
rasa.pirc@ijs.si

Reinecker Marius,
Physik Funktioneller Materialien
Universität Wien,
Austria
marius.reinecker@univie.ac.at

Ross Manuel,
Dynamik Kondensierter Systeme
Universität Wien, 1090 Wien
Austria
manuel.ross@univie.ac.at

Rossnagel Kai,
University of Kiel
Olshausenstr. 40, 24098 Kiel
Germany
rossnagel@physik.uni-kiel.de

Rupp Romano A,
Physik Funktioneller Materialien
Universität Wien, 1090 Wien
Austria
romano.rupp@univie.ac.at

Salje Ekhard K. H.
University of Cambridge
Department of Earth Sciences
Downing Street, CB2 3EQ Cambridge
United Kingdom
es10002@esc.cam.ac.uk

Samulionis Vytautas,
Physics Faculty of Vilnius University
Sauletekio al. 9/3, 10222 Vilnius
Lithuania
vytautas.samulionis@ff.vu.lt

Schiebl Markus,
Technische Universität Wien
Institut für Festkörperphysik, 1040 Wien
Austria
markus.schiebl@ifp.tuwien.ac.at

Schranz Wilfried,
Physik Funktioneller Materialien
Universität Wien, 1090 Wien
Austria
wilfried.schranz@univie.ac.at

Sepiol Bogdan,
Dynamik Kondensierter Systeme
Universität Wien, 1090 Wien
Austria
bogdan.sepiol@univie.ac.at

Shuvaev Alexey,
Vienna University of Technology
Wiedner Hauptstraße 8-10, 1040 Wien
Austria
shuvaev@ifp.tuwien.ac.at

Singraber Andreas,
Computergestützte Physik
Universität Wien,
Austria
andreas.singraber@univie.ac.at

Sobieszczyk Pawel,
Instytut Fizyki Jadrowej
ul. Radzikowskiego 152, 31-342 Kraków
Poland
pawel.sobieszczyk@ifj.edu.pl

Soprunyuk Viktor,
University of Vienna
Boltzmanngasse 5, 1090 Vienna
Austria
soprunyuk@mail.ru

Spaldin Nicola,
ETH Zurich, Materials Theory
Wolfgang-Pauli-Strasse 27, 8093 Zurich
Switzerland
nicola.spaldin@mat.ethz.ch

Speziale Sergio,
Deutsches GFZ
Deutsches GFZ, 14473 Potsdam
Germany
speziale@gfz-potsdam.de

Stana Markus,
Dynamik Kondensierter Systeme
Universität Wien, 1090 Wien
Austria
markus.stana@univie.ac.at

Syrykh Gennady,
NRC "Kurchatov Institute"
1, Kurchatov sq., 123182 Moscow
Russian Fed
sgf@isssph.kiae.ru

Tröster Andreas,
Institute of Theoretical Physics
Vienna University of Technology, A-1040 Wien
Austria
andreas.troester@tuwien.ac.at

Toledano Pierre,
Universite de Picardie
Facultes des Sciences, F-80000 Amiens
France
pierre.toledano@wanadoo.fr

Vilarinho Silva Rui,
IFIMUP and IN-Institute of Nanoscience and Nanotechnology
Departamento de Física e Astronomia, 4169-007 Porto
Portugal
ruivilarinhosilva@gmail.com

Wdowik Urszula D.,
Institute of Technology, Pedagogical University
Podchorazych 2, 30-084 Cracow
Poland
sfwdowik@cyf-kr.edu.pl

Wehinger Björn,
European Synchrotron Radiation Facility (FR60338723919), 38043 Grenoble
France
wehinger@esrf.fr

Wirtz Ludger,
University of Luxembourg
162a, avenue de la Faiencerie, 1511
Luxembourg
Luxemburg
Ludger.Wirtz@uni.lu

Zielinski Piotr,
Institute of Physics of Cracow University of Technology and Institute of Nuclear Physics of Polish Academy of Sciences
ul. Radzikowskiego 152, 31-342 Kraków
Poland
Piotr.Zielinski@ifj.edu.pl